การประเมินผลแบบของหน้าสากต่อแผนที่ของการเปลี่ยนรูปพหุสัณฐานของคลอโพรพาไมด์หลังผ่านกรรมวิธีการตอกอัดเชิงกล

นางสาวธนิตา โชติพิบูลย์ทรัพย์

วิทยานิพนธ์นี้เป็นส่วนหนึ่งของการศึกษาตามหลักสูตรปริญญาเภสัชศาสตรมหาบัณฑิต
สาขาวิชาเภสัชอุตสาหกรรม ภาควิชาวิทยาการเภสัชกรรมและเภสัชอุตสาหกรรม
คณะเภสัชศาสตร์ จุฬาลงกรณ์มหาวิทยาลัย
ปีการศึกษา 2555

EVALUATING THE EFFECT OF PUNCH-FACE DESIGN ON POLYMORPHIC TRANSFORMATION MAPPING AFTER MECHANICAL COMPACTION OF CHLORPROPAMIDE

Miss Thanita Chotpiboolsup

A Thesis Submitted in Partial Fulfillment of the Requirements
for the Degree of Master of Science in Pharmacy Program in Industrial Pharmacy
Department of Pharmaceutics and Industrial Pharmacy
Faculty of Pharmaceutical sciences
Chulalongkorn University
Academic Year 2012

Thesis Title	EVALUATING THE EFFECT OF PUNCH-FACE DESIGN ON POLYMORPHIC TRANSFORMATION MAPPING AFTER MECHANICAL COMPACTION OF CHLORPROPAMIDE
By	Miss Thanita Chotpiboolsup
Field of Study	Industrial Pharmacy
Thesis Advisor	Narueporn Sutanthavibul, Ph.D.
Thesis Co-advisor	Jittima Chatchawalsaisin, Ph.D.

Accepted by the Faculty of Pharmaceutical Sciences, Chulalongkorn University in Partial Fulfillment of the Requirements for the Master's Degree

…..……Dean of the Faculty of Pharmaceutical Sciences
(Associate Professor Pintip Pongpech, Ph.D.)

THESIS COMMITTEE

……..Chairman
(Associate Professor Parkpoom Tengamnuay, Ph.D.)

…….……Thesis Advisor
(Narueporn Sutanthavibul, Ph.D.)

……..Thesis Co-advisor
(Jittima Chatchawalsaisin, Ph.D.)

……..Examiner
(Associate Professor Kraisri Umprayn, Ph.D.)

……..Examiner

(Pharnphen Wattanaarsakit, Ph.D.)

……..External Examiner

(Associate Professor Poj Kulvanich, Ph.D.)

ธนิตา โชติพิบูลย์ทรัพย์: การประเมินผลของแบบหน้าสากต่อแผนที่ของการเปลี่ยนรูปพหุสัณฐานของคลอโพรพาไมด์หลังผ่านกรรมวิธีการตอกอัดเชิงกล (EVALUATING THE EFFECT OF PUNCH-FACE DESIGN ON POLYMORPHIC TRANSFORMATION MAPPING AFTER MECHANICAL COMPACTION OF CHLORPROPAMIDE) อ.ที่ปรึกษาวิทยานิพนธ์หลัก : ดร.นฤพร สุตัณฑวิบูลย์, อ.ที่ปรึกษาวิทยานิพนธ์ร่วม : ดร. จิตติมา ชัชวาลย์สายสินธ์, 123 หน้า.

วัตถุประสงค์ของการศึกษา คือ ประเมินผลของแบบหน้าสากที่แตกต่างกันต่อแผนที่ของการเปลี่ยนรูปพหุสัณฐานของคลอโพรพาไมด์เมื่อถูกตอกอัดเชิงกลให้เป็นยาเม็ดและเปรียบเทียบผลการวิเคราะห์เชิงปริมาณของแผนที่ของการเปลี่ยนรูปพหุสัณฐานของยาเม็ดคลอโพรพาไมด์ระหว่างวิธี powder X-ray diffractrometry กับ confocal microscopic Raman spectroscopy พบว่าเมื่อผงยาคลอโพรพาไมด์พหุสัณฐานรูปแบบเอได้รับพลังงาน เช่น กระบวนการให้ความร้อน ความแรงของการตอกอัดและระยะเวลาของการตอกอัด เป็นต้น ผงยาคลอโพรพาไมด์สามารถเปลี่ยนรูปพหุสัณฐานได้ ซึ่งภายใต้สภาวะแรงตอกอัดและเวลาการตอกอัดที่เพียงพอ วิธีวิเคราะห์โดยใช้ powder X-ray diffraction พบว่าพหุสัณฐานรูปแบบเอสามารถเอาชนะพลังงานส่วนหนึ่งและสามารถเปลี่ยนเป็นรูปแบบอสัณฐานซึ่งไม่คงตัวจากนั้นจึงเปลี่ยนเป็นพหุสัณฐานรูปแบบซีซึ่งมีปริมาณน้อยกว่าร้อยละ 10 ในทางกลับกันปริมาณพหุสัณฐานรูปแบบเอหลังจากได้รับพลังงานความร้อนก่อนที่จะนำไปตอกอัดจะมีปริมาณลดลงครึ่งหนึ่ง แต่หลังจากได้รับแรงตอกอัดโดยใช้ระยะเวลาการตอกอัดที่ต่างกัน พบว่าปริมาณพหุสัณฐานรูปแบบเอจะลดลงน้อยกว่าร้อยละ 20 ขณะเดียวกันปริมาณพหุสัณฐานรูปแบบซีมีปริมาณเพิ่มขึ้นเป็นร้อยละ 40 ซึ่งปริมาณเหล่านี้ไม่สัมพันธ์กับหน้าสากที่แตกต่างกัน ดังนั้นวิธีวิเคราะห์โดยใช้ powder X-ray diffraction ไม่สามารถแยกความแตกต่างระหว่างหน้าสากที่แตกต่างกันได้แต่สามารถแยกผลของแรงตอกอัดและเวลาในการตอกอัดที่สภาวะพื้นและสภาวะกระตุ้นได้

ส่วนวิธีวิเคราะห์โดยใช้ confocal microscopic Raman spectroscopy สามารถแยกผลของแรงตอกอัดและเวลาในการตอกอัดที่สภาวะพื้นและสภาวะกระตุ้นได้เช่นกัน นอกจากนี้ยังสามารถแยกผลหน้าสากที่แตกต่างกันของพื้นผิวเม็ดยาได้ แต่อย่างไรก็ตามวิธีวิเคราะห์นี้ไม่สามารถแยกหน้าสากที่บากและไม่บากออกจากกันได้ ดังนั้นวิธีวิเคราะห์โดยใช้ confocal microscopic Raman spectroscopy สามารถให้ข้อมูลการวิเคราะห์โดยใช้หน้าสากที่แตกต่างกันได้ชัดเจนกว่าวิธี powder X-ray diffractrometry

ภาควิชาวิทยาการเภสัชกรรมและเภสัชอุตสาหกรรม	ลายมือชื่อนิสิต.....
สาขาวิชาเภสัชอุตสาหกรรม	ลายมือชื่อ อ.ที่ปรึกษาหลัก.....
ปีการศึกษา 2555	ลายมือชื่อ อ.ที่ปรึกษาร่วม.....

5276567733 : MAJOR INDUSTRIAL PHARMACY
KEYWORDS : PUNCH-FACE / POLYMORPHIC TRANSFORMATION / MAPPING/ MECHANICAL COMPACTION / CHLORPROPAMIDE

THANITA CHOTPIBOOLSUP: EVALUATING THE EFFECT OF PUNCH-FACE DESIGN ON POLYMORPHIC TRANSFORMATION MAPPING AFTER MECHANICAL COMPACTION OF CHLORPROPAMIDE. ADVISOR: NARUEPORN SUTANTHAVIBUL, Ph.D., CO-ADVISOR: JITTIMA CHATCHAWALSAISIN, Ph.D., 123 pp.

The purpose of this study was to evaluate the effect of different punch-face designs on the polymorphic transformation of chlorpropamide after tablet compaction using comparative results obtained from quantitative powder X-ray diffractometry (Q-PXRD) and Quantitative Raman spectroscopy (Q-Raman). When energy was introduced to chlorpropamide powder Form A, such as heating, compaction forces and dwell time, changes in solid state morphology occurred. Under sufficient pressure and dwell time, Q-PXRD showed that approximately half of Form A overcame the energy barrier and transformed to metastable amorphous form after which it eventually converted to less than 10% of Form C. On the other hand, when Form A was heated prior to compaction, half was converted due to heating. After compaction of the heated Form A with various dwell times, further reduction to less than 20% was observed while Form C increased dramatically beyond 40% with no correlation on punch face designs. Thus, Q-PXRD cannot be used to differentiate the polymorphic interconversion due to punch face designs but can distinguish between the effects of compaction forces and dwell times at ground and excited states.

Q-Raman was able to discriminate the polymorphic transition due to compaction forces and dwell times at ground and excited states similar to Q-PXRD. In addition, the technique was most sensitive in detecting the effects of concave and flat-faced punch designs on polymorphic conversion on tablet surfaces. However, indentation was shown not to have significant impact on inducing changes of chlorpropamide polymorphs. Thus, Q-Raman was able to deliver more information on the polymorphic transformation due to punch face designs when compare to conventional Q-PXRD.

Department : Pharmaceutics and Industrial Pharmacy Student's Signature……
Field of Study : Industrial Pharmacy Advisor's Signature……
Academic Year : 2012 Co-advisor's Signature……

ACKNOWLEDGEMENTS

This thesis was successfully achieved through the cooperation of many individuals. First, I would like to express my sincere gratitude to my advisor, Dr. Narueporn Sutanthavibul for her advice, creative guidance, encouragement, valuable comments and support given throughout my time in graduate school.

I am also indebted to my co-advisor, Dr. Jittima Chatchawalsaisin for her kind assistance, helpful consultation and everlasting support.

I also wish to express deep appreciation to all members of the thesis committee for spending their times to be on my thesis committee and for their suggestion and comments.

I would like to express my infinite thanks and deepest gratitude to staffs in the Department of Pharmaceutics and Industrial Pharmacy for their assistance and encouragement. I am really thankful to my seniors and my friends for their friendship, consultation, guidance, suggestion, helpful thoughts and kindness.

The other special thank to T.O. Chemical Co., Ltd for supplied chlorpropamide powder to my study.

Finally, I would like to express my deep gratitude and appreciation to my family for their assistance, care cheerfulness endless love and encouragement.

CONTENTS

Page

Page

Page

LIST OF TABLES

Table **Page**

Table **Page**

LIST OF FIGURES

Figure **Page**

Figure **Page**

Figure **Page**

Figure **Page**

Figure **Page**

LIST OF ABBREVIATIONS

Q-XRPD	quantitative powder X-ray diffractometry
Q-Raman	quantitative Raman spectroscopy
%	percentage
DSC	differential scanning calorimetry
FT-IR	transformed infrared spectroscopy
cm^2	square centimetre (s)
MPa	megapascal (s)
min	minute (s)
°C	degree Celsius (centrigrade)
µm	micron (s)
NMR	nuclear magnetic resonance spectroscopy
NIR	near-infrared spectroscopy
PXRD	powder X-ray diffractometry
NQR	nuclear quadruupolar resonance
Å	angstrom (s)
θ	angle
FT-Raman	Fourier Transform Raman
nm	nanometre (s)
CCD	charge-coupled device
cm^{-1}	centimetre-gram-second
sec	second (s)
cm^3	cubic centimetre (s)
cm	centimetre (s)
kV	kiloVoltage (s)
mm	millimetre (s)
psi	pound per square inch (es)
R^2	coefficient of determination
SD	standard deviation
et al.	et alli, and others

Chapter I

INTRODUCTION

Tablet dosage form is most popular dosage form in the pharmaceutical industry of Thailand. The critical control of processes during tablet making is very important because of many steps involved such as grinding, sieving, drying and tabletting.

These different procedures may affect the polymorphism of active ingredient in the formula. Over 85% of active pharmaceutical ingredients have been shown to have multiple polymorphic forms in solid state (Byrn 1995; Karpinski 2006). The polymorphic transformation can change physicochemical properties of active pharmaceutical ingredients, such as, melting point, vapor pressure, density, solubility, stability, dissolution rate and bioavailability which have further effect on efficacy (Newman 2003; Yu 2003; Ayala 2012). The solid transformations occurred during manufacturing process, especially compaction (Sanchez-Castillo 2003; Koivisto 2006; Wildfong 2007; Mazel 2011). Because of the pressure distribution during the compaction in the tablet die is not homogeneous, the region in which the different pressure is distributed is also uneven on the surface of the tablet. This caused different polymorphic transition in the tablet during the compaction process. Thus, the physicochemical properties of the outer layers of the tablet surface are shown to be different from the tablet interior (Koivisto 2006; Lin 2007).

Moreover, the designs on the punch-face may be another factor affecting polymorphic transformation. During compaction, interactions between powder and part of the equipment, such as die wall or punch-face, occur. This leads to density variation lead to change physicochemical property of drugs (Sixsmith 1980; Sinka 2004). The punch-faces which are designed differently, such as flat-face or concave face, have been shown to influence the mechanical properties of powder compacts by causing uneven pressure distribution during tablet compression (Newton 2000; Eiliazadeh 2004).

Chlorpropamide is chosen as the model drug for this study because it often relates to many tabletting problems. During compaction, chlorpropamide may change the polymorphic form due to local heating, melting or recrystallization. During compaction process punch and die attrition can induce heat causing polymorphic transition inside the tablets (Boldyreva 2008). However, the pharmaceutical industry realized the importance of polymorphic transformation of drugs by mechanical compression but no official quantitative method has been identified. Thus, an appropriate quality control method for tablets using suitable solid state analysis to quantitatively detect polymorphic transformation is essential.

Many techniques have been used to chlorpropamide polymorphic transformation such as powder X-ray diffractometry (PXRD), Raman spectroscopy, differential scanning calorimetry (DSC) and Fourier transformed infrared spectroscopy (FT-IR) (Tudor 1993; Wildfong 2007; Drebushchak 2008). No studies have been done to identify the location of polymorphic transformation on the surface of chlorpropamide tablets after mechanical compaction using various punch-face designs. Consequently, PXRD and confocal microscopic Raman spectroscopy are compared to quantitatively analyze the solid structural change of chlorpropamide tablets in this study. The aim of this study is to evaluate the different quantitative methods which have different advantages and limitations. By quantitative powder X-ray diffractometry (Q-PXRD), the percentage of each polymorph is based on calculation of the whole tablet and it is a destructive method having to grind tablets into fine powder before analysis. Quantitative confocal microscopic Raman spectroscopy (Q-Raman), on the other hand is analyzed only at the surface of the tablet in order to identify the position of each polymorph and it is not a destructive method.

Objectives of the present study were:

1. To evaluate the effects of different punch-face design on polymorphic transformation of chlorpropamide tablets after mechanical compaction
2. Compare the results analyzed by PXRD and confocal microscopic Raman spectroscopy on polymorphic mapping of chlorpropamide tablet surface

CHAPTER II
LITERATURE REVIEW

1. THE MODEL DRUG

Chlorpropamide, ($C_{10}H_{13}ClN_2O_3S$) (Figure 1), is used as clinical treatment of Type II (noninsulin-dependent) diabetes mellitus for a long time. It has problems of physical property, practically insoluble in water which caused absorption problem. Many pharmaceutical researches used chlorpropamide as a model drug in the study to increase the bioavailability of low water soluble drug in a pure form (Chesalov 2008).

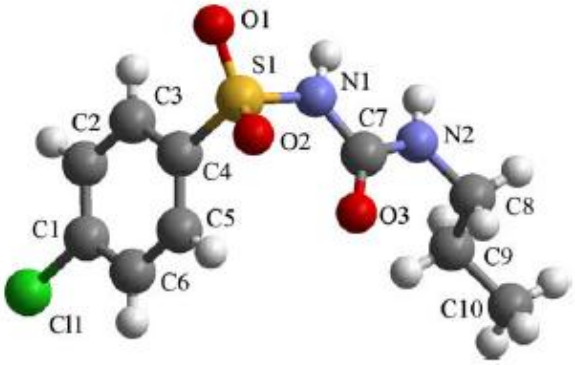

Figure 1 A molecule of chorpropamide (Chesalov 2008).

Moreover, it was reported that chlorpropamide had several polymorphs. Simmons reported the first three chlorpropamide polymorphs. Form A is a stable form. Form C is unstable at room temperature but stable at higher temperature. Each polymorph has slightly different dissolution rates (Simmons 1973). More researchers discovered several polymorphs of chlorpropamide. Burger screened the crystalline forms and identified five polymorphs (Burger 1975; Burger 1976). These forms exhibit very complex thermodynamic relationships involving temperature, pressure and kinetics-induced phase transformations (Ayala 2012). Ueda investigated the dissolution behavior of chlorpropamide polymorphs by dispersing excess amount using stationary disk method.

The results are shown in Figure 2. In addition to this study observed chlopropamide Form C transformed to Form A during compression under 2 ton/cm^2 or 196 MPa (Ueda 1984).

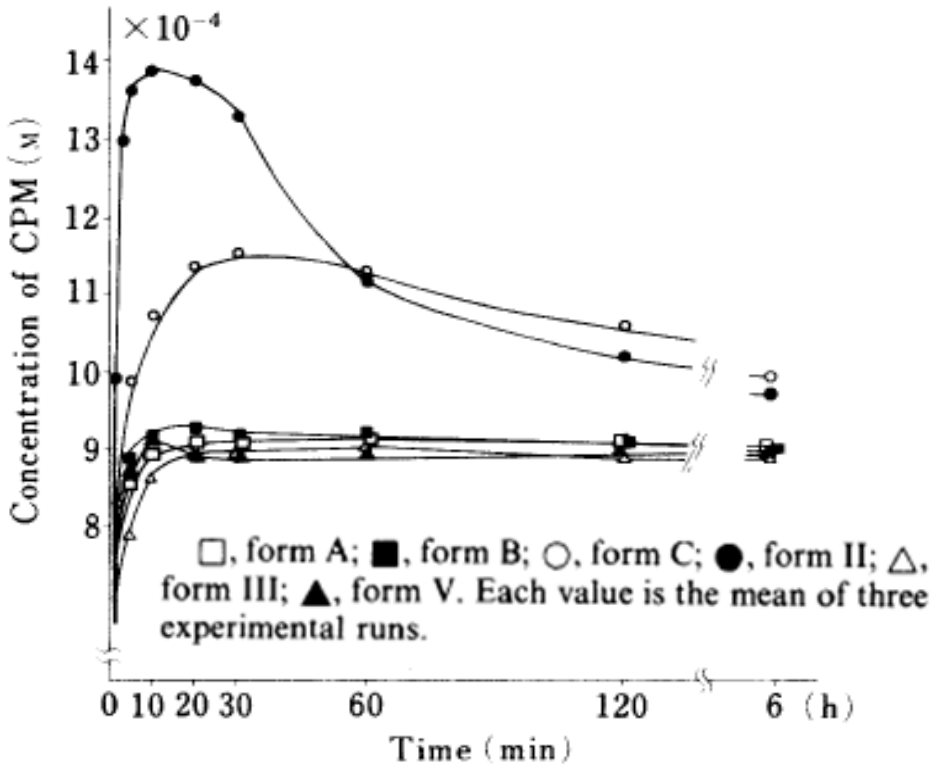

Figure 2 Dissolution profiles of chlopropamide polymorphs in 50 ml of pH 2.0 at 30°C (Ueda 1984).

As above, the polymorphs of chlorpropamide showed to transform by compression so it has related between polymorphic transformation and tabletting compression. In 1993, Otsuka confirmed polymorphic transformation between chlorpropamide Form A and Form C by multi-tabletting compression. Theses suggested the both forms were transformed into each other by mechanical energy during tabletting that mean the phase transformation required the alternation of both crystalline forms to an amorphous intermediate, which then transformed into the equilibrium ratio of 45% Form A and 25%

Form C (Brittain 2002). Figure 3 showed the change in the powder X-ray diffractogram of chlorpropamide Form A and Form C during multi-compression.

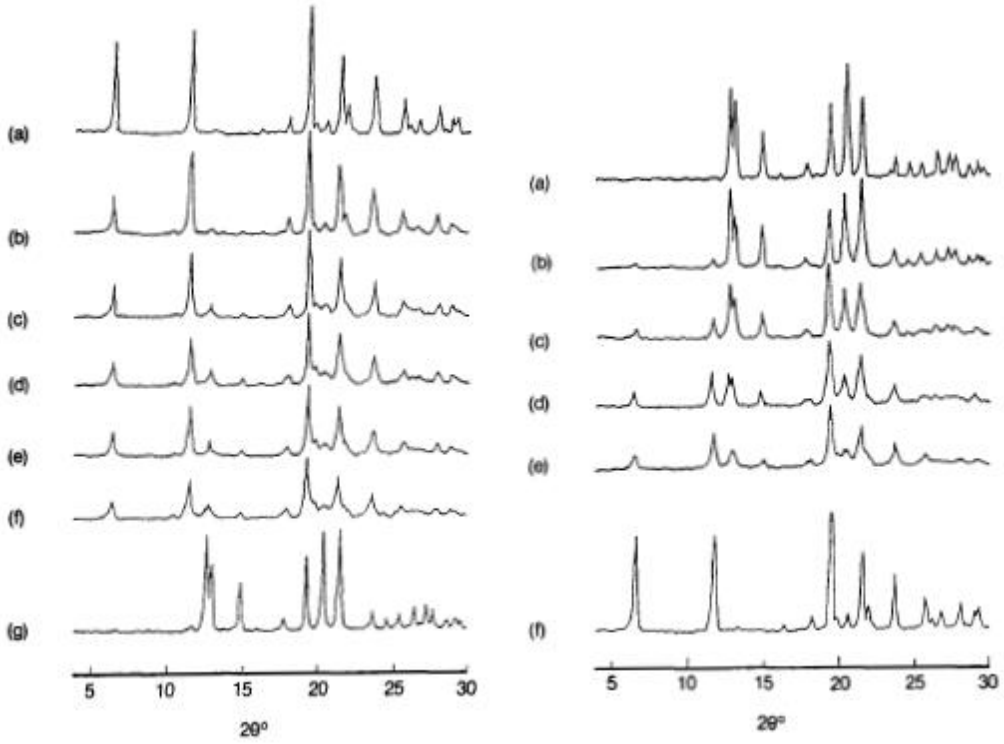

Figure 3 The X-ray diffractogram of Form A (left) and Form C (right) due to compression: (a) intact Form A (left) and Form C (right), (b) after 1 compression, (c) 3 cycles, (d) 5 cycles, (e) 10 cycles (f) 30 cycles and (g) intact Form C (left) but right not showed intact Form A (Otsuka 1989).

Wildfong confirmed the observation of Otsuka by using Raman spectroscopy compared with PXRD. The chlorpropamide polymorphic transformation has compaction pressure approximately 10.5 MPa. The range of phase interconversion increased with applied compaction pressure (Wildfong 2007).

Subsequently, Matsumoto investigated the effect of temperature and pressure during compression and proposed that the mechanochemical effect by controlled temperature at 0 ^{O}C and 45 ^{O}C of Form A depended on the compression temperature, but Form C was independent of temperature. The results were showed in Figure 4. The crushing strength of chlorpropamide tablets depends on the kinds of polymorphic forms and the compression temperature (Matsumoto 1991). It was concluded all phase transformations occurred by a process whereby a metastable amorphous form (non-crystalline form) was formed from the starting materials (crystalline form) and the intermediate could be transformed into whether Form A or Form C (Brittain 2002).

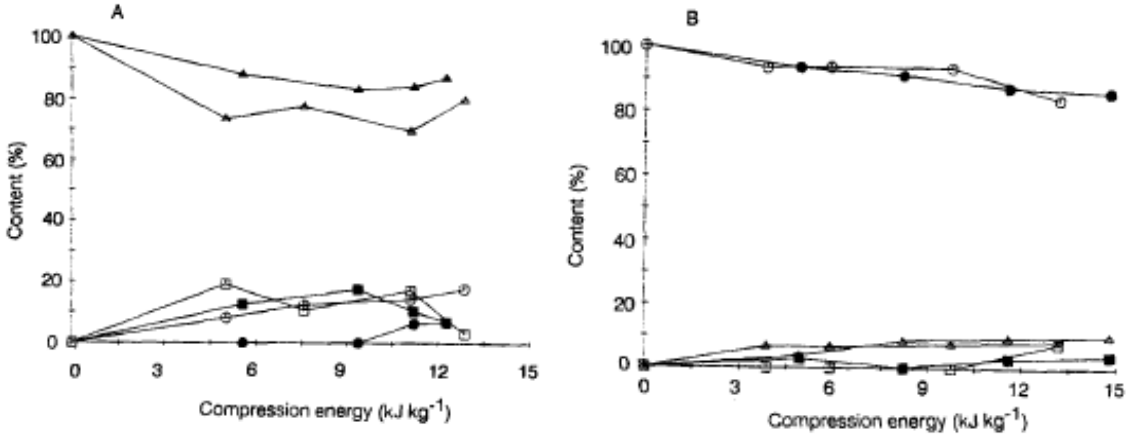

△, Form A at 45 ^{O}C; □, Form C at 45 ^{O}C; ○, non-crystalline solid at 45 ^{O}C;
▲, Form A at 0 ^{O}C; ■, Form C at 0 ^{O}C; ●, non-crystalline solid at 0 ^{O}C;

Figure 4 Effects of temperature on polymorphic transformation of chlorpropamide during tabletting at different compression energies by (A) Form A; (B) Form C (Matsumoto 1991).

In 2008, chlorpropamide polymorphs were discovered the information about 16 polymorphs, Thirteen entries were collected in the Powder Diffraction Files database (PDF-50) and three X-ray diffractogram which reported by Simmon, not included in the database. According to the Burger's nomenclature, the polymorphs are labeled I, II, III, IV, and V, which form I, II and III are usually referred to as Form C, Form B, and Form A

with reference to Simmons, respectively. Furthermore, Debrushchak suggested a new notation based on the order of crystal structure by used Greek characters as follows α, β, γ, δ and ε which referred to Form III, II, IV and I, respectively. Figure 5 presented two conformers of chlorpropamide Form A and Form C (Drebushchak 2006; Drebushchak 2007; Drebushchak 2008; Ayala 2012).

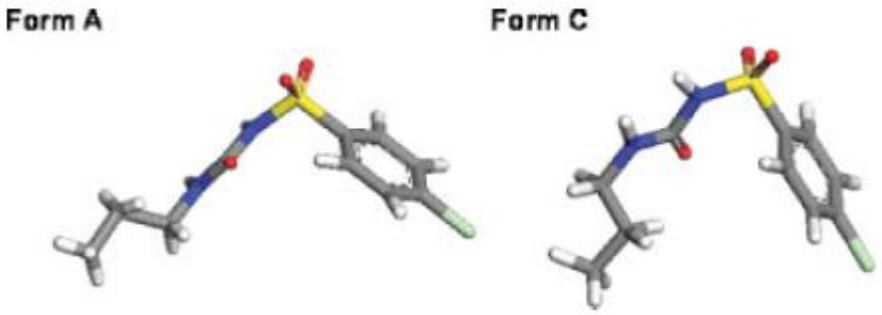

Figure 5 The molecular conformation of chlorpropamide polymorphs Form A and Form C (Wildfong 2007).

2. EFFECT PUNCH-FACE AND PRESSURE

Tablets are one of the most dosage forms produced in pharmaceuticals industry. The polymorphic transformations are observed during unit operations such as milling and compaction (Morris 1998). The energy of compression is dispersed in many processes such as rearrangement, fragmentation, bond formation, deformation of particles or crystals, friction between particles and the die wall. It was used in the process and led to crystallographic changes, in other words the amorphous form is usually undesirable energy therein it must be thermodynamically metastable form and will opportunity spontaneously transform to crystalline form (Otsuka 1989; Brittain 2002). These physical changes can be change the physicochemical property of drug such as dissolution rate and affect to efficacy of drug.

Generally, the pressure was produced during the tabletting are in the range 20-400 MPa. During the tabletting process, the particles of the powder may be deform or fracture in order to form the tablet. The compaction force could not homogeneous due to the pressure distribution during the compression in the tablet die was not uneven. The surface of the tablet is the most area which the pressure is uneven. This is a cause of the change different polymorphic transition in the tablet during the compaction process. These means the physicochemical properties in the outer layers of the tablet surface may different from the tablet interior. Koivisto discovered the amount of crystal defects in the chlorpropamide tablets increased as the more inner regions of the tablets because the compression which broke up the crystalline on the tablet surface thus the crystal defects had occurred (Koivisto 2006). Figure 6 showed chlorpropamide powder tolerated a phase transition from Form A to Form C during the compaction process.

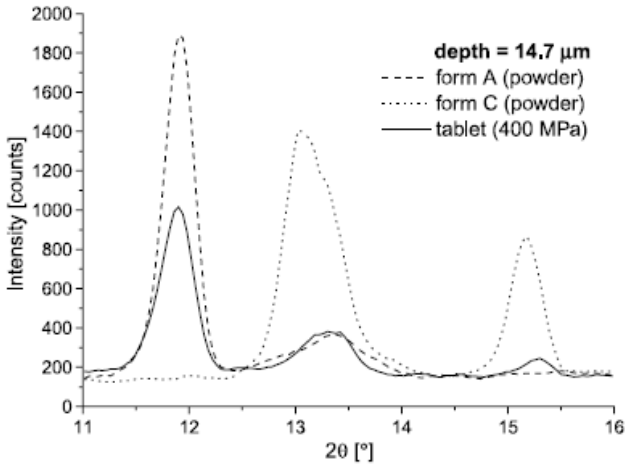

Figure 6 The effect of compression on the chlorpropamide powder (Koivisto 2006).

The fraction of Form A was the smallest on the surface of the tablets. The fraction of Form C was not the highest on the surface but in the interiors of the tablets. The other transformation took place during the compression was the amorphous of the surface. But this situation was not happen the whole actuality because of the chlorpropamide crystals seemed to orient preferentially in compression. The preferred orientation effect may be

dependent on the depth. Compaction force of chlorpropamide independent the phase transition. But the higher pressure, the less Form A was observed in the tablets. The lowest amount of Form C was observed from tablets compacted using the lowest compression pressure (100 MPa). The increase of compaction force increased the bonding and crushing of the particles. Commonly, the dissolution rate decreased when increased compaction pressure but the effect of the compression force could be opposite. The effect of compaction pressure on the dissolution properties of the tablet is a complex matter. (Koivisto 2006). So the compression pressures will affect the conversion to another form, for instance the chlorpropamide powder Form A and Form C were transformed into each other by mechanical energy during tabletting (Otsuka 1989). The phenomenon of polymorphic transition under mechanical force occurred through a mechanism of nucleation and growth of a second phase. The nucleation tended to process from dislocations in a crystal because of their higher free energy hence the energy for transformation is lower at these sites. Moreover, during compression, the plastic flow induced dislocation strains in a crystal (Chan 1985).

Moreover, the punch-face is a factor of change polymorphic transformation. The pharmaceutical industries are manufacturing tablets in many shapes such as flat-face or curved faced, which have influenced mechanical properties of the powder compacts cause of uneven pressure dispersion during compacts the tablets (Newton 2000; Eiliazadeh 2004). The die compaction is a unit operation employed in pharmaceuticals. During compaction tablets, interaction between the powder and the equipments such as die wall or punch-face affect to density variation and lead to change physicochemical property of drugs (Sixsmith 1980; Sinka 2004). Resolution of compression forces act on the particles when the curved faced were used. As showed the force to act downwards towards the centre of the compact. The angle of this force is depends on the curvature of the punch-face. However, this force acts higher the compact for the curved face than the flat faced (Sixsmith 1980).

Nevertheless no have evidence on the study of the position of polymorphic transformation on the various design of punch-face.

3. QUANTITATIVE ANALYSIS

The Solid pharmaceuticals consist of polymorphs, solvates, or amorphous forms. The solid state chemistry of drug was defined as the most drugs are used in a crystalline form. The crystals are held together by molecular forces. The arrangement of molecules in a crystal form was determined its physical properties and the physical properties can affect its performance. But the amorphous solids are not crystalline therefore they do not have powder X-ray diffraction pattern. The most amorphous solid is a glass, which the atoms and molecules exist in a non-uniform array. The amorphous solids cannot be identified as either habits or polymorphs because the properties are direction independent. These are called isotropic (Byrn 1999).

The solid state form of drugs can be have significant influence on both bioavailability and stability, thus the identification and characterization of solid state form is a necessary part of the development process (Byrn 1994). There are many methods that can be used to investigate the solid state form of the drug such as Tudor analyzed binary mixtures of chlorpropamide powder Form A and Form B by near-infrared Fourier transform Raman spectroscopy (FTRs) to distinguish between two major polymorphs and used differentail scanning calorimetry (DSC), Fourier transform infrared microscopy (FT-IR) for identification and characterization (Tudor 1993).

Furthermore, PXRD, nuclear magnetic resonance spectroscopy (NMR), Fourier transform infrared microscopy (FT-IR), near-infrared spectroscopy (NIR), and Raman spectroscopy are excellent techniques for obtaining structural information and have been regularly utilized to discriminate crystalline and amorphous forms and also to differentiate between polymorphs of active pharmaceutical and the ingredients (Bugay 2001; Stephenson 2001).

3.1. POWDER X-RAY DIFFRACTOMETRY

The solid forms of chlorpropamide were traditionally characterized by PXRD, DSC, vibrational spectroscopy and nuclear quadruupolar resonance (NQR) (Otsuka 1989; Matsumoto 1991; Tudor 1993; Koivisto 2006; Wildfong 2007; Chesalov 2008; Drebushchak 2008). PXRD is the primary tool for the study polymorphic transformation traditionally methods is an effective method of distinguishing solid phases having different internal structure where the peak heights or the integrated intensities of the peaks compared to an internal standard usually are used as a measure of the crystalline. The method is simple and does not require large single crystals but can be apply to any powder sample. Moreover, PXRD has also been used to quantify the percentage of a crystal form in the mixture of forms or determine the amounts of the active ingredient in multi-component tablet formulations (Suryanarayanan 1991; Byrn 1999). The accuracy quantitative analysis can be more complex cause of geometry errors associated with traditional Bragg-Brentano reflectance mode application and signal attenuation due to sample densification. The quantitative analysis usually requires extensive calibration using known mixtures of the two components which are easily prepared and ascended onto a standard calibration (Cao 2002; Cao 2003).

FUNDAMENTAL PRINCIPLES OF X-RAYS DIFFRACTION

The X-rays are short-wavelength electromagnetic radiation produced by the deceleration of high energy electrons or by electronic transitions of electrons in the inner orbital of atoms. The wavelength range of conventional X-rays spectroscopy is about 10^{-5} to 100 Å, however, mainly confined to the region of about 0.1 Å to 25 Å. When the X-radiation passed through a sample, the electric vector of the radiation interacts with the electrons in the atoms of the substance to produce scattering. When the X-rays are scattered by the ordered environment in a crystal, constructive and destructive interference occurs among the scattered rays because the distances between the scattering

centers are of the same order of magnitude as the wavelength of the radiation. This result is the diffraction.

When an X-ray beam ran into a crystal surface at some angle (θ), the part of the beam was scattered by the layer of atoms at the surface. The non-scattered part of the beam penetrated to the second layer of atoms where again a fraction is scattered, and the remainder passes on to the third layer and so on Figure 7 (Skoog 2007).

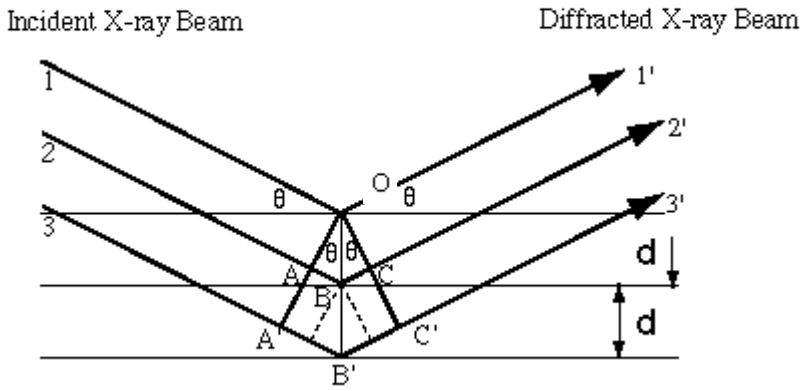

Figure 7 The diffraction of X-rays beam (http://www.geology.wisc.edu/~g203/xray.htm).

ANALYSIS OF POWDER X-RAY DIFFRACTOMETRY

1. Qualitative analysis

The qualitative information can be converted to semi-quantitative data by careful measurement of peak heights. To obtain a rough estimate of concentration, the following relationship is used:

$$P_X = P_S W_S$$

P_X is the relative line intensity measured in terms of number of counts for a fixed period

W_X is the weight fraction of the desired element in the sample

P_S is the relative intensity of the line that would be observed under identical counting condition if W_X were homogeneity. The value of P_S is determined with a sample of the pure element or a standard sample of known composition

Agatonovic-Kustrin developed the qualitative and quantitative assay of the two crystalline of ranitidine hydrochloride by PXRD. Due to the powder X-ray diffraction widely used for identification crystalline solid phase and can be quantify of mixtures. But there are various sources of error in the Q-PXRD. Figure 8 showed the characteristic diffraction of ranitidine Form 1 and Form 2 for identification. The peaks which no, or only minor interfere diffraction signals were chosen as the quantitative assay (Agatonovic-Kustrin 1999).

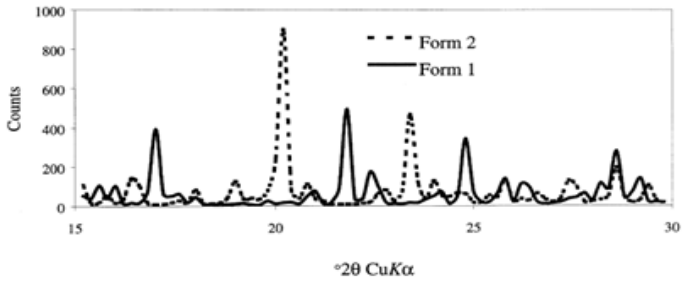

Figure 8 The X-ray diffractogram of two polymorphic form of ranitidine hydrochloride (Agatonovic-Kustrin 1999).

2. Quantitative analysis

The basic quantitative analysis by PXRD used the individual peaks or the whole patterns to verify the relationship between phase composition and the intensity of individual peaks or patterns of the phases. Moreover, It can be applied by determination of amounts of different phases in multi-phase mixtures by peak-ratio calculations or

determination of crystalline size or shape from analysis of peak broadening (Stephenson 2001; Connolly 2007). Currently, the many research develop the quantitative procedure using powder X-ray diffraction, which the first method, combine with the secondary method such as Raman spectroscopy and used multivariate analysis for quantitative with two equipments (Chieng 2009).

Wlidfong chose chlorpropamide as a model compound because of its affectability to polymorphic transformations when using moderately low pressures. It was presented for in situ whole compact detection and quantification of solid state phase transformations using parallel-beam transmission PXRD. The pure chlorpropamide Form A was prepared at pressure range 3.5-35.1 MPa. The intensity of the 2 1 0 reflection for chlorpropamide Form C increased with increasing applied pressure (Figure 9 left). These result that the transformation from chlorpropamide Form A to chlorpropamide Form C does not occur below pressures of 10.5 MPa. On the other hand, the same experiments prepared from pure chlorpropamide Form C (Figure 9 right), yielding the same results (Wildfong 2005).

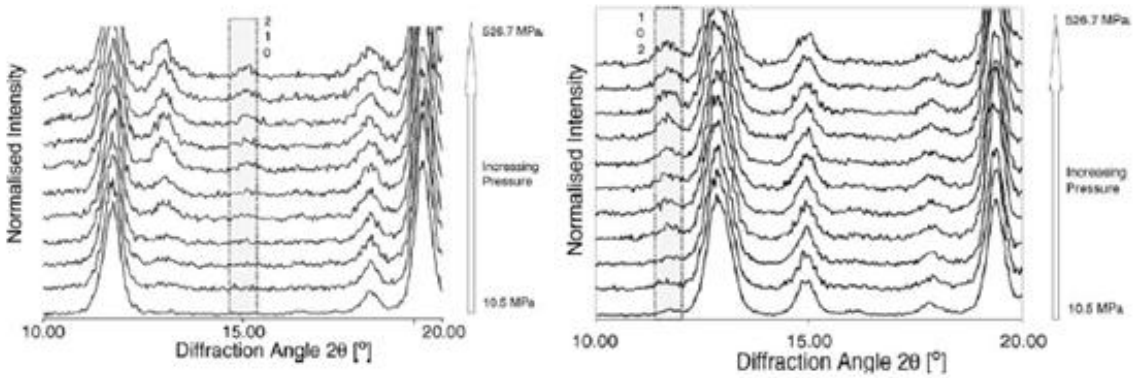

Figure 9 The powder X-ray diffractogram of pure chlorpropamide Form A (left) and Form C (right) at various increasing pressures. (Wildfong 2005).

3.2. RAMAN SPECTROSCOPY

Vibrational spectroscopy methods are verified tools for the characterization of active pharmaceutical ingredients in the solid state apart from PXRD, DSC and thermal gravimetric analysis (TGA) because it provided fingerprint spectra that are unique to each specific compound. In addition, the low wavenumber region, the most of the significant vibrational information on the solid state is contained, is easily to accessible by Raman spectroscopy (Ayala 2007; Haefele 2011). Both infrared (IR) and Raman spectra are concerned with measuring associated molecular vibration and rotation energy changes. However, the requirement for vibrational activity in Raman spectra is not a change in dipole moment, as it is in IR spectra, but a change in the polarizability of the molecule during the vibration (Vankeirsbilck 2002; Newman 2003). Figure 10 showed the Raman spectrum and IR absorption spectrum. They transmitted strong degree of similarity because of the different origins of each process, differences in the character of functional groups cause the techniques to be complementary and not duplicative (Bugay 2006).

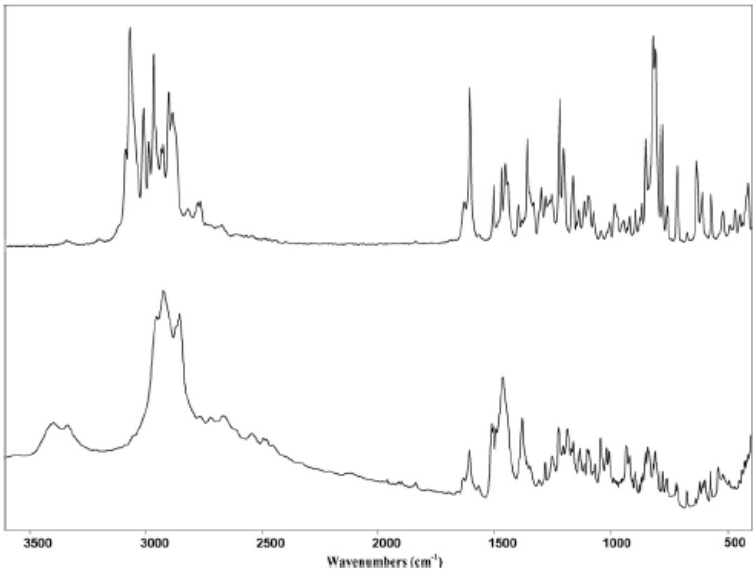

Figure 10 Compared of the diffuse reflectance infrared adsorption spectrum (lower) and FT-Raman spectrum (upper) of an active pharmaceutical ingredient (Bugay 2006).

Raman spectroscopy is one of the first choice methods in the study of polymorphism in pharmaceuticals due to the ability of small volume sampling, fingerprint capabilities, speed of data acquirement, automated high-throughput analysis of multi-well plates and the sensitivity of Raman scattering spectroscopy can detect structural changes (Kojima 2006; Ayala 2012). The Raman spectra were obtained from intact the solid dosage forms such as tablets or capsules. Taylor showed it was possible to detect the active ingredients in the intact dosage form even though the substance comprised less than 1% of the total mass of the tablet. The Raman signals of excipients or diluents are generally weaker than the active ingredients. Hence, it will be not difficult to identify the active ingredients that have strong Raman signals even when they were presented in lower concentrations. Because the most of excipients are composed of non-aromatic or aliphatic and non-crystalline in comparison to drug compounds that are mostly aromatic heterocyclic that are strong Raman scatters. The advantage of Raman analysis is non-destructive method, requires little sample preparation, the time of analysis is short and can be used study small particles within inhomogeneous sample matrices. In addition, Raman spectroscopy is also operated as process analytical technology (PAT) because of its insensitive to aqueous solvents. The signals are usually in the visible or near-infrared region, glass or quartz cells can be employed so it is a suitable tool for monitoring. (Taylor 2000; Vankeirsbilck 2002; Haefele 2011). Although the spectral analysis can be useful to extract information on spatial distributions and discriminate crystalline from amorphous forms, it may not give an accuracy data analysis especially when the spectrum highly overlap bands are involved and when only subtle spectral differences exist between the amorphous and crystalline forms (Widjaja 2011). Moreover, the drawback of Raman spectroscopy such as a major problem for Raman measurements lies in the high levels of fluorescence overlay the Raman spectral, the cost of equipment for adapt the Raman spectroscopy for routine analysis.

THEORY OF RAMAN SPECTROSCOPY

Raman spectra are obtained by irradiation a sample with a powerful laser source of visible or near-IR monochromatic radiation. The sample has been energy ($h\nu_{ex}$) because of the excitation wavelength is well away from an absorption band. The excitation wavelength can be considered to involve a virtual state. A molecule in the ground level can absorb a photon of energy ($h\nu_{ex}$) and remit a photon of energy. The most of the scattered energy comprises radiation of the incident frequency is Reyleigh scattering. The fraction of photons scattered from molecular centers with less energy or lower frequency than they had before the interaction is Stokes scattering. The anti-Stokes photons have greater energy or higher frequency than those of the exciting radiation. Figure 11 compared the different scattering events observed in Raman spectroscopy with the light absorption in IR spectroscopy. During the irradiation, the spectrum of the scattered radiation is measured at some angle (often 90^{O}) with a suitable spectrometer. At the very most, the intensities of Raman lines are 0.001% of the intensity of the source. Because of this, it might seem more difficult to detect and measure Raman bands than IR vibrational bands. However, the Raman scattered radiation is in the visible or near-infrared regions which more sensitive detectors are available. Hence, the measurement of Raman spectra is nearly as easy as measurement of IR spectra (Lin-Vien 1991; Skoog 2007).

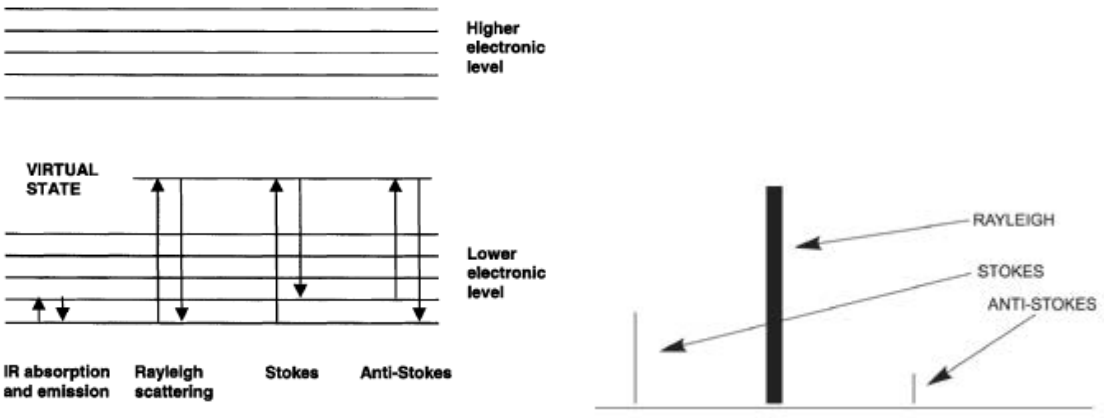

Figure 11 Schematic represents energy transitions in infrared and Raman spectroscopy (http://www.azooptics.com/article.aspx?ArticleID=309 and Vankeirsbilck 2002).

INSTRUMENTS OF THE RAMAN SPECTROSCOPY

The two technologies are used to collect the Raman spectra:

1. Dispersive Raman
2. Fourier Transform Raman (FT-Raman)

The differences between both technologies are the laser is used and the way of Raman scattering is detected and analyzed. Each technique has unique advantages see in Figure 12 (Vankeirsbilck 2002).

Dispersive Raman	FT-Raman
	Laser
VIS : 785 nm, 633 nm, 532 nm, ...	NIR : 1064 nm
	Spectral analysis by
Grating	Interferometer
	Detector
Silicon CCD detector	- room temperature indium gallium arsenide - liquid nitrogen-cooled germanium
	Advantages
- higher sensitivity - higher spatial resolution for microscopy applications - lower laser power	- limited fluorescence - maximal compatibility with libraries and analysis software
	Applications
- minor component analysis - more sensitive for aqueous samples - analysis of dark samples - depth or cross-sectional information in samples	- in the pharmaceutical industry: - unknown identification - incoming raw material characterisation - final product quality - quantitative analyses - investigating polymorphs - forensic analysis through sample containers or evidence bags

Figure 12 Compared of dispersive and FT-Raman spectroscopy (Vankeirsbilck 2002).

The basic configuration and components of a dispersive Raman spectrometer are shown in Figure 13. The source of monochromatic radiation is a laser, which could be helium-cadmium and has the wavelength 325, 354 or 442 nm, or air-cooled argon-ion which has wavelength 488 or 514 nm, or doubled continuous wave neodymium yttrium aluminum garnet (Nd:YAG or $Nd:Y_3Al_5O_{12}$) which has wavelength 532nm, or helium-

neon which has wavelength 633 nm, or stabilized diode which has wavelength 785nm. The stability of the laser radiation, is a key property of a good spectrometer and good stability, is essential for good function. Laser lifetimes and cost are also considerations of choice to use the laser. The one consideration associated with laser selection in the dispersive Raman systems concerns the use of wavelengths that could potentially generate molecular fluorescence. If fluorescence does not pose a problem for a given sample, lower frequency lasers can be used (532 or 514 nm) for enhanced sensitivity. But if fluorescence is a problem when using these high-energy sources, then lower energy sources, such as those used in FT-Raman spectroscopy, can be used to minimize the fluorescence effects.

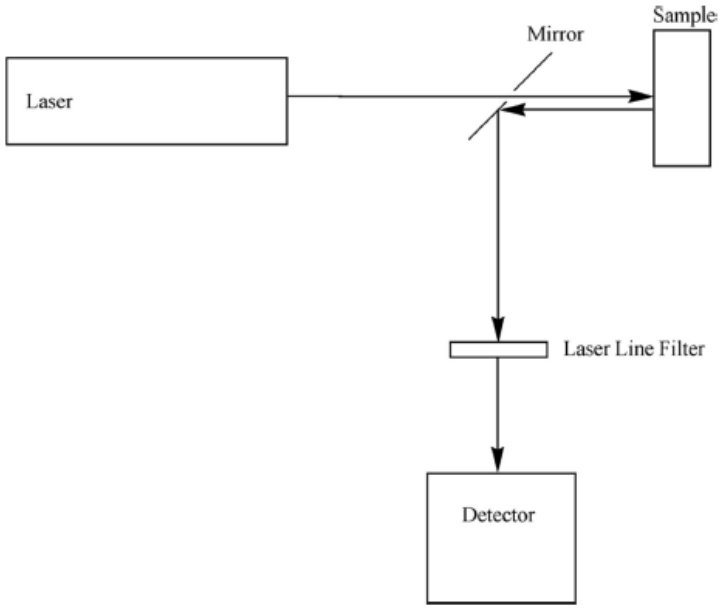

Figure 13 The basic configuration and components of a dispersive Raman spectrometer (Bugay 2006).

Figure 13, the sample is positioned in the laser beam and the scattering radiation is collected in the 180^{O} (the backscattering method) or 90^{O} (the right-angle method) scattering configuration. Accordingly, a laser-line rejection filter is placed in the scattering beam path to filter out Rayleigh scattering and the intensity of scattered light

measured by a detector positioned in the spectrometer. For the dispersive systems, a charge-coupled device (CCD) is typically utilized. Silicon CCD detectors are normally used for Raman spectrometers in which visible wavelength lasers are used.

The basic configuration and components of the FT-Raman spectrometer is shown in Figure 14. The advantages of the FT-Raman spectrometer are wavelength accuracy and the use of a near-infrared (NIR) laser that usually gets rid of the false effects due to fluorescence. In the FT-based system, a Nd:YVO_4 laser which has wavelength output 1064 nm is used to irradiate the sample. The sample is positioned in the laser beam and the scattering radiation is collected in the 180^O (the backscattering method) or 90^O (the right-angle method) scattering configuration, same the dispersive Raman spectrometer. By utilizing the longer wavelength of the Nd:YVO_4 laser in the FT-Raman spectrometer, the fluorescence effect is minimized because it is unlikely that a change in electronic state could be promoted through the use of a low-frequency laser. The scattered photons are passed into an interferometer with laser line filtering. Detection of the scattered photons from systems that application lasers emitting light with wavelengths greater than 1000 nm are of the single element type such as high purity *p*-type germanium or indium/gallium/arsenic (InGaAs) detectors. The detectors are noisier than the charge coupled device (CCD) detectors, but they do exhibit high quantum efficiencies. Unfortunately, germanium detectors are subject to interference by cosmic rays and the creations in their output may be generated. However, the corrections to these creations have been incorporated into hardware or software methods (Bugay 2006).

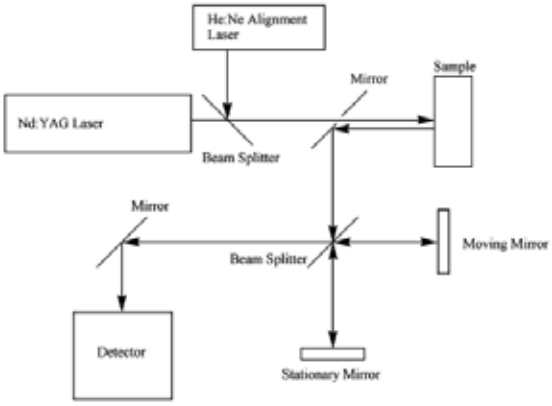

Figure 14 The basic configuration and components of a FT-Raman spectrometer (Bugay 2006).

Confocal Raman microscopy is a choice for investigated heterogeneous systems on the micrometer scale and a useful technique for non-destructive method. It is usually attached to a light microscope. It can selectively probe any given XYZ-location in a sample with a spatial resolution in the micron range. The confocal points are defined as the point source, the in-focus sample location and the focus image of the sample point. Axial resolution, defined as the distance away from the focal plane in which the Raman intensity from the sample decreases to 50% of the in-focus intensity, can be approximated from the numerical aperture used in the microscope. The depth resolution and optical slicing of a sample are provided by a pinhole that restricts the signals come out from out-focus zones. Confocal Raman microscopy is the best done by dispersive Raman spectroscopy with short wavelengths. Its laser light from the probe-head is focused onto diffraction limited spot in the sample by the microscope objective. The Raman scattered light is collected with the same objective through which the excitation is fulfill. The backscattered Raman signal was refocused onto a small confocal aperture that acts as a spatial filter, passing the Raman signal excited at the beam waist, but can be eliminating Raman produced at other points above and below the beam waist. Regularly, the backscattering geometry is employed in Raman microscopy, making it possible to

measure the Raman spectrum from the sample surface without sample preparation. The filtered Raman signal returned to the spectrometer where it was dispersed onto a charge coupled device (CCD) camera to produce a spectrum (Figure 15). Although the Raman scattering is a very weak incident so the improvement in instrumentation have been essential to make confocal Raman microscopy a well-established method of chemical analysis in the field of molecular spectroscopy (Vankeirsbilck 2002; Vyorykka 2004).

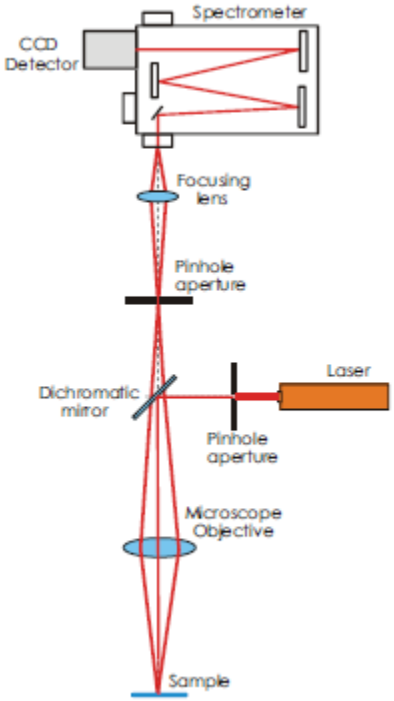

Figure 15 The scheme of confocal spectroscopy (http://content.piacton.com/Uploads/Princeton/Documents/Library/UpdatedLibrary/Confocal_raman_microscopy_note.pdf).

Another technique is surface-enhanced Raman spectroscopy (SERS). The Raman scattered from a compound or ion adsorbed on a structured metal surface can be $10^3 - 10^6$ times greater than in solution. The surface-enhanced Raman scattering is the strongest on silver, but can be observed on gold and copper as well. The surface-enhanced Raman

spectroscopy arises from two mechanisms. The first is an enhanced electromagnetic field produced at the surface of the metal. Second is enhanced formation of a charge-transfer complex between the surface and the analyze molecule. The molecules with lone-pair electrons showed the strongest surface-enhanced Raman scattered (Vankeirsbilck 2002).

MAPPING AND IMAGING

In confocal Raman microscopy, a light source, which usually a laser, is focused onto the sample and the image of this spot is detected through a small pinhole in front of the detector. The pinhole, which is confocal with the illuminating spot, is located in the image plane of the microscope. Besides the Raman microscope is incorporated a programmable, xyz-movement stage so it is a possible to generate a chemical image of a two-dimensional area of a sample (Figure 16(a)). Since the use of a mapping stage, the sample such as a tablet can be moved in the x- and y- directions, obtained spectra at each step. If the sample required defocus at different locations, the z-direction can be automated as well. The distance, which the stage moves in the x- and y- directions, is called the step size and usually can be analyzed uninterruptedly, but the spectra are not related to each other spatially. The line map (Figure 16(b)) defines a series of spectra to be obtained along one dimension. In the line maps, chemical changed that occured along this dimension were investigated. An example of an line map sample is a cross-sectioned pharmaceutical pellet that has several different layers disclosed. One of the more practical reasons that line map are so popular is that they can provide detailed information concerning the chemacal changes that occur across a sample without the need to collect as many spectra as is required for area maps. The final, area map type (Figure 16(c)) defines a series of spectra to be collected in two dimensions such as over an whole region. The mapping can be arranged in two ways; by scanning the light beam along the sample with a system of oscillating mirrors or by moving the sample itself using an X-Y or X-Y-Z scanning stages. This type of map provides a Raman image that can be directly compared with the visual image, often allowing nonvisible to the eye features to be identified. A

common area map sample is a tablet. The tablet can be mapped and the various ingredients can be monitored for content uniformity. If a map is being performed to search for a particular component, the step size need only be in the order of the particle size of that substance. A good approach would be to first obtain a larger area map on the sample with larger step sizes and short sampling times per point. Once an area of interest is defined by analyzing the data from the first map, a smaller, higher resolution map can then be defined. As above, the image of the sample can be obtained by either scanning the sample or the excitation spot point by point or line map. This make the confocal microscope more complex than the conventional microscope (Bugay 2006; Hollricher 2011).

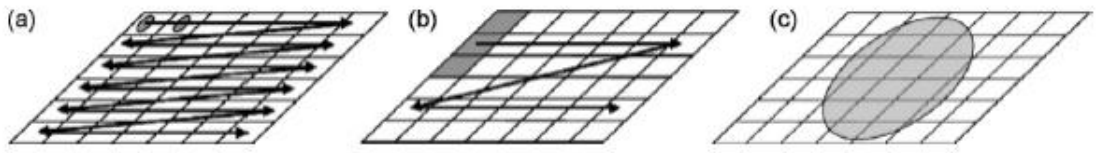

Figure 16 Three methods of Raman imaging data: (a) point mapping, (b) line mapping and (c) area mapping (Gendrin 2008).

The confocal Raman microscopy has been widely applied in several fields, imaging microscopy is one of the most extended applications. Because of it furnishes 3D spatial resolution. There are several imaging methods such as point by point or line map. The line mapping or area mapping experiments have been performed, profiles are created that enable certain spectral features to be monitored spatially on the sample. The data sets generated by mapping can consist of hundreds or even thousands of spectra and view all of these spectra concurrent are impractical. Profiles can be reduce the data set into a more easily viewed format or image. A profile is a representation of map data in which a measurement of spectral intensity or some other characteristic is shown for each sample point. A profile will ascertain the presence, location and extent of the defined spectroscopic feature in the sample. There are many types of profiles. Some profiles such

as chemigram or component profiles compare an entire reference spectrum to every spectrum in the map, with the resulting image show spectral similarity across the mapping region. Other images can be created based on profiling a specific peak area, peak height, peak area ratio or peak height ratio. Profiles can also be performed based on a group of peaks specific for certain functional groups such as alkanes or even on a quantitative method (Baena 2004; Bugay 2006).

Chemical imaging analysis were probed intrinsic properties of a molecule or atom, often in a non-destructive method. Spatially resolved the chemical heterogeneity information with high resolution and molecular specificity and transported prosperity of new information. Furthermore, the image can be often reveal more information than any table result. A color-coded distribution map of a system is very uncomplicate to illustrate the complexity of the system. The Raman chemical imagimg combines Raman spectroscopy with digital imaging technology to imagine chemical composition and molecular structure at the same time. In an imaging mode can be collecting data reduces the effect of interfereces in the field of view because of each pixel in an image contains chemical data specific to the species in that pixel, which corresponds to a limit sampling volume. Raman imaging techniques may be broadly classified as either spontaneous or nonlinear. The Raman imaging may produced more hundreds or thousands of independent spectra. The mean spectrum shows a bulk spectral measurement and has the ability to envelop signals from all interfernces, including a fluorescence background, in the field of view. The analytical value of Raman imaging is achieved when discrete spectroscopic information can be obtained from a unique spatial location within a sample (Lin 2006; Haefele 2011; Stewart 2012). However, the Raman mapping data was reported that it was analyzed by:

- Integrated the characteristic Raman band (Taylor 2000)
- Rationing the characteristic Raman band intensities (Kontoyannis 1995; Breitenbach 1999)
- Observed the full-width at half maximum of certain Raman bands in order to distinguish crystalline and amorphous regions (Furuyama 2008)

CONFOCAL RAMAN MICROSCOPY IN PHARMACEUTICAL

As Raman spectroscopy can be capable of rapid, non-destructive method and non-invasive (Vankeirsbilck 2002). Raman microscopic imaging is the one analytical technique for measuring active pharmaceutical ingredients heterogeneity in tablet cores, controlled release systems, and orally inhaled and nasal drug products. Its suitability as a process analytical tool for the pharmaceutical industry, for both process monitoring and quality control in the many stages of the pharmaceutical manufacture (Gowen 2008; Stewart 2012). The tablets are ideal to be investigated by confocal Raman microscopy. The active ingredients and excipients often exhibit major spectra differences. The concentrations of the active pharmaceutical ingredients below 1% weight by weight can be detectable (Sasic 2007). So it is an extremely powerful tool. Moreover, the confocal Raman microscopy system permits large area mapping, even whole tablets which size up to centimeters can be characterized content uniformity. The ability of confocal Raman microscopy is not only to investigate content uniformity but also to confirm the solid state of the active ingredient. (Haefele 2011). Bugay concluded the analytical using Raman spectroscopy in pharmaceutical (Bugay 2006);

1. Qualitative analysis
- Identification of pharmaceutical compounds
- Polymorphic screenings
- Characterization of solvatomorphic systems
2. Quantitative analysis
- Quantitative determination of active pharmaceutical ingredients in different formulations
- Supporting chemical development process scale-up

QUALITATIVE ANALYSIS OF RAMAN SPECTROSCOPY

1. Identification of pharmaceutical compounds

Taylor observed the active ingredients in intact dosage forms. Mostly the active ingredients have aromatic groups and contain functional groups not found in excipients for example carbonyl vibration thus the spectral regions such as aromatic C-C and C-H stretching initiated. Figure 17 showed the Raman spectrum of ibuprofen and two common excipients were alpha-lactose monohydrate and microcrystalline cellulose. Both the aromatic C-C and the carbonyl group of the acid function rise to peaks break down from any excipient peaks (Taylor 2000).

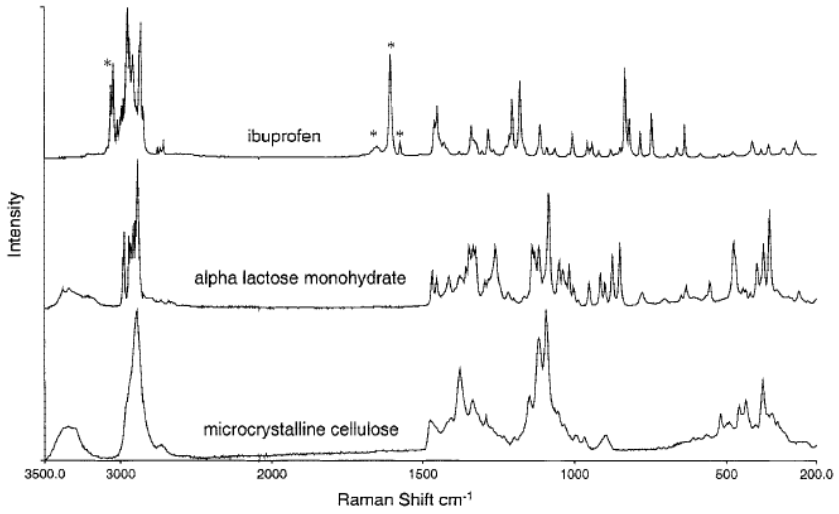

Figure 17 Compared of ibuprofen spectrum and two commonly excipients (Taylor 2000).

2. Polymorphic screenings

Raman spectroscopy has been utilized for the characterization as above. It can be use characterization of substances in low dose for example in Figure 18 showed the Raman spectrum of the prednisolone tablet compared with the spectrum of two prednisolone polymorphs. The tablet spectrum below 1500 cm^{-1} is dominated by

excipients peaks. The peak between 1550 and 1750 cm^{-1} are prednisolone peaks. In these result, Raman spectroscopy can be used to determine the content of polymorph even though a low dose the active ingredient.

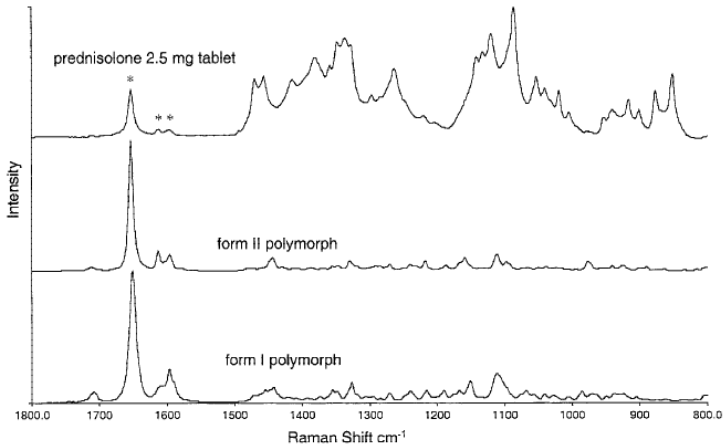

Figure 18 Raman spectra of low dose prednisolone tablet and polymorphs Form I and II (Taylor 2000).

3. Characterization of solvatomorphic systems

The characterization of solvates and hydrates by Raman spectroscopy also requires that the differing crystal structures of the crystal forms cause a perturbation of the pattern of molecular vibrations. Figure 19 showed Naproxen sodium which has been exhibited to crystallize in an anhydrate, a monohydrate, and a dehydrate crystal form. These two solvatomorphs were present very similar Raman spectra. However, the two similar forms can still be distinguished on the basis of a few characteristic Raman peaks (Bugay 2006).

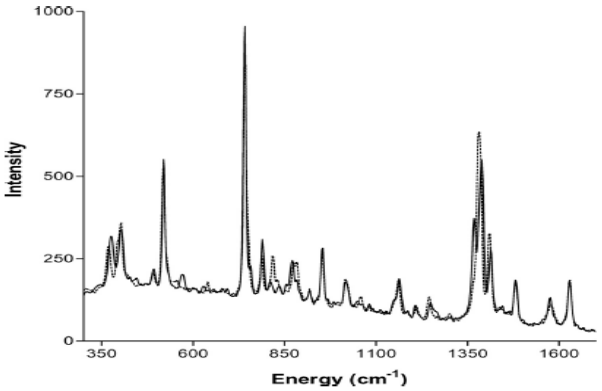

Figure 19 The fingerprint region of Raman spectra for the anhydrate form of Naproxen sodium; solid trace and monohydrate phase; dashed trace (Bugay 2006).

QUANTITATIVE ANALYSIS OF RAMAN SPECTROSCOPY

Raman spectroscopy has been utilized widely for quantitative analysis. The quantitative analysis used the linear relationship existed between scattering intensity and concentration in Raman spectra. It can be exposed as (Bugay 2006):

$$I_R = (I_L \sigma \mathrm{K}) PC$$

Where I_R is the measured Raman intensity (units of photons/sec)

I_L is the laser intensity (units of photons/sec)

σ is the absolute Raman cross-section (units of cm^2/molecule)

K is a constant composed of measurement parameters such as utilizing the same spectrometer (collection optics efficiency), sample positioning and the over efficiency of the Raman spectrometer

P is the sample path length (units of cm)

and C is the concentration (units of molecules/cm^3)

Due to the calibration is based, the Raman sampling devices are not subject to attack by moisture, and small amounts of water in a sample do not interfere so it was used

widely for quantitative analysis. However, on the relative intensities of characteristic bands of the components depend upon various parameters such as the excitation intensity, alignment of the experimental set up, the sample orientation and temperature. The band shifts can be occurred caused of the interaction of molecules (Szep 2003).

It is known that the changes in polymorphic behavior may have affect to the pharmaceutical stability, suspendibility and bioavailability. So it is important to characterize the polymorphic transition and the spatial distribution in solid pharmaceuticals (Lin 2006). As above, the quantitative analysis of active pharmaceutical ingredients in different formulations using Raman spectroscopy in pharmaceutical that is;

The dipyrone tablets which from different laboratories was studied by Fourier transform (FT)-Raman spectroscopy. The figure 20 showed the FT-Raman spectra of six commercial tablets of dipyrone. This quantitative analysis was not used to mean of partial least-squares (PLS) because all the correlation coefficients (R) between FT-Raman band area or height and concentration are more than 0.99. The results of analysis using band area or height agree with the contents of dipyrone tablets which showed in Figure 20 (Izolani 2003).

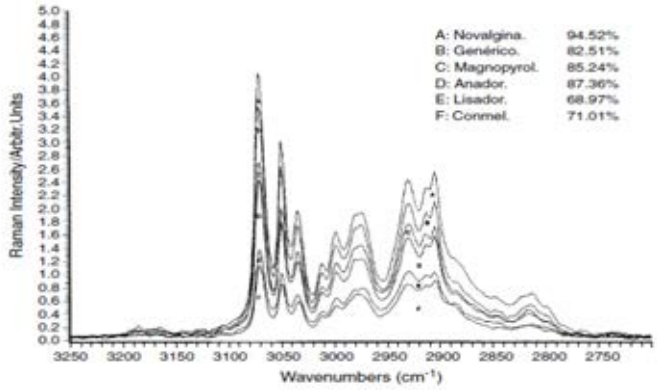

Figure 20 The FT-Raman spectra of six commercial tablets of dipyrone (Izolani 2003).

Moreover, the quantitative analysis by Raman spectroscopy can be used ratio of relative peak intensities such as the quantitative percentage of glycine and calcium carbonate in antacid tablets by Raman spectroscopy with the argon laser. The plot of intensity ratio of the peak calcium carbonate to peak glycine against the reciprocal of the molar fraction of glycine. The quantities of two active ingredients in the antacid tablets were successful and easily determined (Kontoyannis 1995).

Furthermore, the mixtures of three solid forms of Ranitidine hydrochloride prepared by three mixing methods and was develop to reliable quantified by PXRD and Raman spectroscopy combined with multivariate analysis. The principal component analysis (PCA) was studied the effect of mixing method, while partial least squares (PLS) regression was built the quantification models. PXRD and Raman spectroscopy which combination with PLS regression were used to quantify the amount of single components in ternary mixtures of ranitidine hydrochloride solid forms. The result showed that the Raman spectroscopy gave better PLS regression models than PXRD. Due to the packing sample of powder X-ray diffraction was more sensitive when the sample of Raman spectroscopy was homogeneity (Chieng 2009).

Q-Raman can be used to measure in aqueous systems and overcame the poor peak resolution of mixtures by using peak ratio, peak area or peak height and/or multivariate methods. Raman spectroscopy has been used widely in dosage form such as tablets, capsules, microspheres and suspension. Moreover, it used to quantify structural changes in proteins and monitor processes for example wet granulation or batch crystallization (Strachan 2007).

CHAPTER III

MATERIALS AND METHODS

Materials

Chlorpropamide polymorph Form A (Lot CP 1008) was obtained from Kothari Phytochemicals International, India.

Instruments

1. Differential scanning calorimeter (D244e, Mettler Toledo, Switzerland)
2. Powder X-ray diffractometer (MiniFlex II Desktop X-Ray Diffractometer, Rigaku, Japan)
3. Confocal microscopic Raman spectrometer (DXR Raman Microscope Spectrometer, Thermo Fisher Scientific Inc., USA)
4. Hydraulic Press (Carver®Press, USA)
5. Analytical balance (XP205, Mettler Toledo, Switzerland)
6. Hot air oven (Model UL 80, Memmert, Schwabach, Germany)
7. Ball mill (Dimension grinding chamber 5 inches, Ball size 1 centimeters and weight 200 grams)
8. Image analysis software (ImagePro® Plus, Media Cybernetics, Inc., USA)

Experimental methods

1. Identification of chlorpropamide polymorphs

Chlorpropamide polymorph Form C was self-prepared by grinding commercial Form A using ball mill for 0.5 hour and heated at 90^{O}C for additional 6 hours.

Amorphous form was prepared using differential scanning calorimetry (DSC) under constant purge (60 mL/min) of nitrogen gas. Chlorpropamide powder Form A approximately 3-5 mg were weighed and sealed in 40µL aluminium DSC pans and heated from 25-250 ^{O}C at the rate of 10^{O}C/ min and then reduced temperature quickly until -40 ^{O}C at the rate of 20^{O}C/ min. The sample was analyzed by PXRD for identify.

Chlorpropamide polymorph Form A and Form C were identified by Differential scanning calorimetry (DSC), powder X-ray Diffractometry (PXRD) and Confocal microscopic Raman spectrometry (Raman).

1.1. Differential scanning calorimetry (DSC) was operated under constant purge (60 mL/min) of nitrogen gas. Calibration was done using Indium as reference standard. Chlorpropamide polymorphs of approximately 1-3 mg were weighed and sealed in 40µL aluminium DSC pans and heated from 25-250 ^{O}C at the rate of 10^{O}C/ min.

1.2. powder X-ray Diffractometry (PXRD) studies used MiniFlex II (Rigaku, Japan) equipped with CuKα anode (λ = 1.5406 Å), 15.0 mA and 30.0 kV. Diffraction data were collected at $1^{O}2\theta$/min using an angular step size of 0.01^{O} 2θ. The scanning range was from 5 $^{O}2\theta$ - 30 $^{O}2\theta$. Fine powder were measured in continuous scan mode using quartz sample holder with 0.5 mm thickness. Analyses of the diffractograms were done by generating intensity integration of the selected peak by Peak Search® software.

1.3. Confocal microscopic Raman spectrometry (Raman) used dioade laser source of 532 nm at 10 mW in mode laser power at 100% and an Olympus TH4-200 microscope. Each Raman spectrum was collected with 10x objective using an acquisition

time of 2 seconds and accumulating four measurements at a time. The system was controlled by OMNIC® 8.0 software.

2. Calibration curve development for quantitation by PXRD (Q-PXRD)

Pure chlorpropamide polymorphs, Form A and Form C, were passed through sieve number 100 to disperse any aggregates to fine particles and classified into similar size. Prepare different polymorph mixtures with the ratios of Form A: Form C at 100:0, 90:10, 70:30, 50:50, 30:70, 10:90 and 0:100. Each ratio was quantitatively analyzed by PXRD in triplicates to construct standard curves of the two polymorphs.

Powder X-ray diffraction peaks at position 6.6^{O} 2θ and 15.0^{O} 2θ were chosen for quantitative analysis of chlorpropamide Form A and Form C, respectively, similar to previous reports (Ueda 1984; Otsuka 1989; Otsuka 1993). The standard curves to determine the quantitative amounts of chlorpropamide polymorphic of Form A and Form C analyze of the diffractograms by generating intensity integration of the selected peak by Peak Search® software using intensity ratio and estimated by the following linear equations.

3. Quantitative powder X-ray diffraction analysis

PXRD was selected to quantitatively analyze the relative amounts in percentage of each polymorph after tabletting. All Q-PXRD experiments used the same condition as in experiment 1.2. Tablets were prepared by varying conditions during tabletting process as follows.

3.1. Effect of heating duration

Chlorpropamide powder Form A was divided into two parts. The first part was ground by ball mill for 30 minutes prior to future treatment and the second half was not. Heat both halves of chlorpropamide powders in hot air oven at 90^{O}C for 1, 2, 3, 4, 5,

and 6 hours. Sampling the powder after each heating duration and evaluate by Q-PXRD. Every sample was evaluated in triplicates. Analyses of the diffractograms were done by generating intensity integration of the selected peak by Peak Search® software.

3.2. Effect of time

3.2.1. Effect of compression dwell time with constant compaction pressure on non-heated samples

Chlorpropamide powder Form A 350 mg were compressed by Carver® hydraulic press at dwell time of 0, 15, 30 and 60 minutes with constant force of 3000 psi using punch size of 3/8 inches and various punch-face designs, i.e. concave, concave with incision, flat-face and flat-face with incision. Sampling three tablets from each batch produced by each compression dwell time and evaluate by Q-PXRD. Analyses of the diffractograms were done by generating intensity integration of the selected peak by Peak Search® software.

Note: code for various punch-face designs for experiment 3.2.1.

Concave	Concave with incision	Flat-face	Flat-face with incision
CC	CI	FF	FI

3.2.2. Effect of compression dwell time with constant compaction pressure on heated samples

Heat chlorpropamide powder Form A in hot air oven at 90^{O}C for 6 hours. Compress 350 mg of powder using Carver® hydraulic press at varying dwell time of 0, 15, 30 and 60 minutes and with constant force of 3000 psi using punch size of 3/8 inches and various punch-face designs, i.e. concave, concave with incision, flat-face and flat-face with incision. Sampling three tablets from each batch produced by each

compression dwell time and evaluated by Q-PXRD. Analyses of the diffractograms were done by generating intensity integration of the selected peak by Peak Search® software.

Note: code for various punch-face designs for experiment 3.2.2.

Concave	Concave with incision	Flat-face	Flat-face with incision
HCC	HCI	HFF	HFI

3.3. Effect of compaction pressure with constant dwell time of non-heated samples

Chlorpropamide powder Form A 350 mg were compressed by Carver® hydraulic press at various compaction pressures of 1000, 2000, 3000, 4000 and 5000 psi and at a constant dwell time of 15 minutes with punch size of 3/8 inches and various punch-face designs, i.e. concave, concave with incision, flat-face and flat-face with incision. Sampling three tablets from each batch produced with each compaction force and evaluate by Q-PXRD. Analyses of the diffractograms were done by generating intensity integration of the selected peak by Peak Search® software.

Note: code for various punch-face designs for experiment 3.3.

Concave	Concave with incision	Flat-face	Flat-face with incision
PCC	PCI	PFF	PFI

3.4. Effect of compaction pressure with constant dwell time on heated samples

Heat chlorpropamide powder Form A in hot air oven at 90^{O}C for 6 hours. Compress 350 mg of heated by Carver® hydraulic press at various compaction pressures of 1000, 2000, 3000, 4000 and 5000 psi and at a constant dwell time of 15 minutes with punch size of 3/8 inches and various punch-face designs, i.e. concave, concave with

incision, flat-face and flat-face with incision. Sampling three tablets from each batch produced by each compaction force and evaluate by Q-PXRD. Analyses of the diffractograms were done by generating intensity integration of the selected peak by Peak Search® software.

Note: code for various punch-face designs for experiment 3.4.

Concave	Concave with incision	Flat-face	Flat-face with incision
HPCC	HPCI	HPFF	HPFI

3. Quantitative Raman spectroscopy analysis

The powder of confocal microscopic Raman spectroscopy is able to create Raman mapping in identifying polymorphic transformation on the surface of tablets without disupting the tablet structure. All Confocal microscopic Raman spectroscopy studies used the same samples prepared similar to experiment 3 for Q-PXRD experiments except the last topic in 3.4, where compaction pressures of 1000, 3000 and 5000 psi were used instead. The tablets which contact the upper punch were chosen for Raman spectroscopic analysis. The Raman spectra were collected using a DXR Raman microscope spectrometer, Thermo Fisher Scientific Inc., USA. Each accumulation of approximately 120 Raman spectra at estimated resolution 2.7 - 4.2 cm^{-1}. The Raman spectra were recorded at room temperature within the range of 50-3600 cm^{-1}, exposure time of 2 seconds and accumulating four measurements for each spectrum. Data for Raman maps were collected over 10000 μm (X-axis) x 10000 μm (Y-axis) area using step size of 1000 μm (X-axis) x 1000 μm (Y-axis). The system was operated under OMNIC® 8.0 software and analyzed the colored maps quantitatively by Image analysis software (ImagePro® Plus).

Chapter IV

RESULTS AND DISCUSSION

1. Identification of chlorpropamide polymorphs

Chlorpropamide polymorph Form A (Lot CP 1008) obtained from Kothari Phytochemicals International and self-prepared Form C were identified by three different techniques and the results are as follow

1.1. Differential scanning calorimetry

Differential scanning calorimetry (DSC) thermograms of Form A and Form C are shown in Figure 21. Form A and Form C exhibit endothermic melting events at the onsets of 125.65 ^{O}C and 127.90 ^{O}C, respectively.

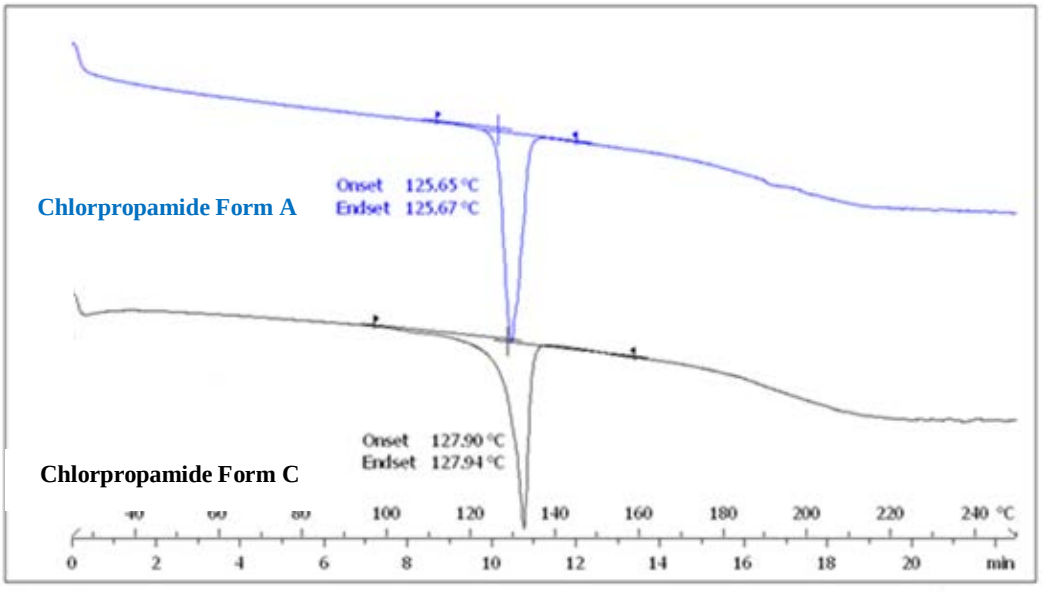

Figure 21 DSC thermograms of chlorpropamide Form A and Form C.

1.2. Powder X-ray diffractometry

Figure 22 shows powder X-ray diffraction profiles of the amorphous form, Form A and Form C of chlorpropamide powder used in this study. The distinct powder X-ray diffraction peak of chlorpropamide Form A are observed clearly at 6.6^{O} 2θ and of Form C at 15.0^{O} 2θ similar to many previous studies (Ueda 1984; Otsuka 1989; Otsuka 1993). In contrast, profile of the amorphous form shows halo pattern and do not exhibit any diffraction peaks. These results suggest that the main diffraction peaks of Form A and Form C do not overlap, so they were used in the future to quantitatively determine the content of polymorphic Form A and Form C in a mixture.

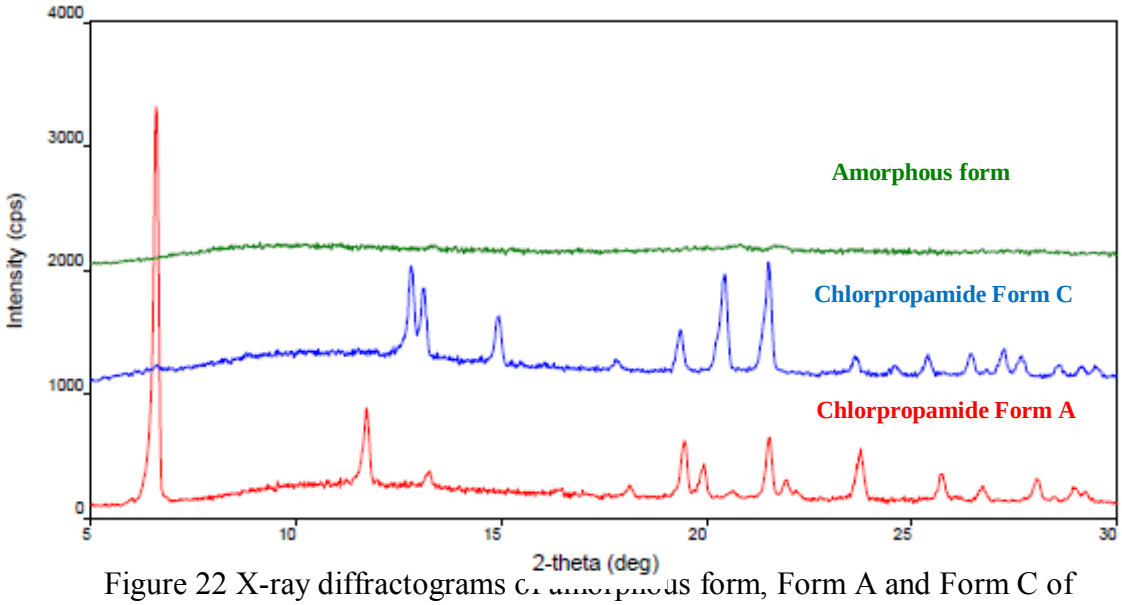

Figure 22 X-ray diffractograms of amorphous form, Form A and Form C of chlorpropamide powder.

1.3. Confocal microscopic Raman spectrometry

The Raman spectra of chlorpropamide Form A, Form C and amorphous form are shown in Figure 23. Differences in Form A compared to Form C were detected at Raman shift of 273 cm^{-1} (Figure 24) for chlorpropamide Form A. While Raman shift at 1306 cm^{-1} (Figure 25) signifies chlorpropamide Form C. Moreover, the two positions in

Raman shifts shown above do not overlap with the Raman shift of amorphous form, so they are used to quantify the content of polymorphic Form A and Form C by Raman.

Characterization results from all three techniques suggest that these samples were pure polymorphic forms. Thus, powder X-ray diffraction peak at 6.6^{O} 2θ and Raman shift at 273 cm^{-1} are selected to quantify amount of polymorphic Form A. Powder X-ray diffraction peak at 15.0^{O} 2θ and Raman shift at 1306 cm^{-1} are utilized for quantitative evaluation of polymorphic Form C.

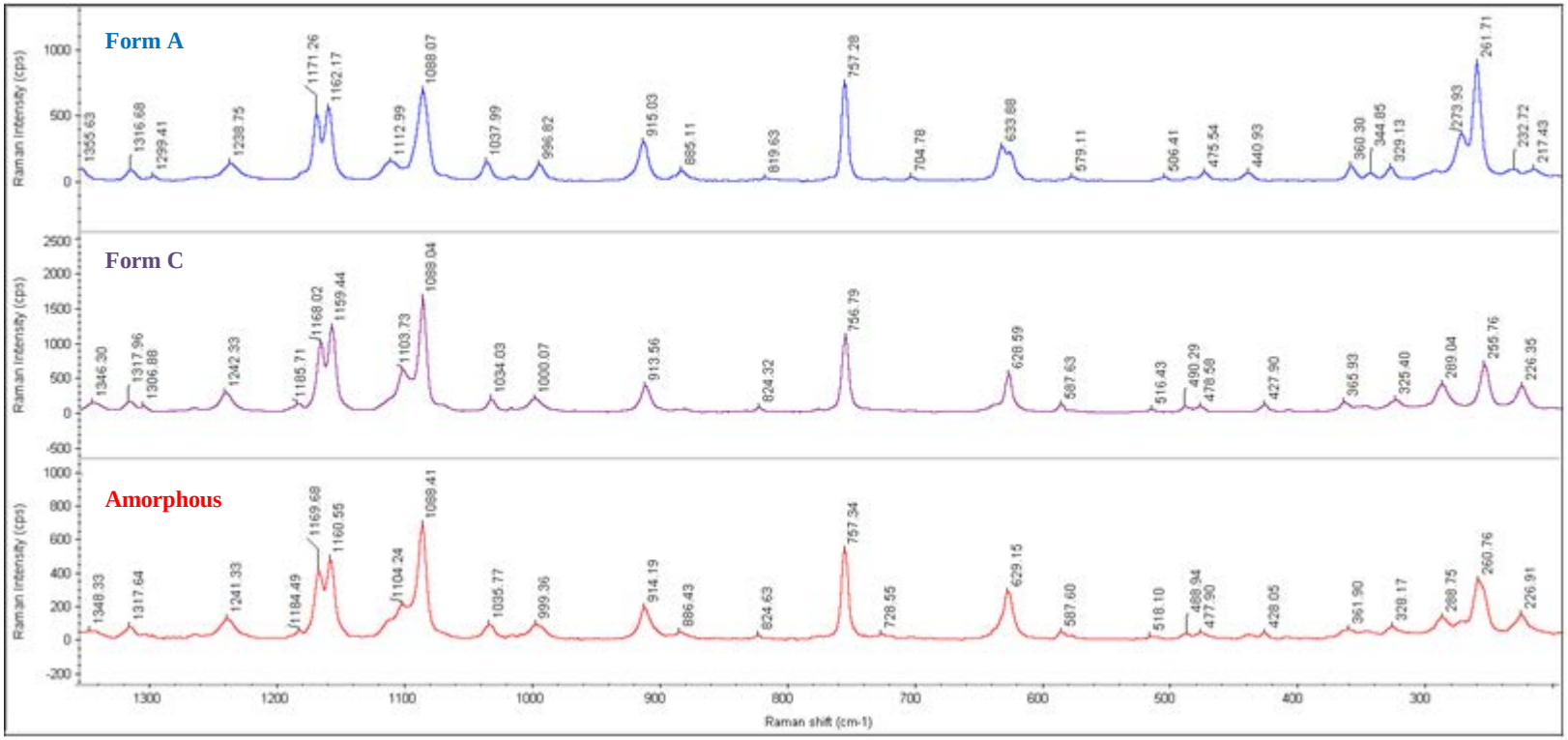

Figure 23 Raman spectra between 1350-220 cm^{-1} of chlorpropamide Form A, Form C and amorphous form.

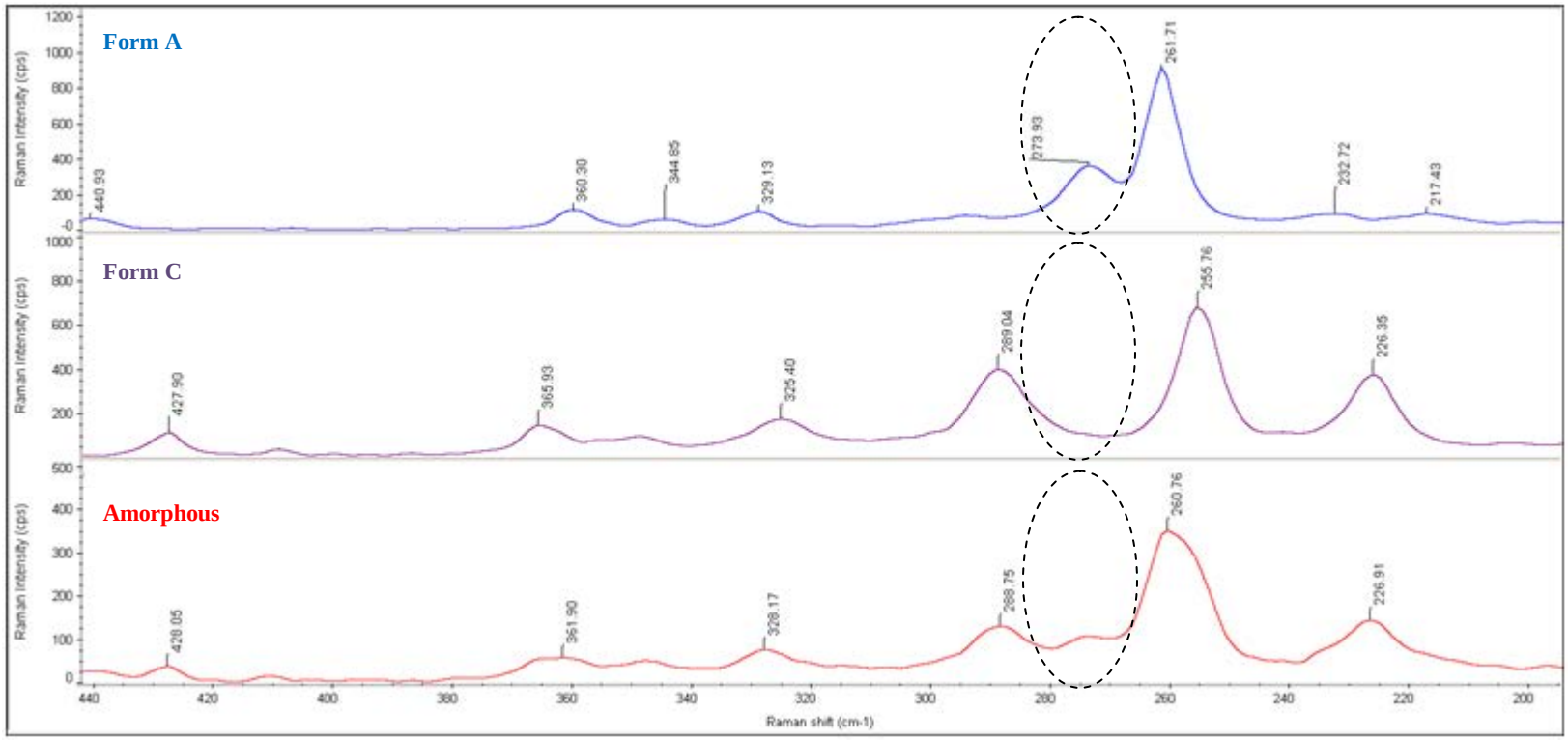

Figure 24 Raman spectra between 200-440 cm^{-1} of chlorpropamide Form A, Form C and amorphous form where reference of Form A appears at Raman shift 273 cm^{-1}.

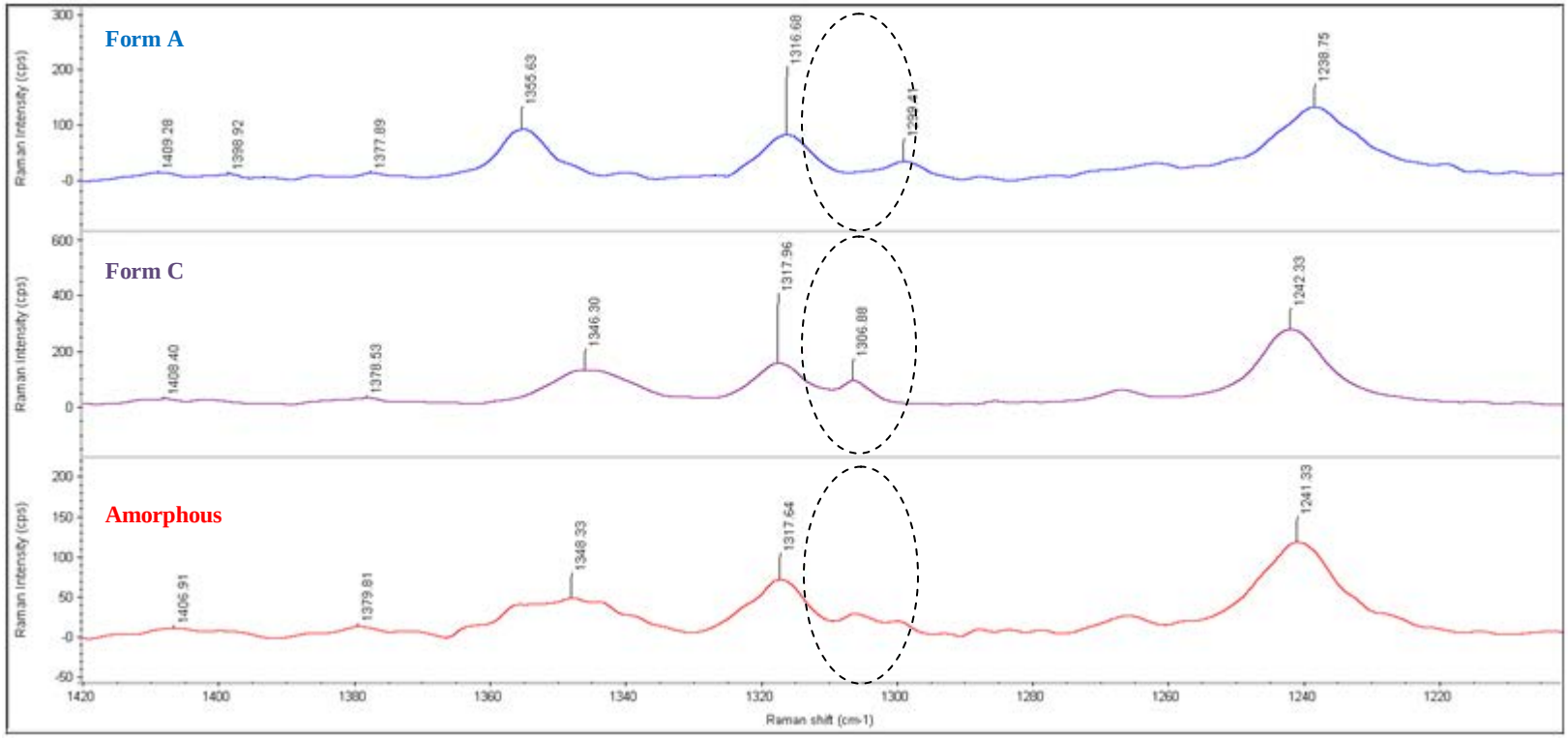

Figure 25 The Raman spectra between 1220-1420 cm^{-1} of chlorpropamide Form A, Form C and amorphous form where reference of Form C appears at Raman shift 1306 cm^{-1}.

2. Calibration curves development for quantitative analysis

Powder X-ray diffraction profile can be affected by various factors such as types of sample holders, particle sizes of samples, powder packing and preferred orientation effects. So all standard powder mixtures prepared was sieved and mixed throughly to ensure homogeneity.

Powder X-ray diffraction peaks at positions 6.6^{O} 2θ and 15.0^{O} 2θ were chosen for quantitative analysis of chlorpropamide Form A and Form C, respectively. The selections of these two positions were based on the resolution and lack of mutual interference between forms.

The standard curves to determine the quantitative amounts of chlorpropamide polymorphic of Form A and Form C are shown to be correlated in a straight line (Figure 26 and Figure 27, Table 11 in appendix A) and are estimated by the following linear equations.

$$y_A = 32.7379x_A \qquad R_A^2 = 0.9923 \qquad [1]$$

$$y_C = 5.4701x_C \qquad R_C^2 = 0.9971 \qquad [2]$$

Where y_A is the average peak intensity of Form A

y_C is the average peak intensity of Form C

x_A is the content (%) of polymorphic Form A

x_C is the content (%) of polymorphic Form C

R^2 is correlation coefficient of determination

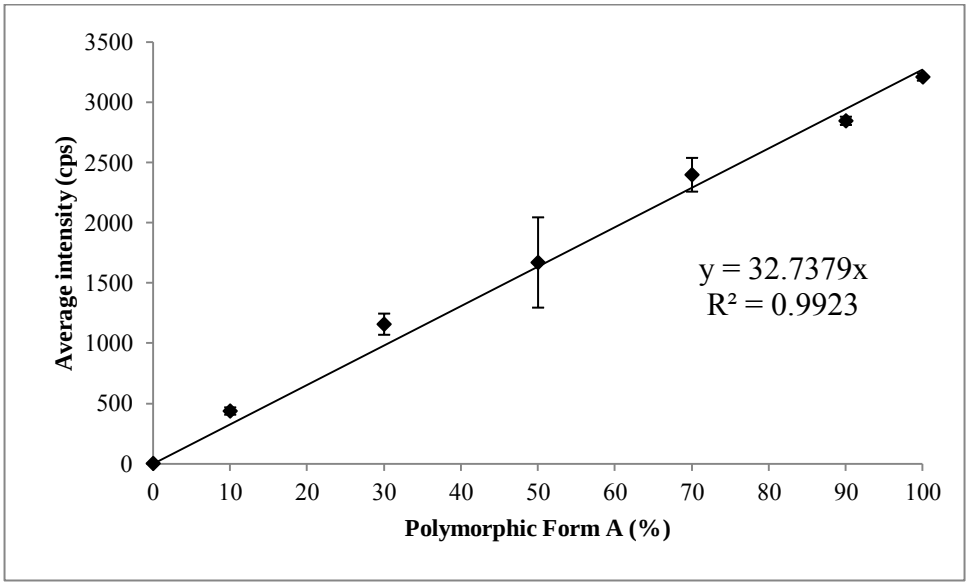

Figure 26 Standard curve for determination of quantitative amounts of chlorpropamide polymorphic Form A by PXRD.

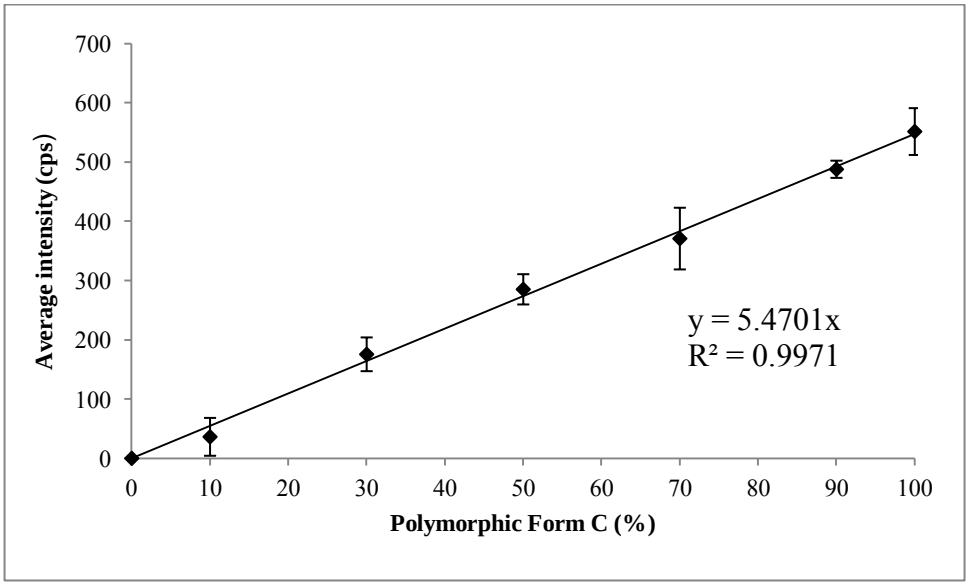

Figure 27 Standard curve for determination of quantitative amounts of chlorpropamide polymorphic Form C by PXRD.

3. Quantitative powder X-ray diffraction analysis

PXRD is selected as a tool for quantitatively analyzed the percentage of each polymorph within the whole tablet as an average. The tablets are evaluated for the different tabletting conditions during their production.

3.1.Effect of heating duration

Chlorpropamide powder Form A was divided in half. The first half was heated in hot air oven at 90^{O}C by varying heating duration of 0, 1, 2, 3, 4, 5, and 6 hours and sampling in triplicates. The results are shown below in Table 1.

Table 1 Effect of heating duration on morphology change of chlorpropamide powder as determined by Q-PXRD.

Heating duration at 90 ^{O}C (hours)	Average content of Form A (percent ± SD) (n=3)	Calculated average content of metastable amorphous form (percent)	Average content of Form C (percent ± SD) (n=3)
0	97 ± 3	3 ± 3	0
1	84 ± 11	16 ± 11	0
2	83 ± 9	17 ± 9	0
3	76 ± 11	24 ± 11	0
4	75 ± 6	25 ± 6	0
5	69 ± 5	28 ± 6	3 ± 6
6	46 ± 4	9 ± 6	45 ± 2

When heating duration of chlorpropamide powder Form A was longer, content of chlorpropamide Form A decreased instantly, however, content of chlorpropamide Form C did not increase until reaching the heated duration of 5 hours (Figure 28).

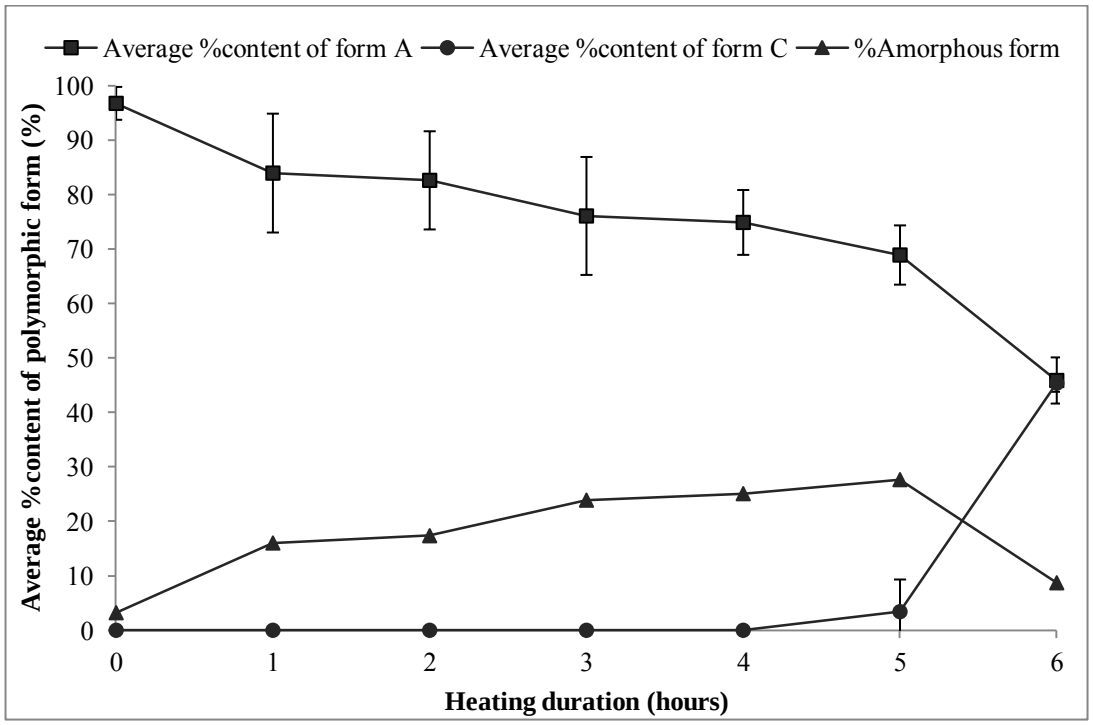

Figure 28 Contents (percent) of each polymorph and metastable amorphous form of chlorpropamide powder when heated by varying the heating duration.

The second part of powder was ground by ball mill for 30 minutes and heated in hot air oven similarly to the previous study. Results are shown in Table 2. Content of chlorpropamide Form A initially decreased to 26 ± 2 percent after ball milling and lower than the initial chlorpropamide powder Form A which was not ground. When the ground samples were heated to 2 hours, one could rarely find content of chlorpropamide Form A. But chlorpropamide Form C appeared instantly after the first hour of heating to 42 ± 2 percent (Figure 29).

Table 2 Effects of heating duration after grinding (30 min) on the morphology change chlorpropamide powder determined by Q-PXRD.

Heating duration at 90 ^{O}C (hours)	Average content of Form A (percent ± SD) (n=3)	Calculated average content of metastable-amorphous form (percent)	Average content of Form C (percent ± SD) (n=3)
0	26 ± 2	74 ± 2	0
1	17 ± 5	41 ± 3	42 ± 2
2	0	18 ± 4	82 ± 4
3	0	15 ± 4	85 ± 4
4	0	9 ±1	91 ± 1
5	0	4 ± 4	96 ± 4
6	0	3 ± 4	97 ± 4

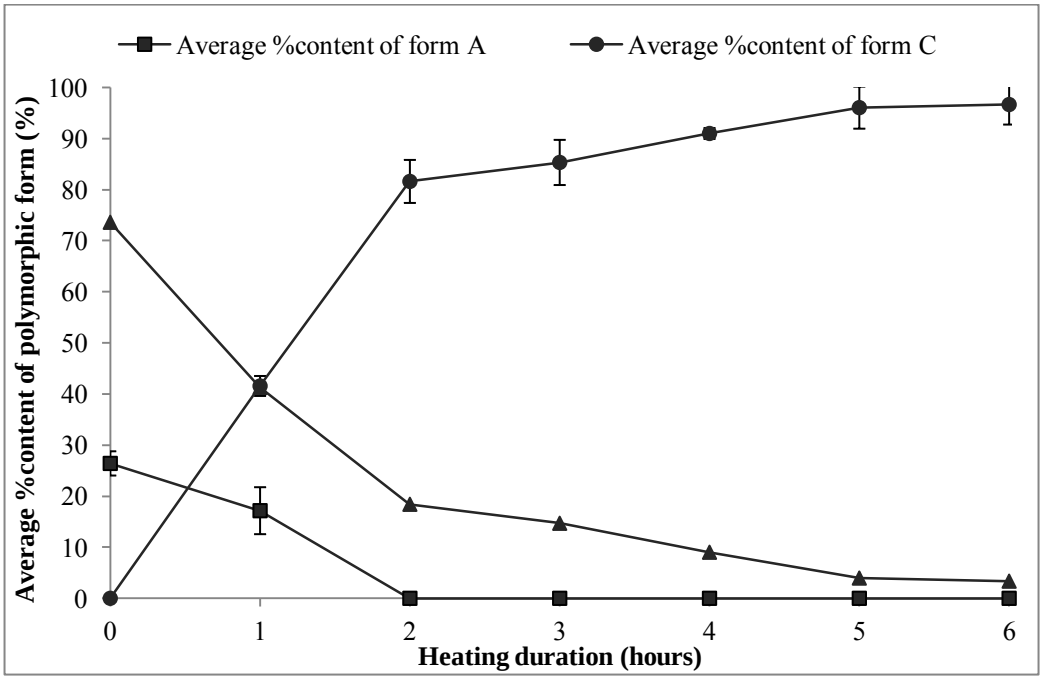

Figure 29 Contents (percent) of each polymorphs and metastable-amorphous form of ground chlorpropamide powder before heated by varying the heating duration.

Moreover, when compare diffractograms of chlorpropamide powders which were heated for 6 hours and not heated. The baseline of diffractogram of powder which was heated for 6 hours had higher amounts of metastable amorphous form than the powder that is not heated (as indicated by an arrow in Figure 30). Contents of metastable amorphous form of not heated chlorpropamide powder is 3% and the heated powder is 9% (as shown in Table 1)

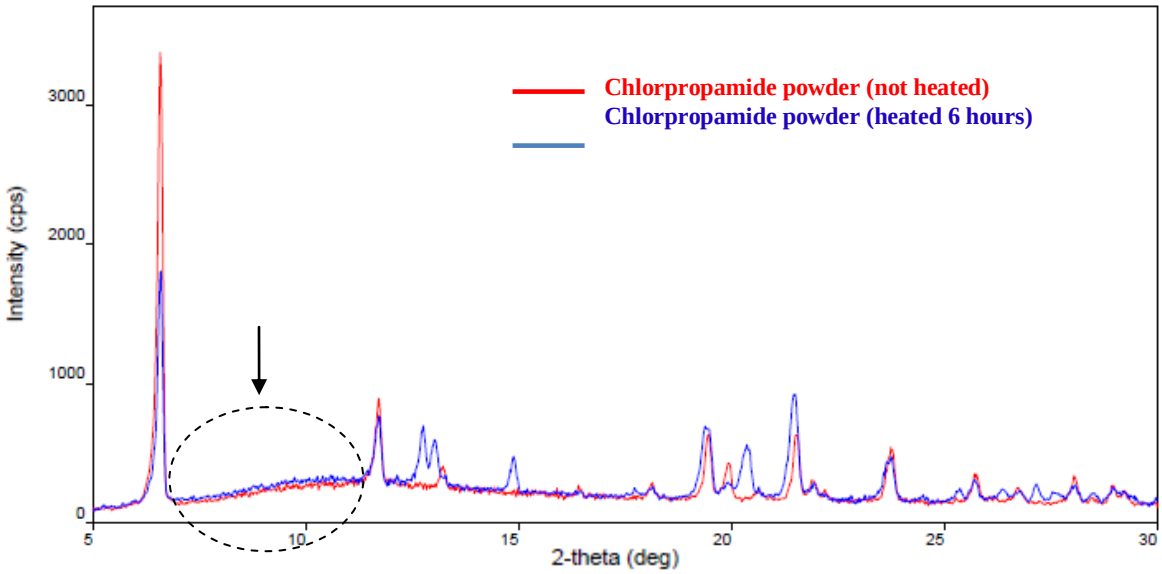

Figure 30 The powder X-ray diffractograms of chlorpropamide powders. (–) not heated and (–) heated for 6 hours

Likewise, when comparing diffractograms of chlorpropamide powders which are ground for 30 minutes and not ground (Figure 31), the diffractogram of ground powder shows clearly a high amount of metastable amorphous form than the powder which is not ground (metastable amorphous form of intact chlorpropamide powder is 3% and the ground powder is 74%) as shown in Table 2. The powders are then heated for another 6 hours. The resulted a solid powder with very high amount of polymorphic Form C while Form A disappeared since the first 2 hours of heating. It can be concluded that heating

alone is insufficient to transform Form A to Form C. However, grinding prior to heating accelerate this interconversion efficiently by helping to produce metastable amorphous form by grinding energy. It was in accordance with Brittain (Brittain 2002) that all crystalline phase transformations occurs through the formation metastable amorphous structure and could be transformed back to the initial Form A or the final product Form C.

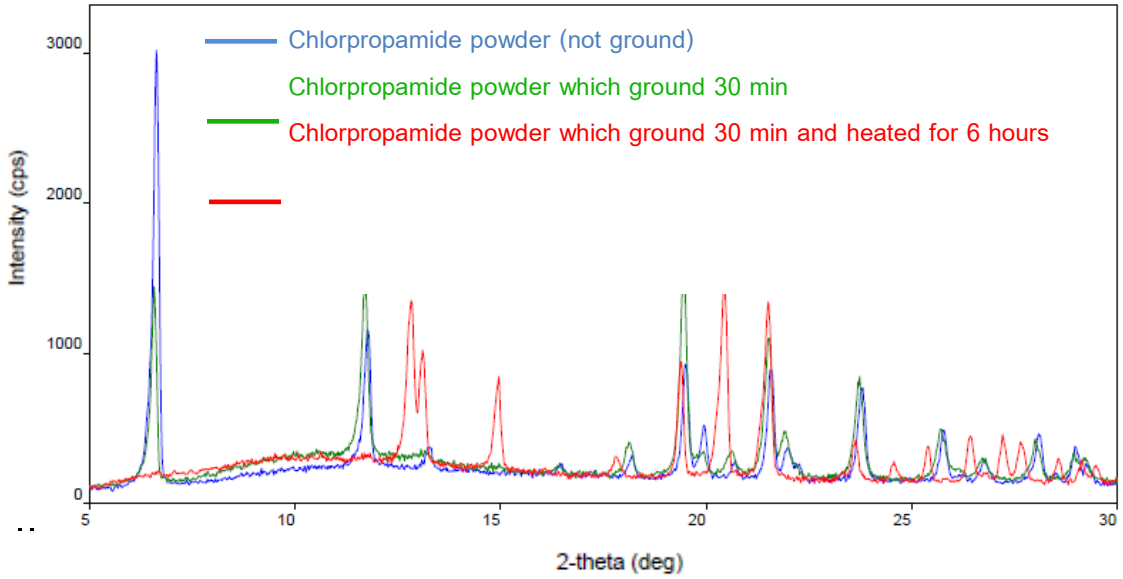

Figure 31 The X-ray powder diffractograms of chlorpropamide powder.
(–) not ground, (–) ground for 30 min and (–) ground and heated for 6 hours

3.2.Effect of time

The solid transformations occur during manufacturing process, especially during tablets compaction process (Sanchez-Castillo 2003; Koivisto 2006; Wildfong 2007; Mazel 2011). During the process, heat can be generated which cause the crystal form to undergo mechanochemical changes (Bertran 1999; Braga 2006). Dwell time of compaction may be one of the factor which determine the extent of change in the

polymorphic forms. Thus, this section intends to consider effects of compression dwell time of the various punch face designs and the heating duration on polymorphic transformation as determined by Q-PXRD.

3.2.1. Effect of compression dwell time with constant compaction pressure on non-heated samples

Chlorpropamide powder Form A was compressed by Carver® hydraulic press (with constant force of 3000 psi) at 0, 15, 30 and 60 minutes dwell time using various punch-face designs. The results of various punch-face designs are shown in Table 3. When polymorphic Form A was compacted, the content of polymorphic Form A decreased drastically and showed trace of polymorphic Form C. This is to show that the tabletting procedure can induce polymorphic transition. The energy of compression is dispersed due to rearrangement, fragmentation, bond formation, deformation of particles or crystals form. It led to changes in polymorphic form where the amorphous form is usually present as meta-stable phase before spontaneously converts to the final crystalline form (Otsuka 1989; Brittain 2002).

Table 3 Effect of compaction dwell time on the polymorphic transformation of non-heated chlorpropamide under constant compaction pressure analyzed by Q-PXRD.

Punch face designs	Dwell Time (min)	Average content of Form A (percent ± SD) (n=3)	Calculated average content of metastable amorphous form (percent)	Average content of Form C (percent ± SD) (n=3)
Control	-	97 ± 3	3 ± 3	0
CI	0	35 ± 5	60 ± 10	5 ± 5
	15	34 ± 1	64 ± 2	2 ± 3
	30	34 ± 1	58 ± 3	8 ± 4
	60	36 ± 5	60 ± 2	4 ± 3
CC	0	39 ± 2	57 ± 6	4 ± 6
	15	37 ± 2	63 ± 2	0
	30	35 ± 1	59 ± 7	6 ± 6
	60	35 ± 2	57 ± 5	8 ± 7
FI	0	29 ± 3	61 ± 3	10 ± 3
	15	30 ± 3	61 ± 4	9 ± 5
	30	31 ± 1	65 ± 5	4 ± 7
	60	31 ± 2	60 ± 5	9 ± 3
FF	0	33 ± 1	59 ± 4	8 ± 3
	15	35 ± 1	60 ± 5	5 ± 5
	30	32 ± 2	62 ± 5	6 ± 6
	60	33 ± 2	59 ± 3	8 ± 5

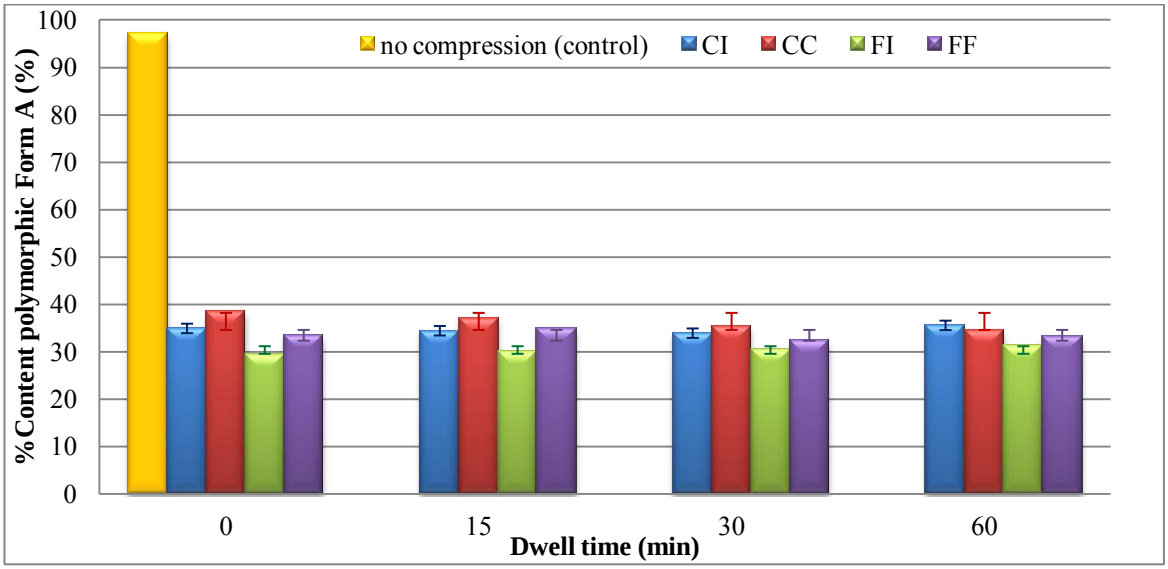

Figure 32 The relative amounts of polymorphic Form A and the compression dwell time analyzed by Q-PXRD.

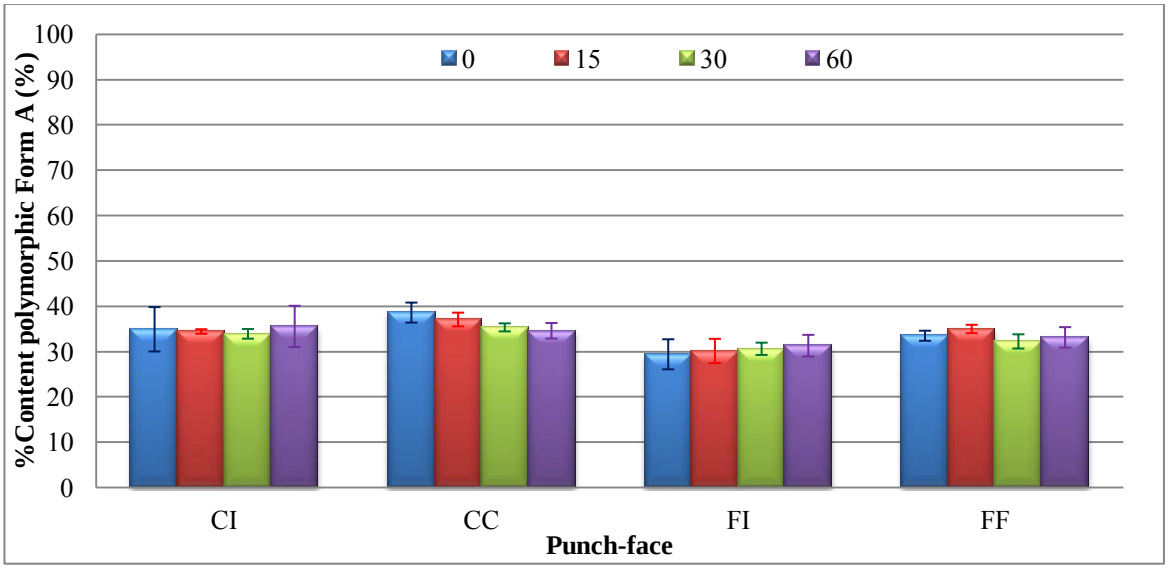

Figure 33 The relative amounts of polymorphic Form A and various punch-face designs analyzed by Q-PXRD.

Figure 32 shows dramatic decrease in the content of polymorphic Form A after compression. Amounts of resulting Form A were all within 30-40% regardless of dwell time or designs of punch-face. However, Figure 33 shows various punch-face designs affects the extent of polymorphic Form A transition. Form A transformed to metastable form and Form C more readily when Flat-face punches were used. On the other hand, compression time was shown not to be the main factors to determine the transformation rate of Form A.

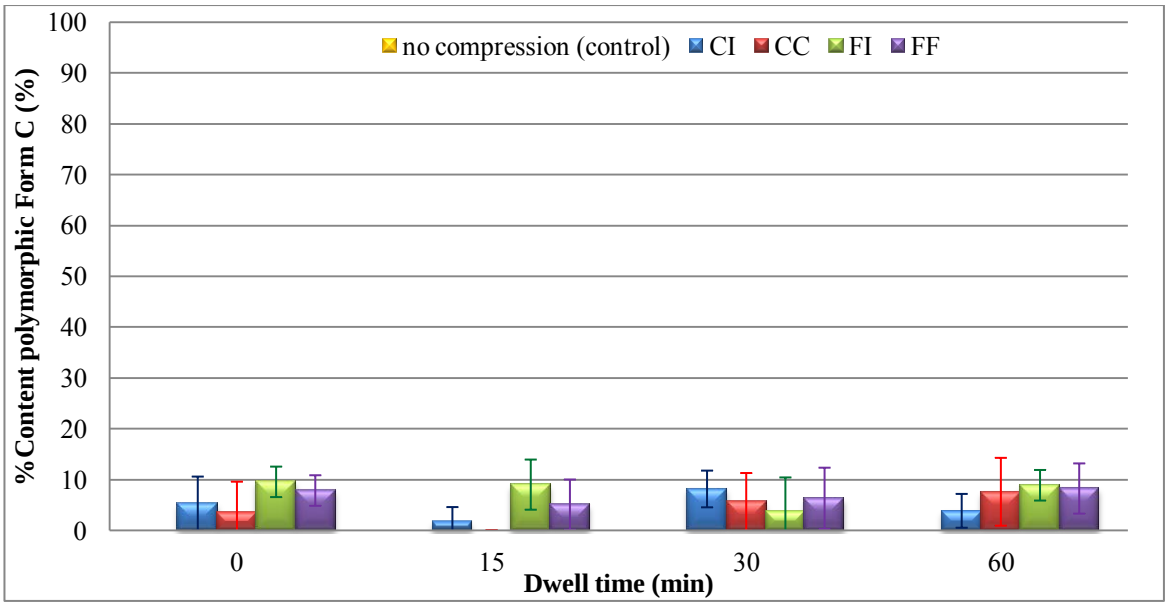

Figure 34 The relative amounts of polymorphic Form C and the compression dwell time analyzed by Q-PXRD.

Every design of punch-face can generate polymorphic Form C of less than 10 percent even at with no compression dwell time (Figure 34). Due to the starting polymorphic Form A can be transformed into polymorphic Form C by mechanical energy exerted during tabletting via the metastable amorphous intermediate. When the upper punch entered the die, particles deformed because it had transferred some energy from the upper punch to the powder. The excess energy will be used to rearrange the

molecules and bond formation, transforming mostly to the metastable amorphous form and eventually to polymorphic Form C if cumulative energy exceeds the required activation energy (Brittain 2002).

3.2.2. Effect of compression dwell time with constant compaction pressure on heated samples

Prior treatment with heat may cause the change in polymorphic form. Therefore, this section will consider the effect of compression dwell time on heated samples.

Chlorpropamide powder Form A was heated at 90ºC for 6 hours. Then, it was compressed by Carver® hydraulic press at 0, 15, 30 and 60 minutes dwell time with constant force of 3000 psi using various punch-face designs. The results are shown in Table 4. The starting heated polymorphic Form A decreased to approximately 46 percent and the polymorphic Form C increased significantly when compared to the powder that was not heat treated in 3.2.1 (Figures 32 and 34). Thus, heating the sample before compression accelerates the change of this polymorphic transformation pathway.

Table 4 Effect of compression dwell time of heated chlorpropamide powder using constant compaction pressure (3000 psi) and analyzed by Q-PXRD.

Punch face designs	Dwell Time (min)	Average content of Form A (percent ± SD) (n=3)	Calculated average content of metastable amorphous form (percent)	Average content of Form C (percent ± SD) (n=3)
Control	-	46 ± 4	9 ± 6	45 ± 2
HCI	0	10 ± 2	47 ± 7	43 ± 9
	15	15 ± 1	41 ± 1	44 ± 1
	30	13 ± 0	24 ± 3	63 ± 3
	60	12 ± 1	41 ± 1	47 ±1
HCC	0	9 ± 1	49 ± 2	42 ± 2
	15	12 ± 3	53 ± 2	35 ± 5
	30	13 ± 1	56 ± 3	31 ± 4
	60	17 ± 2	68 ± 3	15 ± 5
HFI	0	10 ± 1	50 ± 5	40 ± 5
	15	12 ± 2	59 ± 5	29 ± 6
	30	14 ± 1	65 ± 4	21 ± 5
	60	16 ± 1	68 ± 2	16 ± 2
HFF	0	10 ± 2	46 ± 3	44 ± 1
	15	11 ± 2	53 ± 3	36 ± 3
	30	15 ± 1	62 ± 2	23 ± 3
	60	15 ± 3	61 ± 7	24 ± 10

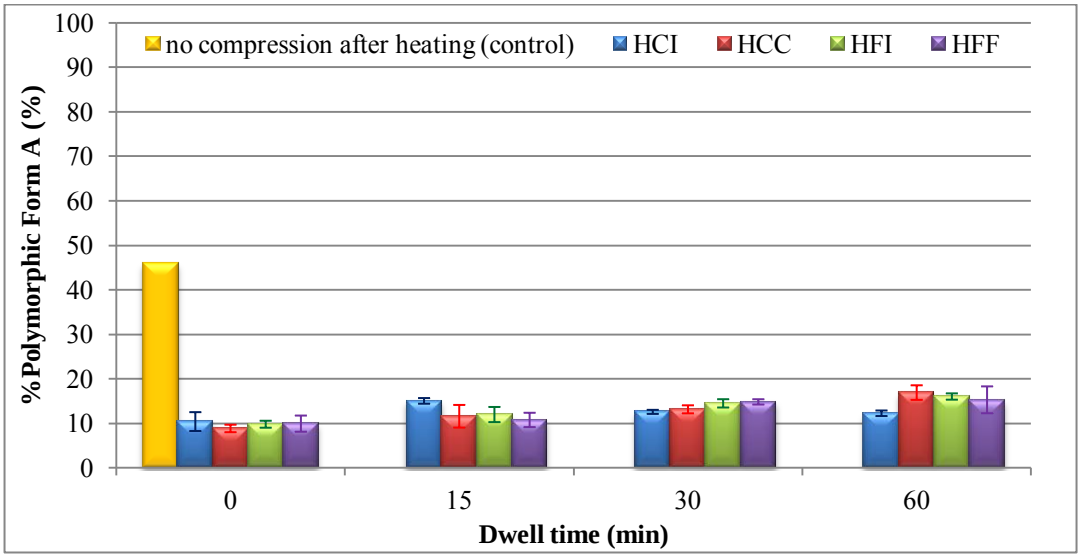

Figure 35 The relative amounts of polymorphic Form A and the compression dwell time of heated chlorpropamide powder analyzed by Q-PXRD.

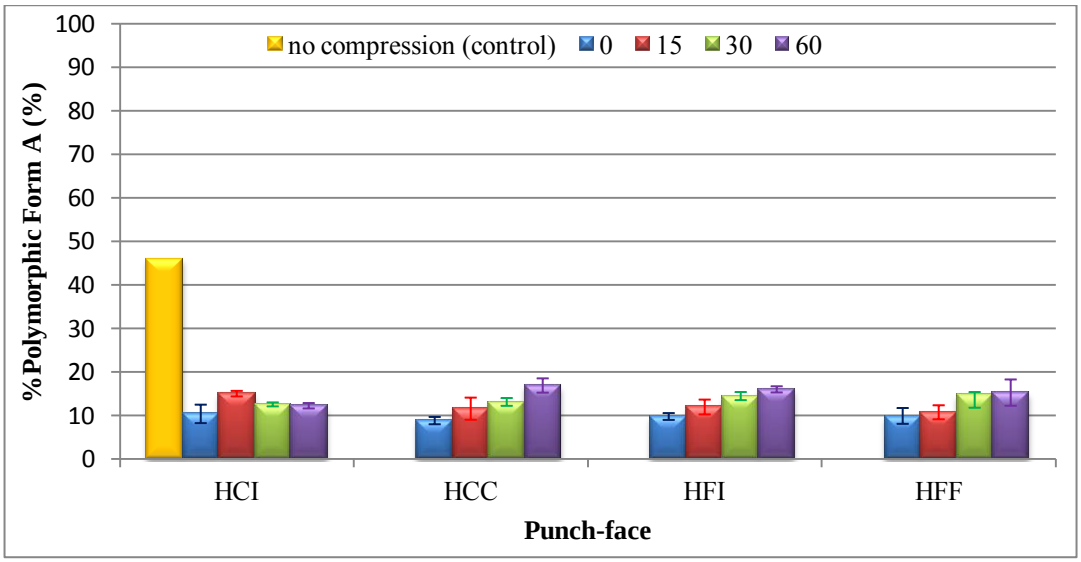

Figure 36 The relative amounts of polymorphic Form A and various punch-face designs of heated chlorpropamide powder analyzed by Q-PXRD.

Heated chlorpropamide powder when underwent compression, content of Form A was reduced to below 20%. Every punch-face design resulted in increased amounts of polymorphic Form A as compression dwell time increased. This is true for every punch-face designs except HCI which shows no correlation on dwell time.

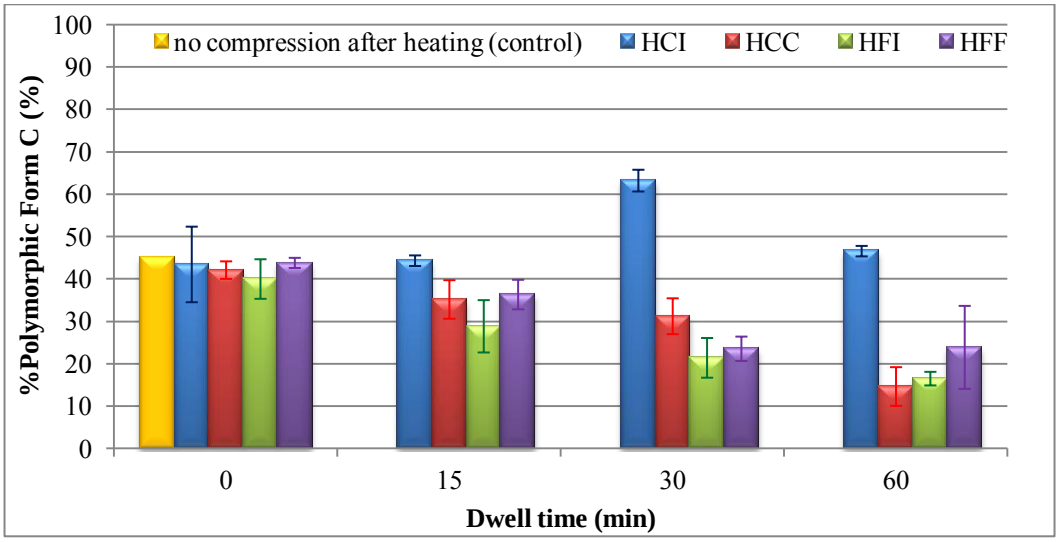

Figure 37 The relative amounts of polymorphic Form C and the compression dwell time of heated chlorpropamide powder analyzed by Q-PXRD.

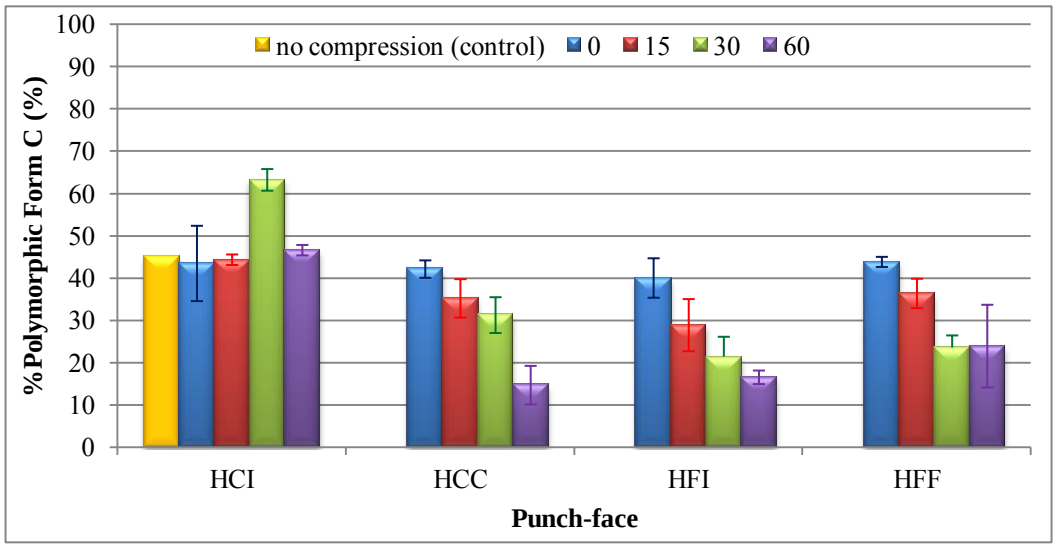

Figure 38 The relative amounts of polymorphic Form C and various punch-face designs of heated chlorpropamide powder analyzed by Q-PXRD.

Every punch-face designs resulted in reduced amounts of polymorphic Form C of heated chlorpropamide powder as compression dwell time increased. This is true for every punch-face designs except HCI which shows no correlation on dwell time as with Form A.

Typical solid state stability theory states that only one polymorphic form is stable under "one specific condition", such as temperature pressure and composition. However, as shown in Figure 36 and 38, it was observed that under pressure of 3000 psi. The stability of chlorpropamide polymorphic Form A and Form C differs from higher temperature condition (where Form C is more stable than Form A). At this stressed condition of pressure, Form A is hypothetically more stable than Form C. Thus, an increase in dwell time potentiates the reversible change of Form C (obtained after heating) back to Form A through an amorphous transition phase.

3.3. Effect of compaction pressure with constant dwell time of non-heated samples

Solid transformations can occur during manufacturing process especially during tablet compaction process (Sanchez-Castillo 2003; Koivisto 2006; Wildfong 2007; Mazel 2011). The pressure distribution during compaction in the tablet die is not homogenous. The regions in which the uneven pressure is distributed on the surface of the tablet, causing different polymorphic transition (Koivisto 2006; Lin 2007). Thus the influence of compaction force may effect the change in polymorphic forms where various punch-face designs are used.

This section will compress non-heated chlorpropamide polymorphic Form A using various compaction pressures of 1000, 2000, 3000, 4000 and 5000 psi at constant dwell time of 15 minutes with various punch-face designs. The results are shown in Table 5

Table 5 Effect of compaction pressures on the transformation of polymorphic forms of chlorpropamide analyzed by Q-PXRD.

Punch face designs	Pressure (psi)	Average content of Form A (percent ± SD) (n=3)	Calculated average content of metastable amorphous form (percent)	Average content of Form C (percent ± SD) (n=3)
Control	-	97 ± 3	3 ± 3	0
PCI	1000	41 ± 1	54 ± 6	5 ± 5
	2000	36 ± 6	64 ± 6	0
	3000	36 ± 5	59 ± 2	5 ± 4
	4000	36 ± 2	60 ± 1	4 ± 3
	5000	37 ± 1	57 ± 1	6 ± 0
PCC	1000	33 ± 2	59 ± 5	8 ± 4
	2000	35 ± 3	62 ± 6	3 ± 3
	3000	31 ± 4	61 ± 4	8 ± 7
	4000	32 ± 3	62 ± 4	6 ± 1
	5000	31 ± 5	63 ± 5	6 ± 0
PFI	1000	37 ± 2	59 ± 4	4 ± 3
	2000	32 ± 1	63 ± 7	5 ± 8
	3000	31 ± 1	62 ± 3	7 ± 2
	4000	30 ± 2	65 ± 6	5 ± 4
	5000	31 ± 2	67 ± 3	2 ± 4
PFF	1000	37 ± 4	53 ± 3	10 ± 2
	2000	32 ± 1	64 ± 4	4 ± 3
	3000	31 ± 2	59 ± 4	10 ± 3
	4000	30 ± 2	67 ± 5	3 ± 5
	5000	30 ± 1	62 ± 3	8 ± 4

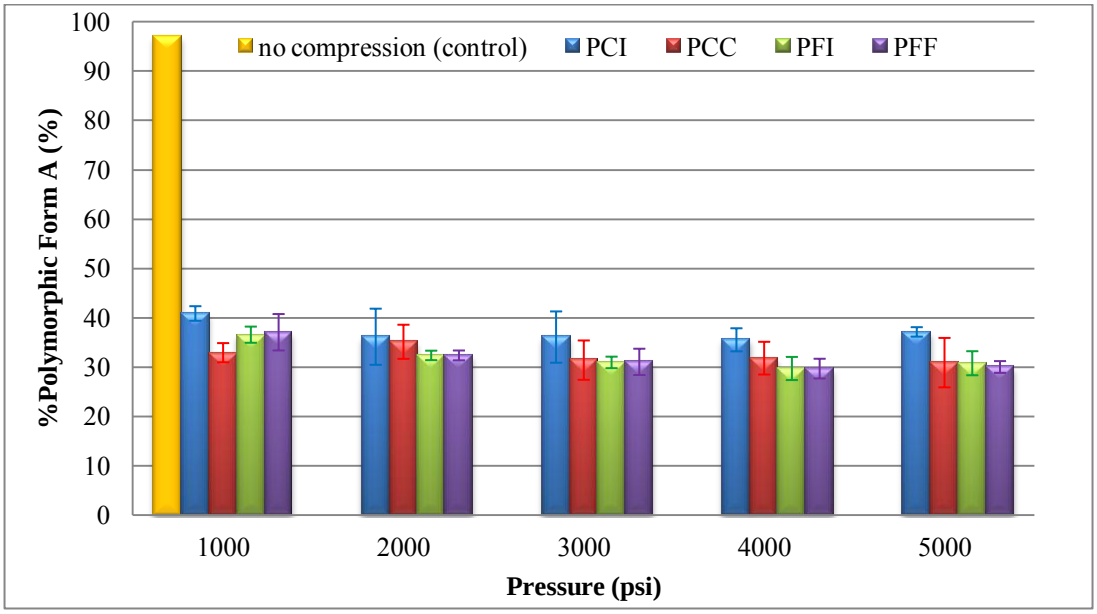

Figure 39 The relative amounts of polymorphic Form A and various compaction pressures of non-heated chlorpropamide powder analyzed by Q-PXRD.

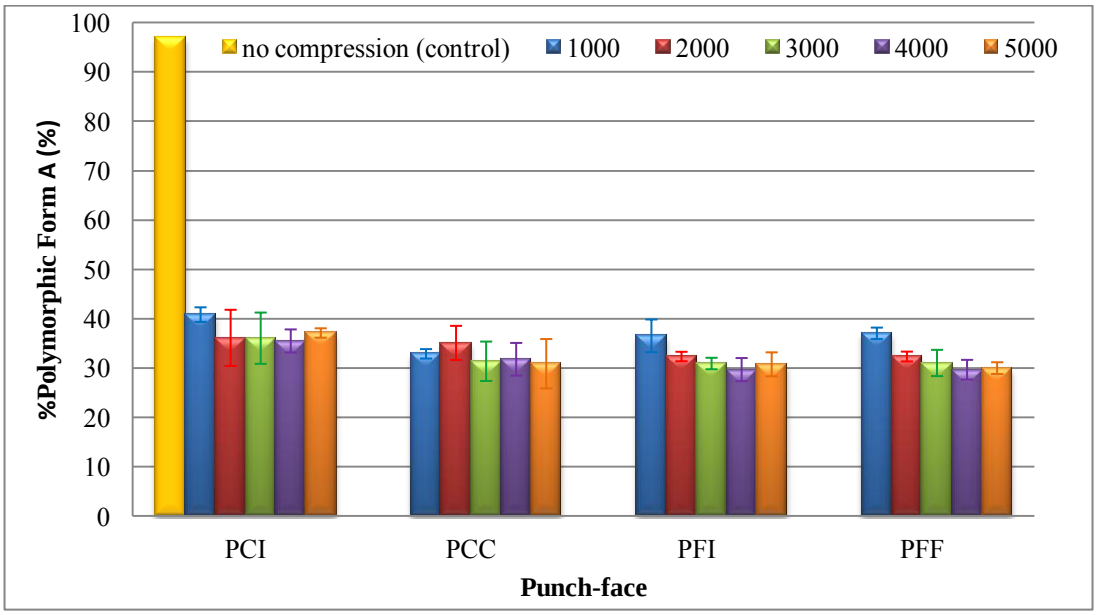

Figure 40 The relative amounts of polymorphic Form A and various punch-face designs of non-heated chlorpropamide powder analyzed by Q-PXRD.

Figure 39 shows dramatic decrease in %content of polymorphic Form A after compaction. Amounts of resulting Form A were all within 30-40% regardless of compaction forces. However, Figure 40 shows that the punch-face designs did not show any differences in the resulting average polymorphic Form A. In summary, various compression forces and the designs of punch-face are not the main factors which determine the transformation rates of Form A analyzed by Q-PXRD.

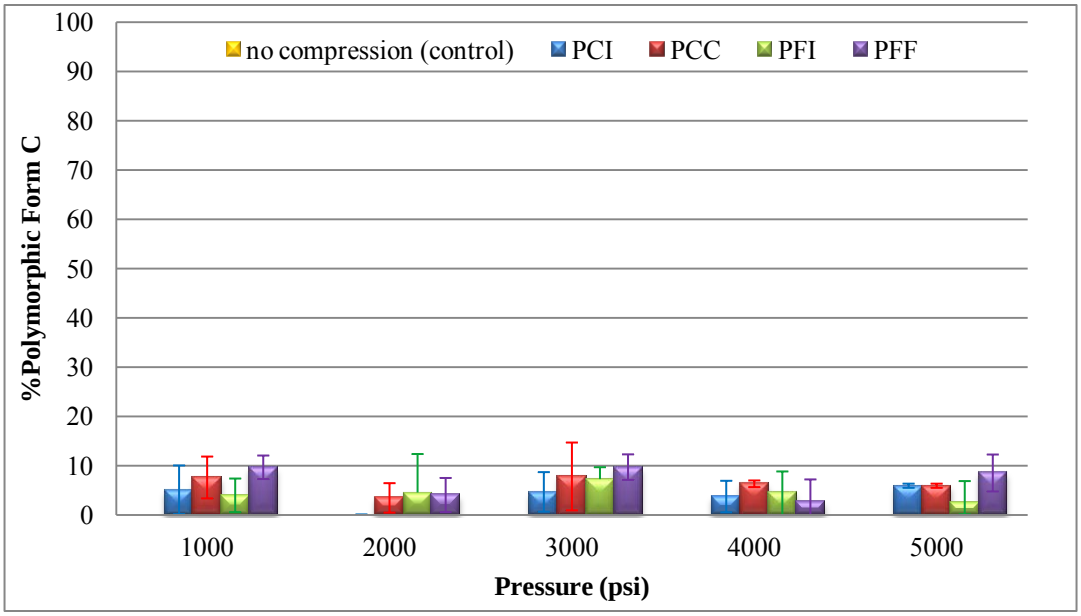

Figure 41 The relative amounts of polymorphic Form C and various compaction pressures of non-heated chlorpropamide powder analyzed by Q-PXRD.

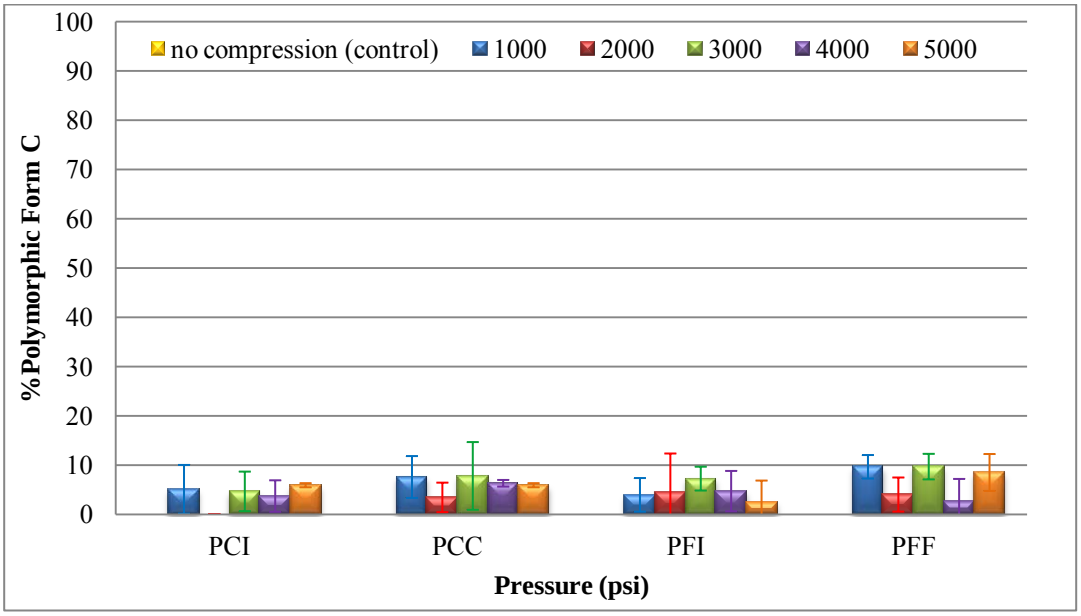

Figure 42 The relative amounts of polymorphic Form C and various punch-face designs of non-heated chlorpropamide powder analyzed by Q-PXRD.

Every compaction pressures used can generate polymorphic Form C even without compression dwell time (Figure 41). The starting polymorphic Form A can be transformed into polymorphic Form C by mechanical energy exerted during tabletting via the metastable amorphous intermediate. When the upper punch entered the die, particles deformed because it had transferred some energy from the upper punch to the powder. The excess energy will be used to rearrange the molecules and bond formation, transforming to the metastable amorphous form and finally to polymorphic Form C. The mechanical compaction induced the transformation from one polymorphic form to another and the results may be a mixture of different forms (Pirttimaki 1993). Both the compaction force and various punch-face designs have no effect on the change in the average polymorphic Form C (Figures 41 and 42).

3.4. Effect of compaction pressure with constant dwell time on heated samples

This section will consider the effect of compaction pressures on heated samples. The results are shown in Table 6. Polymorphic Form C for all punch-face designs and every compaction pressures occurred in significantly high amount. The content of polymorphic Form C can be produced up to 60% even after the least compaction force (1000 psi) was used. On the other hand, amounts of polymorphic Form A of all punch-face designs and compaction pressures were reduced compared to non-heated samples (Figure 41). Because heat is one factor which accelerates the polymorphic forms transitions. The heated powder may collect energy and transformed to metastable amorphous form before compaction by which all will transformed to Form C upon compression. Thus, in this section, polymorphic Form C occurred higher than the previous section (3.3).

Table 6 Effect of compaction pressures of heated chlorpropamide powder using constant compaction dwell time (15 min) by Q-PXRD.

Punch face designs	Pressure (psi)	Average content of Form A (percent ± SD) (n=3)	Calculated average content of metastable amorphous form (percent)	Average content of Form C (percent ± SD) (n=3)
Control	-	46 ± 4	9 ± 6	45 ± 2
HPCI	1000	17 ± 0	19 ± 2	64 ± 1
	2000	12 ± 3	17 ± 7	71 ± 10
	3000	9 ± 2	43 ± 7	48 ± 8
	4000	13 ± 1	35 ± 1	52 ± 2
	5000	6 ± 0	27 ± 0	67 ± 1
HPCC	1000	20 ± 1	16 ± 2	64 ± 2
	2000	17 ± 1	13 ± 3	70 ± 3
	3000	10 ± 0	46 ± 4	44 ± 4
	4000	11 ± 0	30 ± 2	59 ± 2
	5000	10 ± 1	26 ± 6	64 ± 7
HPFI	1000	15 ± 0	17 ± 2	68 ± 2
	2000	18 ± 0	17 ± 1	65 ± 1
	3000	13 ± 0	45 ± 3	42 ± 3
	4000	11 ± 1	52 ± 0	37 ± 1
	5000	8 ± 0	40 ± 3	52 ± 3
HPFF	1000	19 ± 4	11 ± 6	70 ± 4
	2000	19 ± 2	15 ± 1	66 ± 4
	3000	10 ± 2	44 ± 5	46 ± 3
	4000	14 ± 1	42 ± 3	44 ± 3
	5000	7 ± 0	33 ± 2	60 ± 2

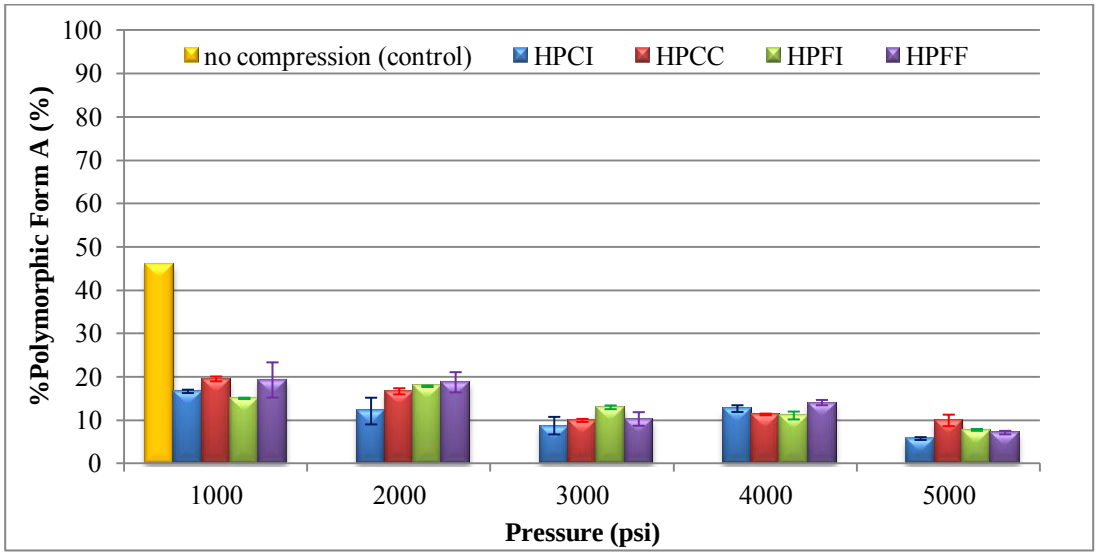

Figure 43 The relative amounts of polymorphic Form A and various compaction pressures of heated chlorpropamide powder analyzed by Q-PXRD.

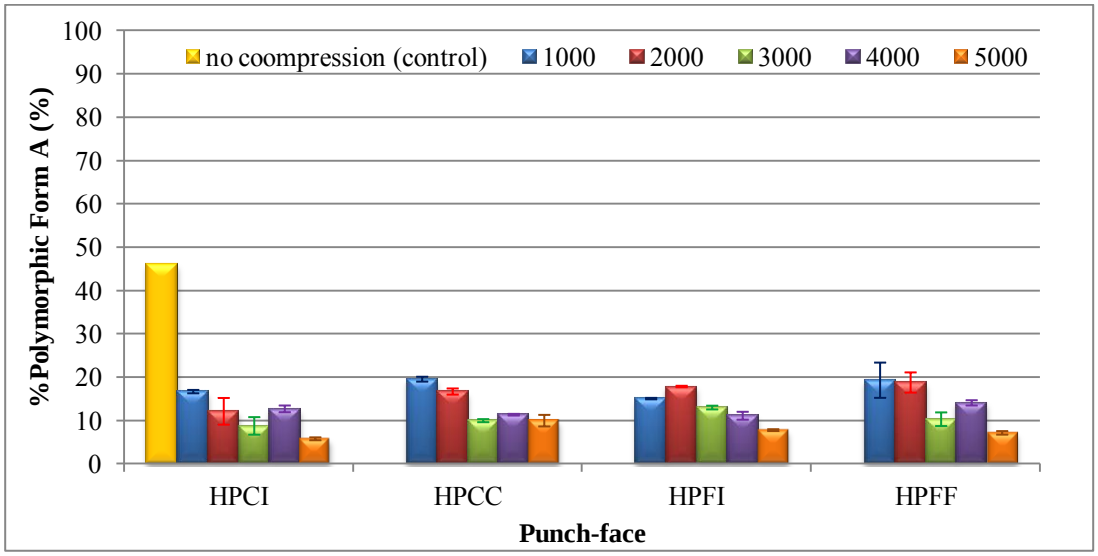

Figure 44 The relative amounts of polymorphic Form A and various punch-face designs of heated chlorpropamide powder analyzed by Q-PXRD.

After heating and compression, every punch-face design resulted in reduced amounts of polymorphic Form A as compaction force increased (Figure 43). The polymorphic Form A reduced to below 20% (Figure 44)

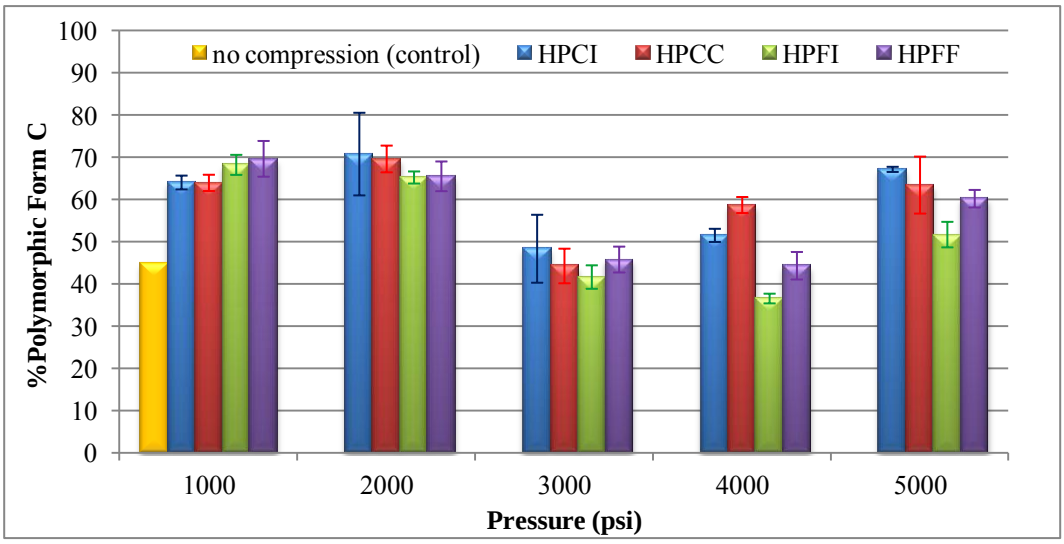

Figure 45 The relative amounts of polymorphic Form C and various compaction pressures of heated chlorpropamide powder analyzed by Q-PXRD.

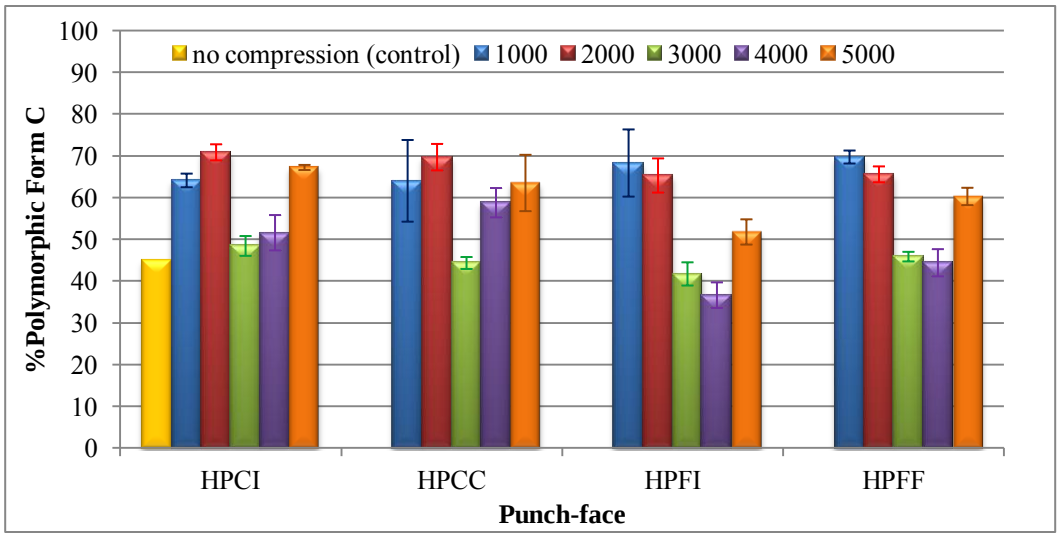

Figure 46 The relative amounts of polymorphic Form C and various punch-face designs of heated chlorpropamide powder analyzed by Q-PXRD.

In this section, the polymorphic Form C occurred up to 50% (Figure 45). The data indicated that the compaction pressures have an effect on the average polymorphic Form C.

Typical solid stated stability theory states that only one polymorphic form is stable under one specific condition such as temperature and pressure. As shown in Figures 44 and 46, at excited state such as heated samples, Form A is hypothetically more stable than Form C. Thus, an increase compaction force potentiates the reversible change of Form C back to Form A through an amorphous transition phase.

Therefore, Q-XRPD cannot be used to differentiate the polymorphic interconversion due to punch-face design but can distinguish between the effects of compaction forces and dwell time at ground and excited states.

4. Quantitative Raman spectroscopy analysis

In the previous section, PXRD was used to characterize the solid forms of chlorpropamide powder as an average percentage of each polymorph based on the whole tablet by grinding the tablet before analysis. However, microscopic Raman spectroscopy is the method which analyzes and identifies the transition of each polymorph only on the tablet surface where it is most prone to transition during compaction process. This method can be done without disrupting the physical tablet structure. In addition, Raman spectroscopy is one of the instruments used in process analytical technology (PAT) due to its insensitive to aqueous solvents. Raman spectroscopy is an excellent technique for discriminating crystalline from amorphous forms and also to differentiate between polymorphs of active pharmaceuticals and excipients (Bugay 2001; Stephenson 2001).

Confocal microscopic Raman spectroscopy is vibrational spectroscopy. When a powerful laser source focuses on the chlorpropamide powder, the molecules of

chlorpropamide powder are excited to a virtual state. Then the molecules fall to the original state and remit photon. Most of the scattered energy comprises radiation of the incident frequency called “Reyleigh” scattering. The fraction of photons scattered from molecular centers with less energy or lower frequency than they had before is called “Stokes” scattering. The anti-Stokes photons have greater energy or higher frequency than those of the excited radiation. The different vibrational modes of a molecule can be identified by recognizing Raman shifts in the spectrum (Lin-Vien 1991; Skoog 2007).

In this section, We tried to use quantitative method using Raman spectroscopy (Q-Raman) to analyze the top surface of the whole tablet and where physical structure of tablets are not destroyed. In the first part, the pure Form A and Form C of chlorpropamide powder are identified by putting pure form powders on a glass slide and focus the powder particles through the microscope. Then collect the Raman spectrum of chlorpropamide polymorphs Form A and Form C. The Raman spectra of chlorpropamide polymorphic Form A, Form C and meatstable-amorphous form are shown in section 1.3 (Figures 23-25). Differences between the two spectra were detected at Raman shift of 273 cm^{-1} (Figure 24) for chlorpropamide Form A. While Raman shift at 1306 cm^{-1} (Figure 25) was used to signified chlorpropamide Form C. The second part is to develop quantitative analytical method. One surface of chlorpropamide tablets are chosen for Q-Raman by placing the whole tablet on a glass slide and focuses the surface of chlorpropamide tablets through the microscope. The program will automatically generate detection grids on the tablet surfaces. Then collect data for each grid and build spectral maps on surfaces of chlorpropamide tablets (Figure 47).

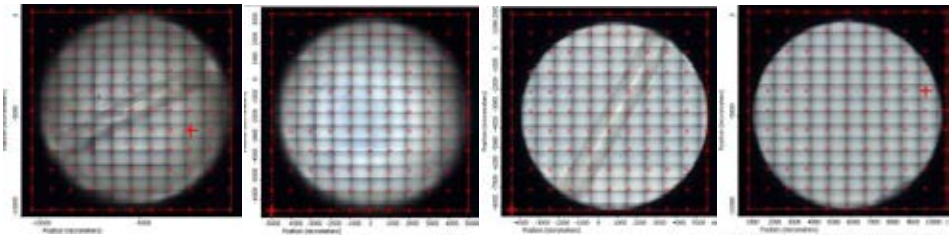

Figure 47 Sampling grid of various punch-face designs.

Collect sample data using identical conditions as the method for identification of chlorpropamide polymorphs. When finish collecting data for each grid, Omnic® software will display analytical results as shown in Figure 48.

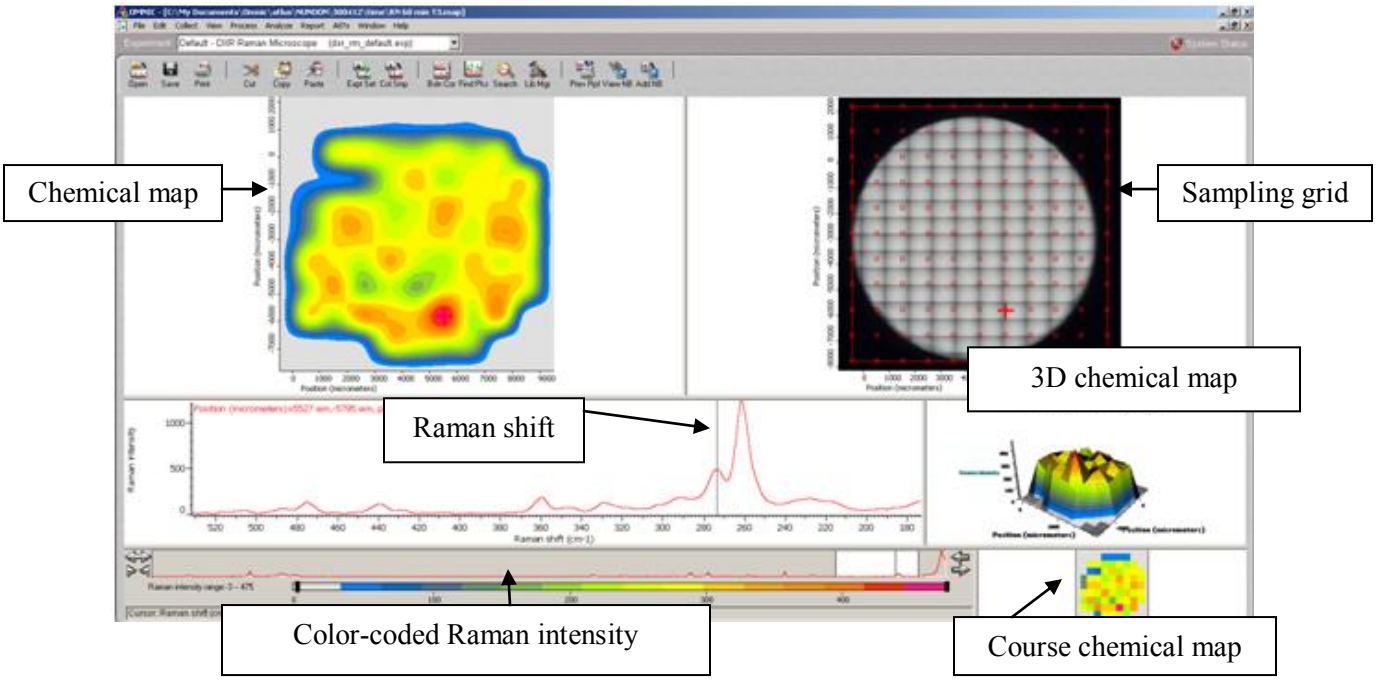

Figure 48 Screen display of resulting Raman map computed by Omnic® software.

One tablet composed of 120 laser shots, hence, 120 spectral data. So if holding Raman shift constant, the chemical map does not change when moving the cursor but the spectrum changes (Figure 49).

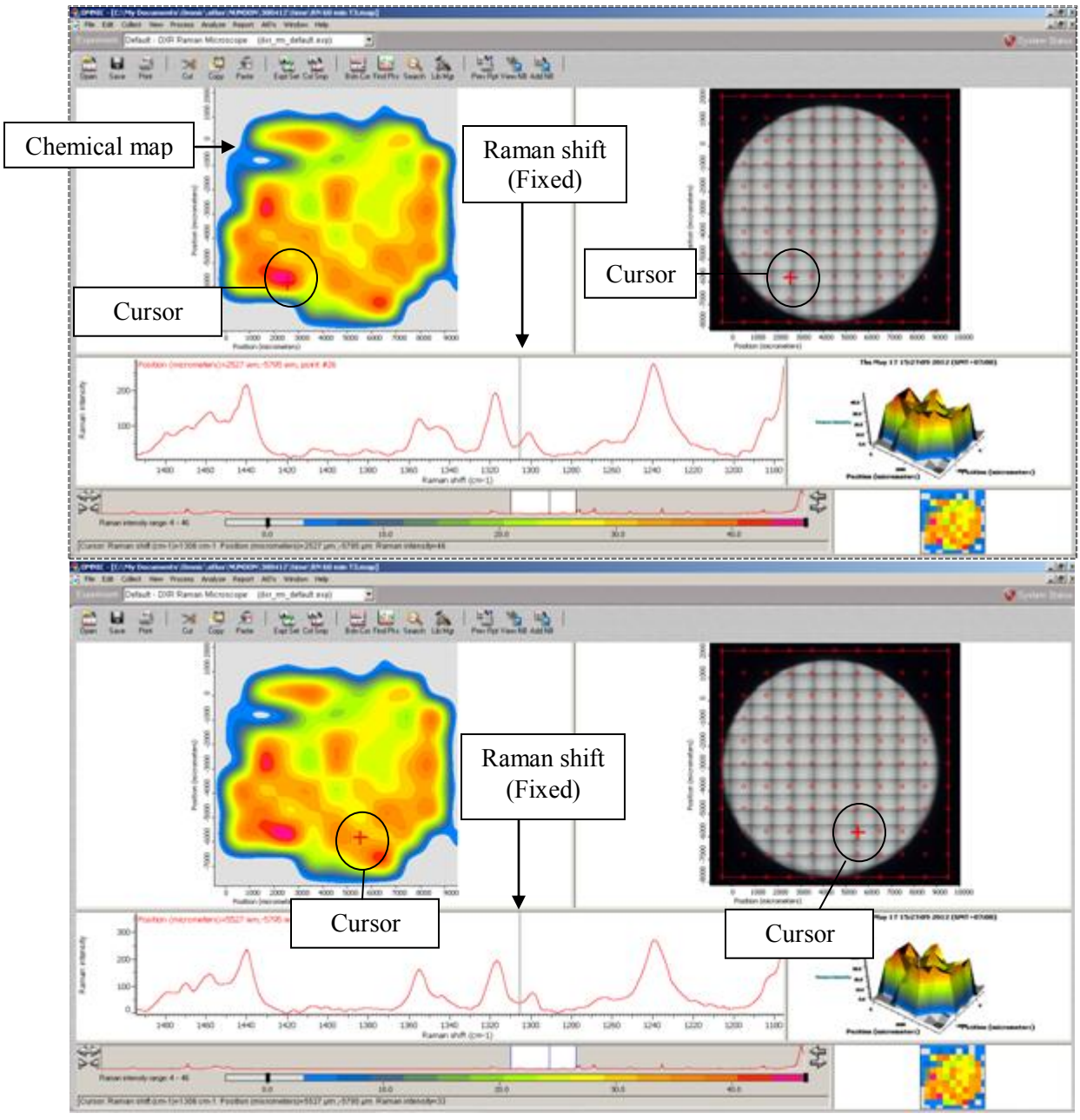

Figure 49 Raman mapping computed by Omnic® software after moving cursor on tablet grids while holding Raman shift constant.

If holding the cursor in place, when moving the Raman shift to another position, the chemical map changes but the spectrum does not changes (Figure 50).

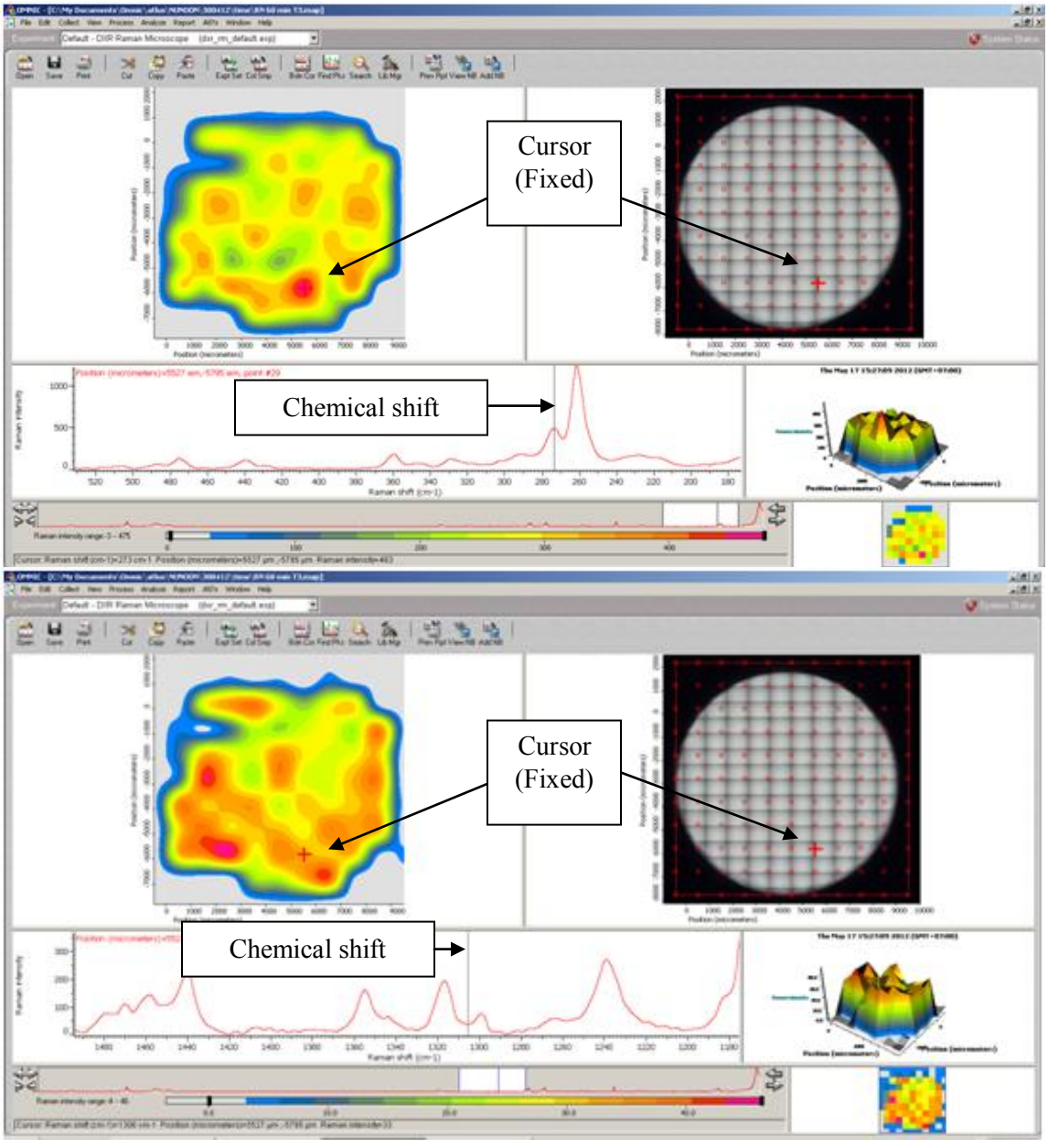

Figure 50 Raman mapping computed by Omnic® software after moving Raman shift on the spectrum while holding the cursor constant.

The color-coded Raman intensity is a relative indicator of the content of each polymorphic form. If the peak position on the spectrum shows highest intensity, the chemical map will appear in red and will reduce to blue if no peak as present. However, one chemical map could not be compared to another chemical map because each color-coded Raman intensity was shown to be in different relative scales. Thus, one chemical map can quantitatively show the relative amounts of a polymorphic form of interest at various positions on the surface of chlorpropamide tablets.

The quantity of chlorpropamide polymorphic forms was analyzed by image analysis software (ImagePro® Plus) using colors that appear on chemical map. ImagePro® Plus quantitate each color and report it in terms of areas. The amount of each polymorphic form is calculated as the sum of areas multiply by the relative intensity (I/I_0) of each color as follows.

$$Q = \sum [A_n(I_n/I_0)]_n$$

Q The amount of each polymorphic form

A_n Total area of each color

I_n Intensity of each color

I_0 Maximum intensity as appears on "color coded Raman intensity" scale

n Colors (total of 16 colors)

4.1. Effect of time

4.1.1. Effect of compression dwell time with constant compaction pressure on non-heated samples

Chlorpropamide powder was compacted by varying the dwell time and analyzed by Raman spectroscopy. Collect samples using the same condition as when identifying chlorpropamide polymorphs in section 3.2.1. Figure 51 shows Raman mapping of chlorpropamide Form A and Form C.

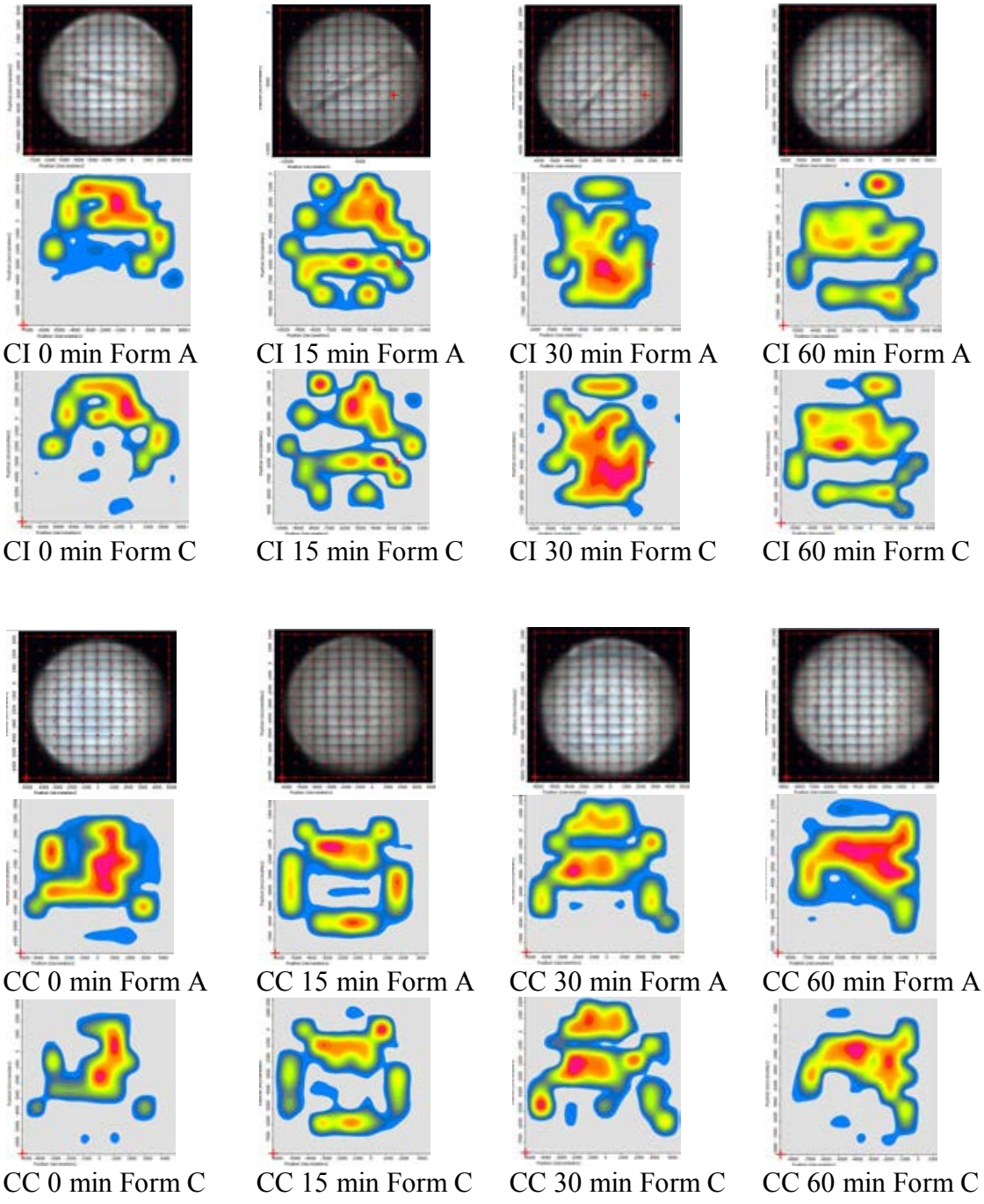

Figure 51 Sampling grid and chemical mapping obtained by Raman spectroscopy of non-heated chlorpropamide polymorphic Form A and Form C on tablet surfaces (CI = concave, indent CC = concave FI = flat-faced, indent FF = flat-faced).

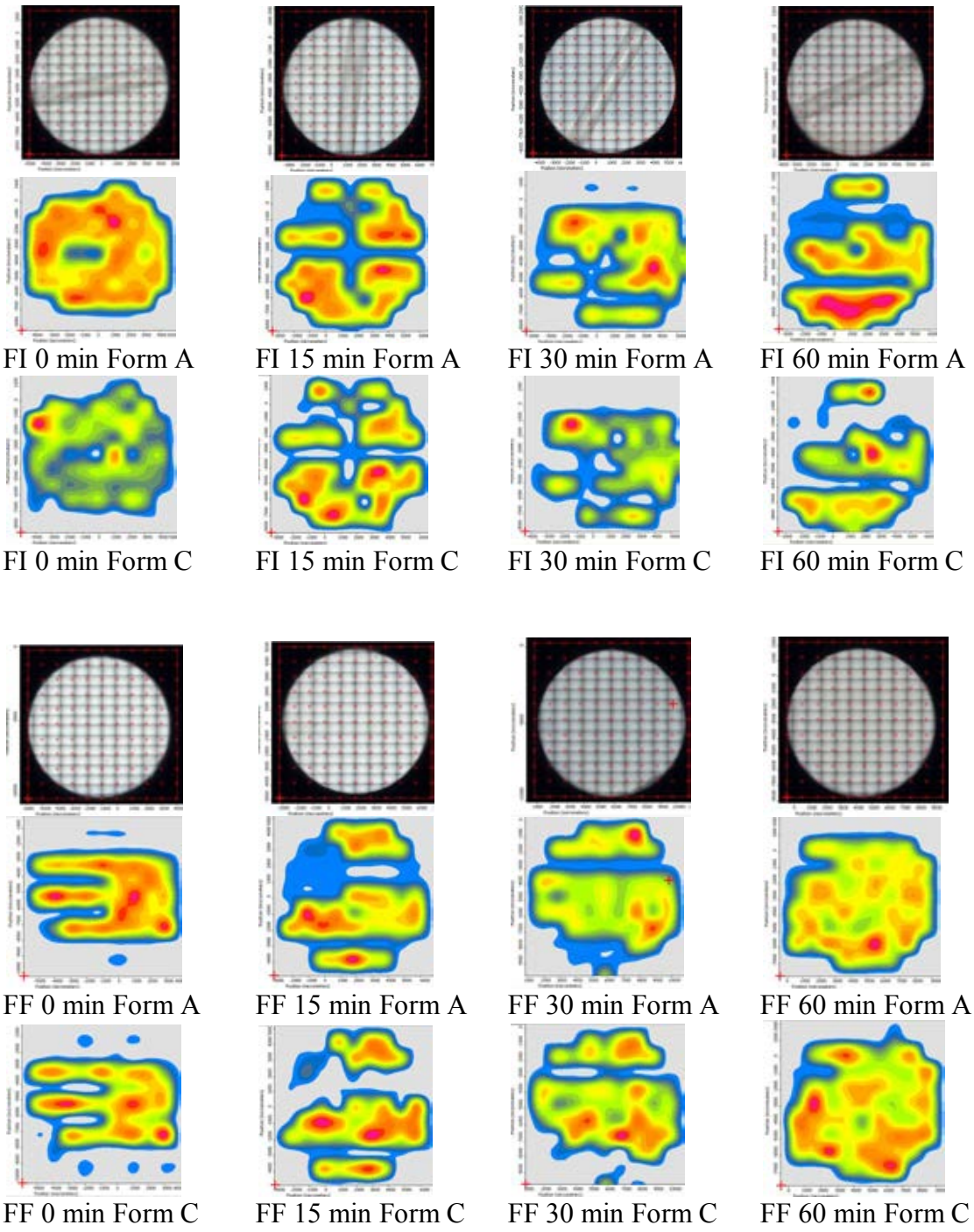

Figure 51 (cont.) Sampling grid and chemical mapping obtained by Raman spectroscopy of non-heated chlorpropamide polymorphic Form A and Form C on tablet surfaces (CI = concave, indent CC = concave FI = flat-faced, indent FF = flat-faced).

Analyze the quantity of each chlorpropamide polymorphic form using image analysis software (ImagePro® Plus) based on area integration of each color. After that, the total amounts of polymorphic Form A or polymorphic Form C are calculated as the sum of every color coded areas multiply by the relative intensity (I/I_0) of each color. The results show that dwell time has no significant effect (Table 12 in appendix B) on the transformation of both polymorphic forms (Table 7) on the surfaces of tablets.

Table 7 Effect of compaction dwell time on the polymorphic transformation of non-heated chlorpropamide under constant compaction pressure analyzed by Q-Raman.

Punch face designs	Dwell Time (min)	Average content of Form A (percent ± SD) (n=3)	Calculated average content of metastable amorphous form (percent)	Average content of Form C (percent ± SD) (n=3)
CI	0	21 ± 3	69 ± 4	10 ± 2
	15	21 ± 3	69 ± 2	10 ± 2
	30	34 ± 16	45 ± 17	21 ± 9
	60	22 ± 4	66 ± 5	12 ± 3
CC	0	20 ± 1	74 ± 2	6 ± 3
	15	19 ± 6	70 ± 9	11 ± 5
	30	20 ± 4	66 ± 8	14 ± 4
	60	26 ± 0	57 ± 3	17 ± 3
FI	0	33 ± 9	55 ± 13	12 ± 5
	15	31 ± 3	56 ± 9	14 ± 6
	30	32 ± 9	45 ± 22	23 ± 13
	60	31 ± 7	50 ± 13	19 ± 10
FF	0	27 ± 2	55 ± 2	18 ± 0
	15	28 ± 4	53 ± 7	19 ± 5
	30	38 ± 9	27 ± 15	35 ± 6
	60	35 ± 3	39 ± 7	26 ± 5

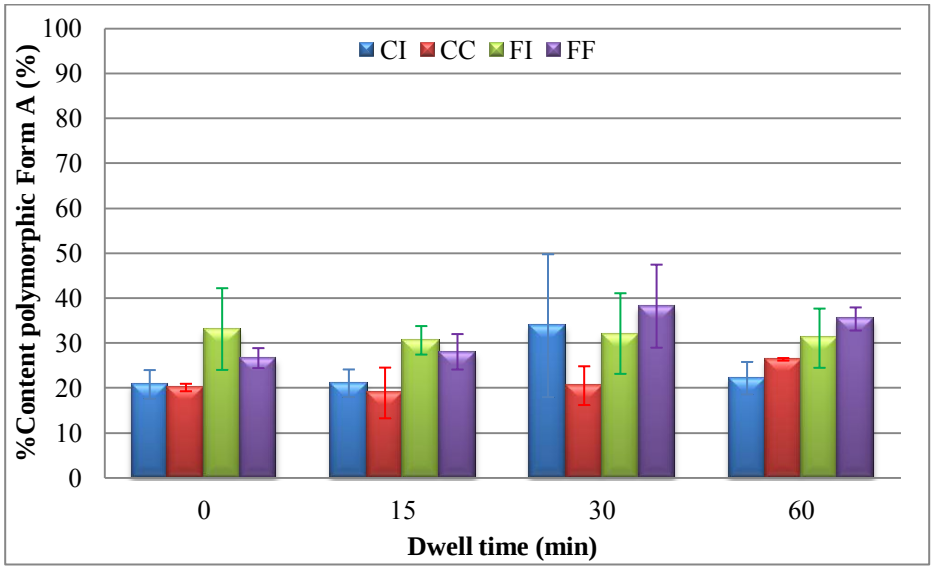

Figure 52 The relative amounts of polymorphic Form A as appears on tablet surfaces and the compression dwell time of non-heated chlorpropamide powder obtained by Q-Raman.

When polymorphic Form A powder is compacted, the content of polymorphic Form A of all punch face designs decreased drastically (Figure 52). Moreover, the statistical data (Table 12, Appendix B) indicated that various punch-face designs show significant effect on the transition of polymorphic Form A content at 95% confidence interval ($p \leq 0.05$) (Figure 53).

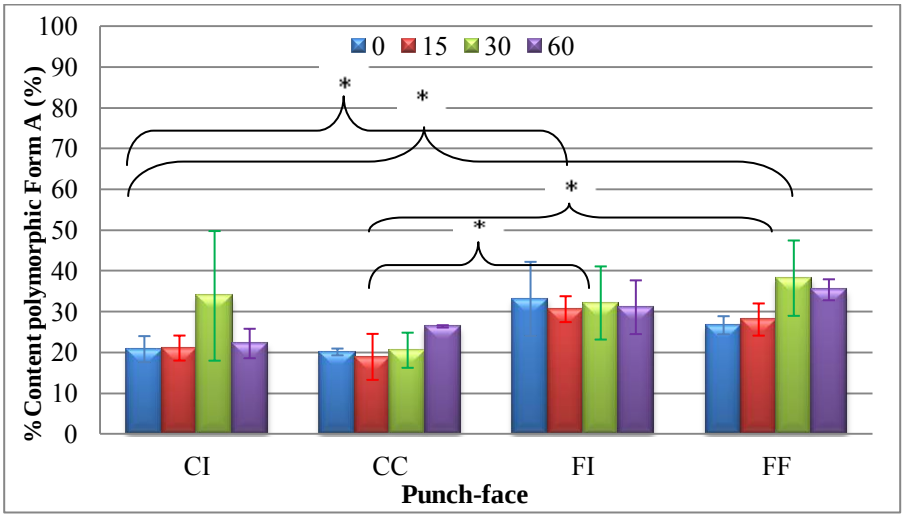

Figure 53 The relative amounts of polymorphic Form A and various punch-face designs of non-heated chlorpropamide powder obtained by Q-Raman (* significantly different at $p \leq 0.05$).

When comparing various punch-face designs used for compression, the average polymorphic Form A obtained between CI and FI, CI and FF, CC and FI and CC and FF were significantly different more than 95% confidence interval ($p \leq 0.05$) (Table 13, Appendix B). From this data, the polymorphic transition of Form A occurred more when using concave punch as compared to flat-faced punch. However, indentation was shown not to have any significant effect.

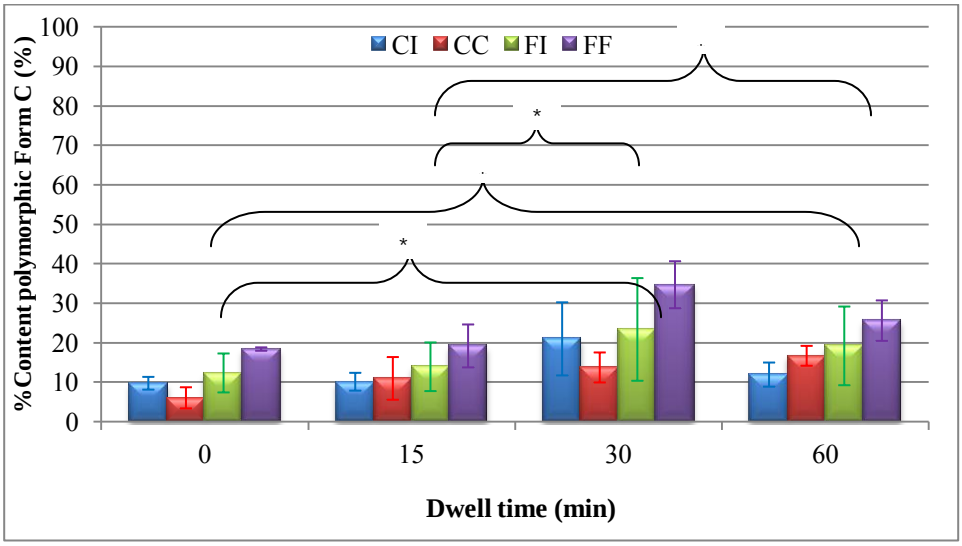

Figure 54 The relative amounts of polymorphic Form C as appears on tablet surfaces and the compression dwell time of non-heated chlorpropamide powder obtained by Q-Raman (* significantly different at $p \leq 0.05$).

Every designs of punch-face used for compression were able to generate polymorphic Form C even with no dwell time (Figure 54). The results are similar to those obtained by Q-PXRD, that is the content of polymorphic Form A decreased and the content of polymorphic Form C increased after compression. The statistical evaluation indicated that both punch-face designs and compaction dwell time affect the change in polymorphic Form C at 95% confidence interval ($p \leq 0.05$) (Table 16, Appendix B). At low dwell time (0 and 15 minutes) resulted in lower amount of Form C, but at higher dwell time (30 and 60 minutes) Form C increased significantly.

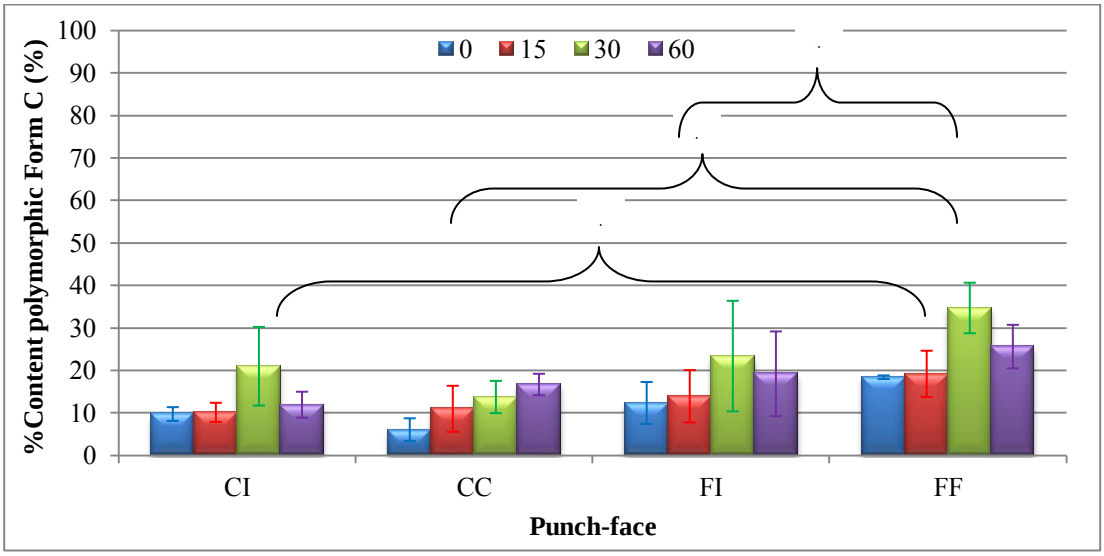

Figure 55 The relative amounts of polymorphic Form C and various punch-face designs of non-heated chlorpropamide powder obtained by Q-Raman (* significantly different at $p \leq 0.05$).

When comparing punch-face designs (Figure 55), the average amount of polymorphic Form C are significantly different at 95% confidence interval ($p \leq 0.05$) (Table 15 in appendix B) when CI and FF, CC and FF and FI and FF were used.

Various punch face designs show impact on transformation of both polymorphic forms. The flat-faced shows higher polymorphic form change than curved face due to more uniform pressure distribution during compression. The high compaction pressure from flat-face punch exerted on polymorphic Form A can change it to polymorphic Form C directly bypassing metastable amorphous form. However, curved face punch distribute uneven compaction force throughout the tablet. After compaction, the polymorphic Form A may change to the metastable amorphous form before more energy is needed to finally transform to polymorphic Form C. Thus, the various designs of punch-face, curved-face and flat-faced, have significant effect on the transformation of polymorphic forms but the incision of punch-face shows little or no effect.

4.1.2. Effect of compression dwell time with constant compaction pressure on heated samples

This section, chlorpropamide powder was heated prior to compaction by varying the dwell time. Raman spectroscopy was used for analysis. The Sampling grid and chemical map of chlorpropamide tablets are shown in Appendix C. The average contents (%) of both polymorphic forms are shown in Table 8.

Table 8 Effect of compression dwell time of heated chlorpropamide powder using constant compaction pressure (3000 psi) and analyzed by Q-Raman.

Punch face designs	Dwell Time (min)	Average content of Form A (percent ± SD) (n=3)	Calculated average content of metastable amorphous form (percent)	Average content of Form C (percent ± SD) (n=3)
HCI	0	7 ± 2	72 ± 9	21 ± 7
	15	5 ± 3	76 ± 4	19 ± 5
	30	3 ± 2	74 ± 10	23 ± 8
	60	3 ± 1	76 ± 5	21 ± 5
HCC	0	3 ± 1	82 ± 2	15 ± 2
	15	4 ± 1	75 ± 5	21 ± 7
	30	2 ± 1	83 ± 3	15 ± 2
	60	3 ± 1	83 ± 3	14 ± 4
HFI	0	7 ± 2	57 ± 6	36 ± 5
	15	14 ± 1	53 ± 9	33 ± 9
	30	3 ± 1	69 ± 4	28 ± 3
	60	7 ± 4	64 ± 8	29 ± 8
HFF	0	5 ± 4	70 ± 7	25 ± 3
	15	7 ± 4	59 ± 5	34 ±5
	30	5 ± 2	73 ± 6	22 ± 5
	60	2 ± 2	78 ± 7	20 ± 5

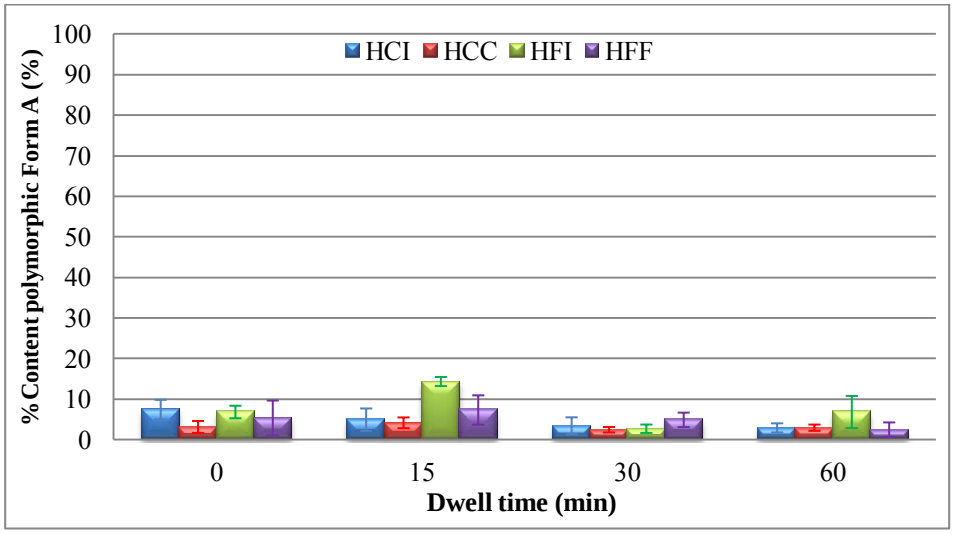

Figure 56 The relative amounts of polymorphic Form A and the compression dwell time of heated chlorpropamide powder analyzed by Q-Raman.

Figure 56 shows heated chlorpropamide powder after compaction at varying dwell time and designs of punch-face. Polymorphic Form A decreased significantly to less than 10%. At higher dwell time (30 and 60 minutes) Form A decreased to lower amounts than when lower dwell times (0 and 15 minutes) were used (Figure 56). The statistical data indicated that the significant influence of punch-face designs in correlation with the compaction dwell time on the transformation of polymorphic Form A at 95% confidence interval (Table 17, Appendix B). Both factors, dwell time and punch face designs, had an integrated effect on the extent of polymorphic Form A transition.

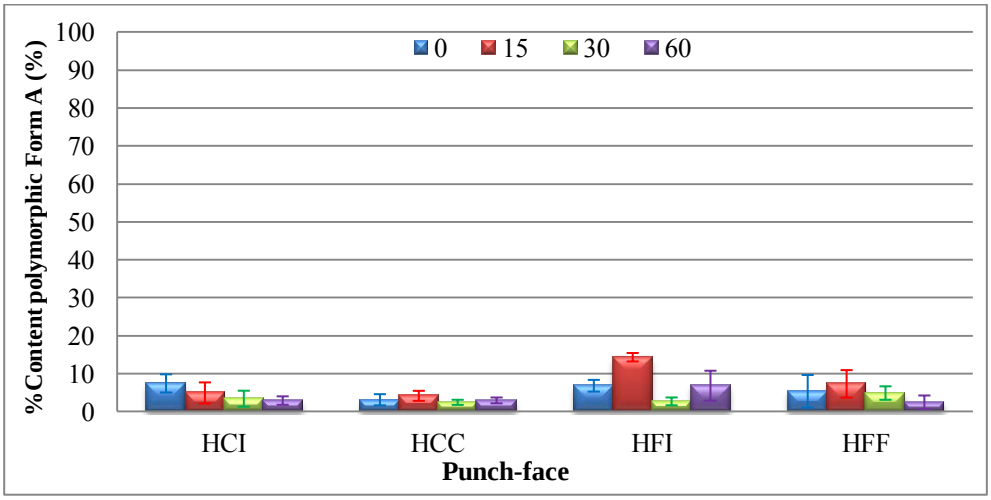

Figure 57 The relative amounts of polymorphic Form A and various punch-face designs of heated chlorpropamide powder analyzed by Q-Raman.

When comparing the various punch-face designs, flat-face designs resulted in higher content of residual polymorphic Form A compare to concave punch designs (Figure 57).

After the heated the polymorphic Form A was compacted, the amount of Form C increased markedly as a result of heating when compare to unheated samples. As can be seen in Figure 58 that the average amount of polymorphic Form C is not significantly different at every dwell time used. The result conforms to that obtained by Q-PXRD. The statistical data indicated that only the punch-face design have significant impact on the conversion to polymorphic Form C at 95% confidence interval (Table 18, Appendix B).

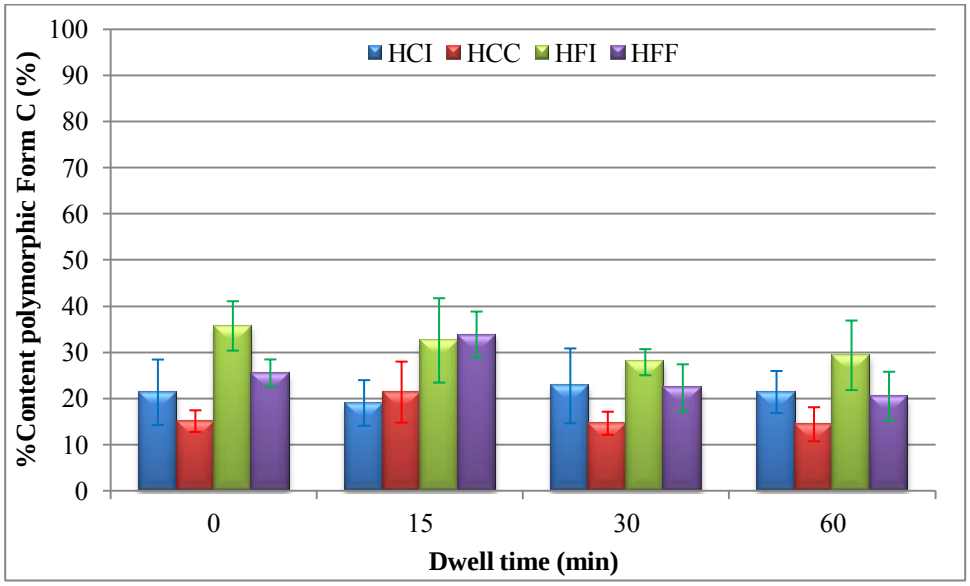

Figure 58 The relative amounts of polymorphic Form C and the compression dwell time of heated chlorpropamide powder analyzed by Q-Raman.

When comparing the various designs of punch-face (Figure 59), the average content of polymorphic Form C compressed between HCI and HFI, HCC and HFI and HCC and HFF are shown to be significantly different at 95% confidence interval (Table 19, Appendix B). Flat-face punches are shown to have higher effect in inducing polymorphic Form C after compaction comparing to concave punch designs. This may be due to flat-face punches exerted higher energy dissipation homogeneously on the tablet surface.

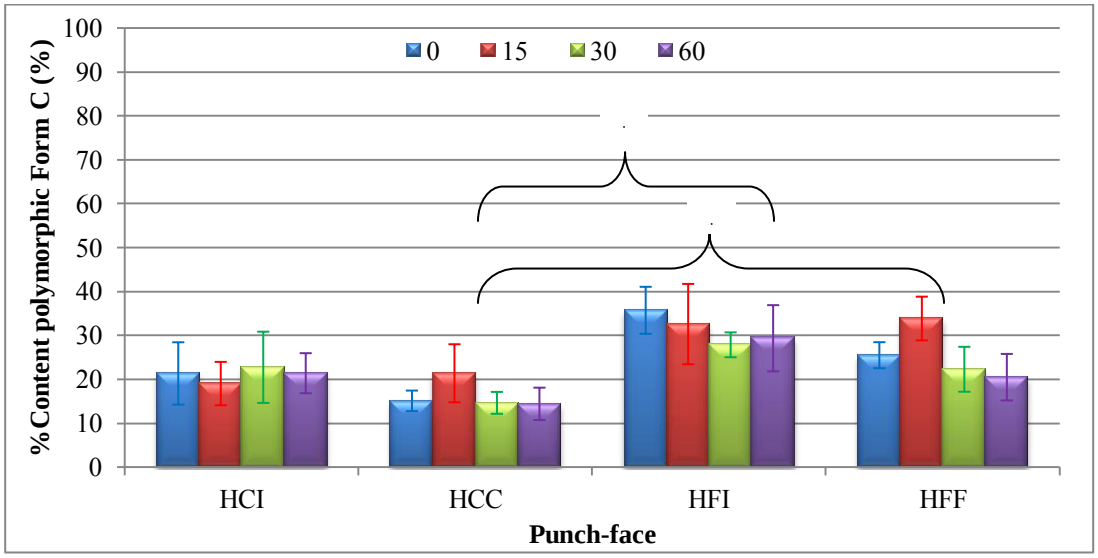

Figure 59 The relative amounts of polymorphic Form C and various punch-face designs of heated chlorpropamide powder analyzed by Q-Raman.
(* significantly different at $p \leq 0.05$)

Hence, the factor which effect the transition of heated polymorphic Form A and Form C after compaction detected by Q-Raman is punch-face design only. Flat-face compared to concave face is shown to result in different quantitative amounts of polymorphic Form A and Form C. However, the effect of indentation on punch faces cannot be distinguished quantitatively by this method.

Flat-face punches shows higher polymorphic form change than curve face due to more even pressure distribution during compression. The compaction force from flat-face punch exerted on polymorphic Form A can induce a change to the polymorphic Form C directly by passing metastable amorphous form. However, curved face punch distribute unhomogeneous compaction force. After compaction force, polymorphic Form A may change to the metastable amorphous form prior to transformation to the polymorphic Form C. Thus, the various designs of punch-face, the curved face and the flat-face, have

significant effect on the transformation of polymorphic forms but the incision of punch-faces have no effect.

4.2. Effect of compaction pressure with constant dwell time of non-heated samples

Non-heated chlorpropamide powder Form A was compacted at various compression pressures of 1000, 3000 and 5000 psi by constant dwell time of 15 minutes using various punch-face designs. The contents of both of polymorphic forms are shown in Table 9.

Table 9 Effect of compaction pressures on the transformation of polymorphic forms of non-heated chlorpropamide analyzed by Q-Raman.

Punch face designs	Pressure (psi)	Average content of Form A (percent ± SD) (n=3)	Calculated average content of metastable-amorphous form (percent)	Average content of Form C (percent ± SD) (n=3)
PCI	1000	22 ± 1	62 ± 2	16 ± 3
	3000	21 ± 3	69 ± 2	10 ± 2
	5000	25 ± 10	62 ± 18	13 ± 8
PCC	1000	22 ± 5	66 ± 3	12 ± 4
	3000	19 ± 6	70 ± 9	11 ± 5
	5000	21 ± 6	63 ± 13	16 ± 9
PFI	1000	31 ± 5	51 ± 8	18 ± 5
	3000	31 ± 3	56 ± 9	14 ± 6
	5000	36 ± 9	44 ± 12	20 ± 8
PFF	1000	29 ± 5	48 ± 8	23 ± 10
	3000	28 ± 4	53 ± 7	19 ± 5
	5000	36 ± 4	42 ± 13	22 ± 10

When polymorphic Form A was compacted, the content of polymorphic Form A on the surface of every punch face designs decreased to approximately 30% (Figure 60). The transformation occurred higher than results obtained by Q-PXRD. Moreover, statistical data indicated that the effect of the various designs of punch-face had significant effect on the extent of average polymorphic Form A conversion (Figure 61). However, various compaction forces were shown not significantly affect the average polymorphic Form A transformation at 95% confidence interval ($p \leq 0.05$) (Table 20, Appendix B).

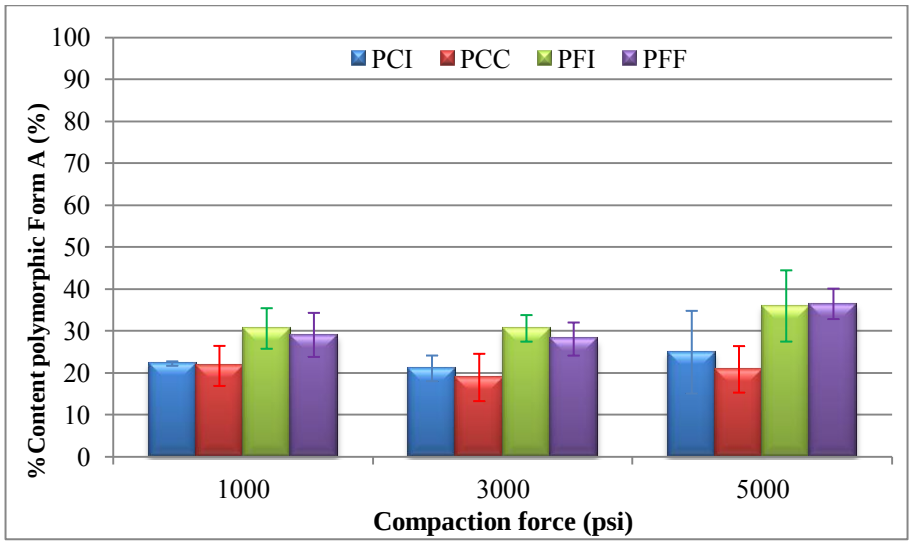

Figure 60 The relative percentages of non-heated polymorphic Form A and various compaction pressures (constant compaction dwell time) obtained analyzed by Q-Raman.

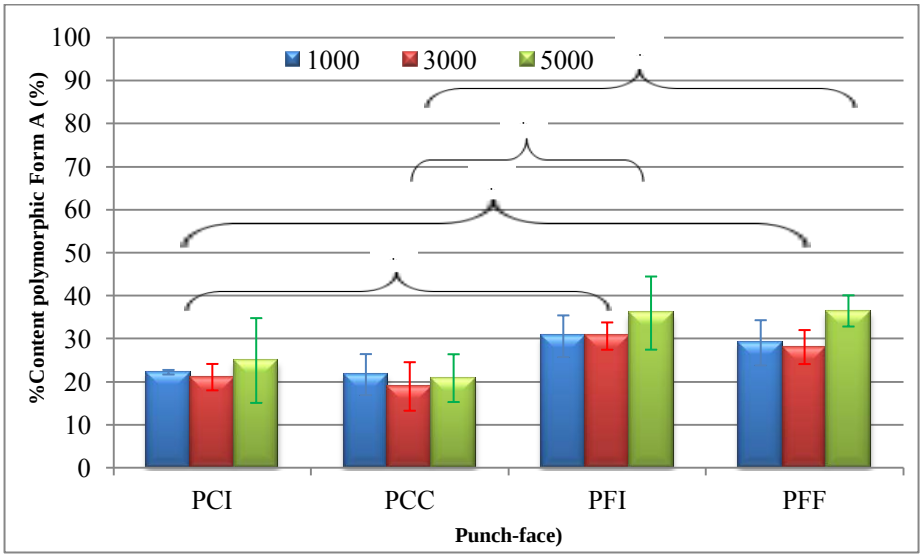

Figure 61 The relative amounts of various punch-face designs and the compaction pressures on non-heated chlorpropamide powder Form A obtained by Q-Raman (* significantly different at $p \leq 0.05$).

Various punch-face designs have an observable effect on the change of polymorphic Form A. The statistical results show that PCI and PFI, PCI and PFF, PCC and PFI and PCC and PFF were significantly different at 95% confidence interval (Table 21 in appendix B). In summary, difference in polymorphic Form A transformation was seen between flat-face and concave punches. Compaction with flat-face punches is shown to result in higher amount of Form A compare to Form C.

Every designs of punch-face can generate polymorphic Form C, even under compression force 1000 psi (Figure 62). However, statistical data shows that both factors (various punch-face designs and the compaction force) had no significant effect on conversion from Form A to Form C at 95% confidence ($p \leq 0.05$) (Table 22, Appendix B).

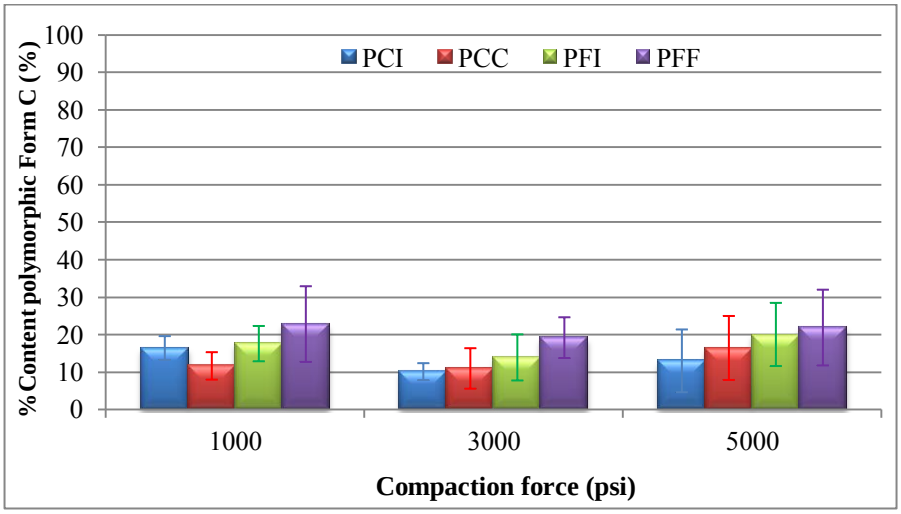

Figure 62 The relative percentages of non-heated polymorphic Form C and various compaction pressures (constant compaction dwell time) obtained analyzed by Q-Raman.

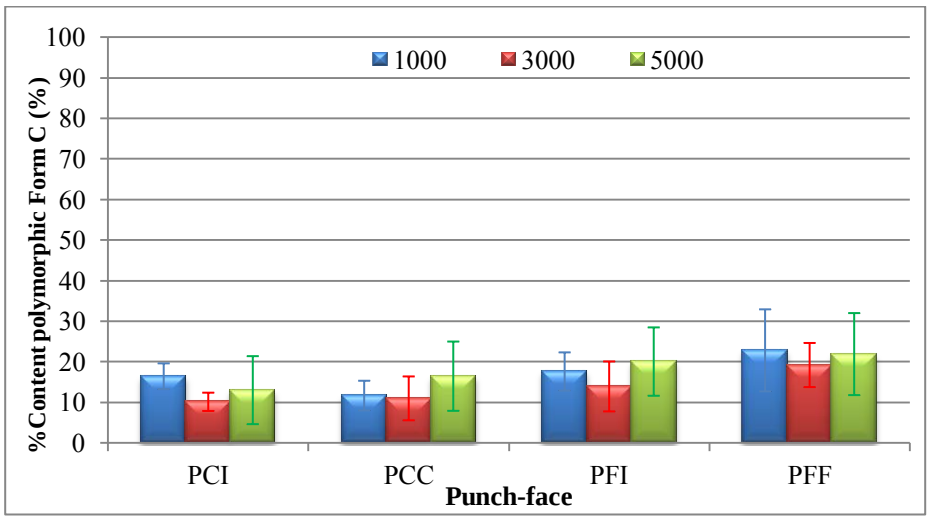

Figure 63 The relative amounts of various punch-face designs and the compaction pressures on non-heated chlorpropamide powder Form C obtained by Q-Raman.

Q-Raman shows the result of punch-face designs. When flat-face punch was used during compaction slightly higher amount of polymorphic Form A remained when compare to concave punch face. Because the pressure distribution during the compression

of curved face is uneven on the surface of tablets. After compaction with flat face punch, the polymorphic Form A changed to polymorphic Form C almost directly without passing through the metastable-amorphous form. So the content of starting polymorphic Form A after using concave punch face will decreased more than the flat-face punch due to the transformation to metastable-amorphous form and stayed as such in addition to conversion to Form C. However, polymorphic Form C were not shown to be different for punch-face designs or various compaction forces at 95% confidence interval ($p \leq 0.05$).

4.3. Effect of compaction pressure with constant dwell time on heated samples

This section will consider the effect of compression pressures on polymorphic of transformation heated chlorpropamide samples. The result is shown in Table 10.

Table 10 Effect of compaction pressures of heated chlorpropamide powder using constant compaction dwell time (15 min) by Q-Raman.

Punch Face designs	Pressure (psi)	Average content of Form A (percent ± SD) (n=3)	Calculated average content of metastable amorphous form (percent)	Average content of Form C (percent ± SD) (n=3)
HPCI	1000	9 ± 4	66 ± 9	25 ± 7
	3000	5 ± 3	76 ± 4	19 ± 5
	5000	8 ± 4	64 ± 5	28 ± 5
HPCC	1000	7 ± 3	71 ± 14	22 ± 12
	3000	4 ± 1	75 ± 5	21 ± 7
	5000	3 ± 0	72 ± 5	25 ± 5
HPFI	1000	10 ± 3	59 ± 7	31 ± 4
	3000	14 ± 1	53 ± 9	33 ± 9
	5000	18 ± 6	49 ± 12	33 ± 8
HPFF	1000	10 ±3	51 ± 3	39 ± 1
	3000	7 ± 4	59 ± 5	34 ± 5
	5000	19 ± 3	54 ± 8	27 ± 9

Every punch-face designs resulted in increased amounts of polymorphic Form C, while polymorphic Form A was reduced significantly. The results are shown in Figures 64 and 66. However, statistical evaluation indicated that both punch face and the compaction force had significant combined influence on the average polymorphic Form A transformation at 95% confidence interval ($p \leq 0.05$) (Table 23, Appendix B).

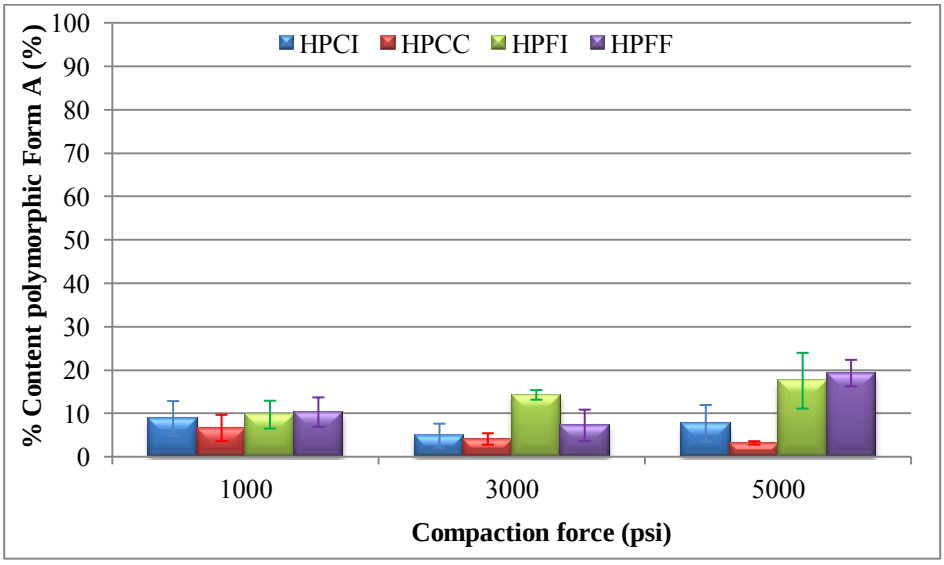

Figure 64 The relative percentages of heated polymorphic Form A and various compaction pressures (constant compaction dwell time) obtained analyzed by Q-Raman.

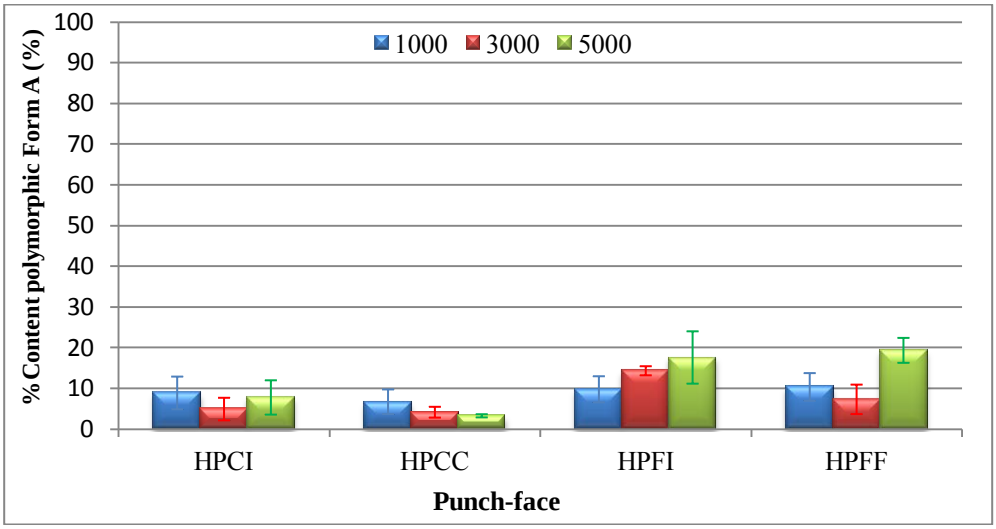

Figure 65 The relative amounts of various punch-face designs and the compaction pressures on heated chlorpropamide powder Form A obtabined analyzed by Q-Raman.

The flat-face punch (HPFI and HPFF) compaction force of 5000 psi was shown to have the highest polymorphic Form A (Figure 65). Because of increasing compaction force had direct impact on the change in polymorphic Form A. Thus, when polymorphic Form A was compacted with concave punch-face, the relationship is straight forward that Form A was reduced as compaction force increased. But if the polymorphic Form A were compacted with the flat-face punch, the results were shown in the opposite direction comparing to results of concave punch. This may be due to the higher compaction force exerted by flat-face punch design potentiates the reversible change of Form C (obtained after heating) back to Form A through an amorphous transition phase.

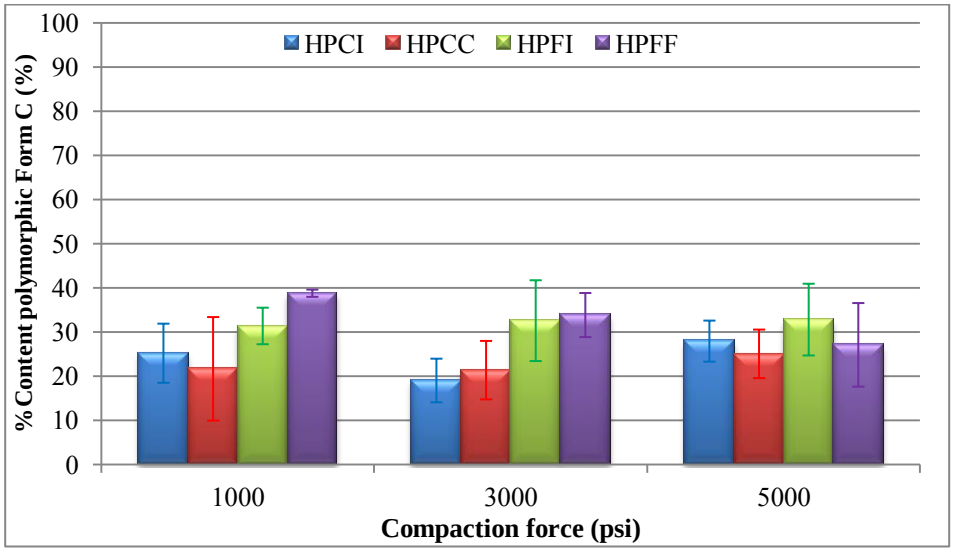

Figure 66 The relative percentages of heated polymorphic Form C and various compaction pressures (constant compaction dwell time) obtained analyzed by Q-Raman.

Polymorphic Form C was obtained after heating the initial polymorphic Form A. The heated samples were compacted at various pressures and resulted in reduced amount of polymorphic Form C as compared to uncompacted sample (data not shown). The statistical evaluation indicated that punch-face designs affected the transition of polymorphic Form C with 95% confidence level ($p \leq 0.05$) (Table 24, Appendix B), where the various compaction pressures did not show this effect.

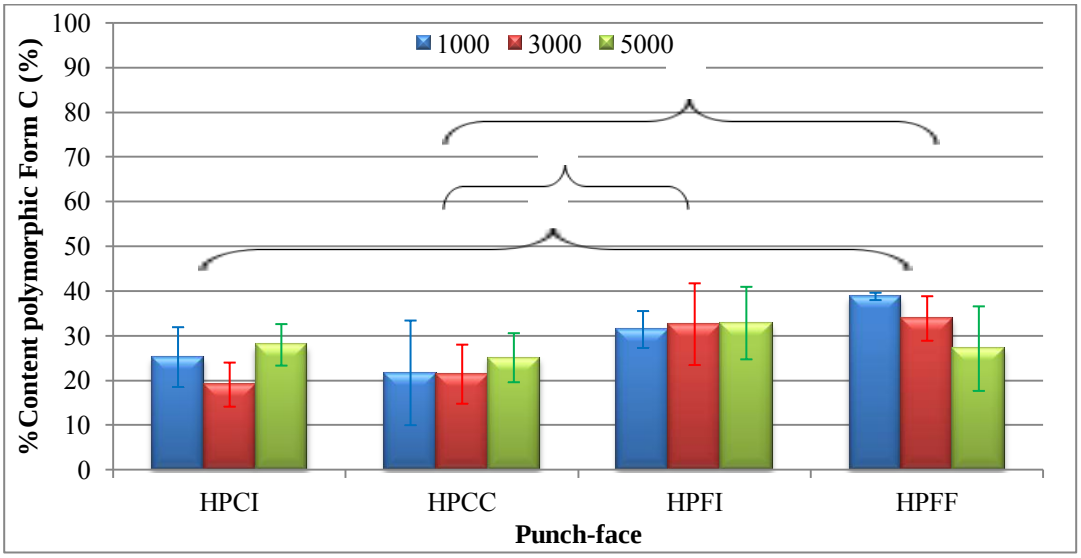

Figure 67 The relative amounts of various punch-face designs and the compaction pressures on heated chlorpropamide powder Form C obtabined analyzed by Q-Raman. (* significantly different at $p \leq 0.05$).

Figure 67 shows that designs of punch-face (especially between concave and flat-face punches) effect the change of polymorphic form C. Significant differences were seen between HPCI and HPFF, HPCC and HPFI and HPCC and HPFF (Table 25, Appendix B).

Thus, when the samples were pretreated by heat, Form A transformed partially to metastable-amorphous form and From C. After compaction, polymorphic transformation of Form C was shown to be effected only by punch-face design and not pressures. The compaction forces affect only polymorphic Form A but punch-face designs show affects on the transformation of both polymorphic Form A and Form C.

The quantitative analysis by PXRD is the perspective seen relative to the whole tablet. Each polymorphic form must have sufficiently high percentages and intensites to be detected. The percent content is as an average of the whole tablet. If the polymorphic

transformation occurred only on the surface of the tablet, as in our research, it may not be detected due to its low amounts and lower than the limit of detection when analyzed by PXRD. Thus, Q-Raman is useful in analyzing the polymorphs present only on the top surfaces of tablets. The percent content is not the average of the whole tablet. So the difference in punch face designs can be observed. However, this study discovered that the effect of indentation on punch face cannot be identified and differentiated by microscopic Raman spectroscopy.

Chapter V
CONCLUSIONS

The results of this study may be concluded as follow:

1. To evaluate the effects of different punch-face design on polymorphic transformation of chlorpropamide tablets after mechanical compaction.

Initial chlorpropamide powder Form A was compacted using punch-face design with concave, concave with incision, flat-face and flat-face with incision punches. After tabletting, chlorpropamide polymorphic Form C is observed for all various designs of punch face even when no dwell time and the least compaction force of 1000 psi were used. Thus, starting chlorpropamide powder Form A undergoes polymorphic transformation after mechanical compaction.

Moreover, the transformation of chlorpropamide powder was amplified by heating before tabletting. Chlorpropamide Form C appeared more after compaction than when unheated powder was used. So heat is a crititcal factor which will increase the extent of polymorphic transformation after compression.

Because only one polymorphic form is stable under one specific condition such as temperature and pressure. The stability of chlorpropamide powder Form A and Form C at ambient condition (Form C is more stable than Form A) differs from higher temperature or higher pressure condition. Under stressed conditions (such as accelerated temperatures, increased compaction dwell time or compaction pressure) Form A is more stable than Form C. Thus, it potentiates the reversible change of Form C back to Form A through an amorphous transition phase.

The various designs of punch-face is another factor which may induce polymorphic transformation. The concave punch face exerted “lower” uneven pressure distribution and will gradually change polymorphic Form A to Form C through

metastable amorphous form. However, flat face punch exerted “higher” even energy distribution, other than transform Form A to Form C as expected, it additionally has more opportunity to reverse polymorphic Form C back to Form A when enough pressure is accumulated. However, indentation of punch face did not show significantly different effect on chlorpropamide polymorphic transformation.

2. Compare the results analyzed by PXRD and confocal microscopic Raman spectroscopy on polymorphic mapping of chlorpropamide tablet surface.

Both quantitative analyses can analyzed the two polymorphic forms of chlorpropamide powder. Powder X-ray diffraction analyzed the whole tablet by gently ground the tablet until fine powder before analysis. However, grinding may affect the change in polymorphs. Moreover, this method is a destructive method where tablet structures must be destroyed. The content of polymorphic forms is an average amounts compare to the whole tablet. Thus, the results from PXRD can differentiate between processes used in tableting but cannot distinguish between punch-face design. However, confocal microscopic Raman spectroscopy is not a destructive method and can discriminate and locate each polymorphic forms present on the surfaces of tablets. In addition, confocal microscopic Raman spectroscopy can discriminate the difference in punch-face designs with better power than PXRD. However, Raman spectroscopy cannot detect polymorphic differences in the presence of indentation on the surfaces of tablets.

REFERENCES

Agatonovic-Kustrin, S., Wu, V., Rades, T. , Saville, D. and Tucker, G. I. Powder diffractometric assay of two polymophpic forms of ranitidine hydrochloride. Int J Pharm. 184 (1999): 107-114.

Ayala, P. A. Polymorphism in drugs investigated by low wavenumber Raman scattering. Vib Spectrosc. 45 (2007): 112-116.

Ayala, P. A., Caetano, C. W. M., Honorato, B. S., MendesFilho, J., Siesler, W. H., Faudone, N. S. and et al. Conformational polymorphism of the antidiabetic drug chlorpropamide. J Raman Spectrosc. 43 (2012): 263-272.

Baena, R. J. and L., B. Raman spectroscopy in chemical bioanalysis. Curr Opin Chem Biol. 8 (2004): 534-539.

Bertran, F. J. Mechnochemistry: an overview. Pure Appl Chem. 71(1999): 581-586.

Boldyreva, V. E., Sowa, H., Ahsbahs, H., Goryainov, V. S., Chernyshev, V. V., Dmitriev, P. V. and et al. Pressure-induced phase transitions in organic molecular crystals: a combination of x-ray single-crystal and powder diffraction, raman and IR-spectroscopy. J Phys. 121 (2008): 1-11.

Braga, D. G., L. S., Grepioni, F., Pettersen, A. Maini, L., Curzi, M. and Polito, M. Mechanochemical preparation of molecular and supramolecular organometallic materials and coordination networks. Dalton T. 14 (2006): 1249-1263.

Breitenbach, J. S., W. and Neumann, J. Confocal Raman-Spectroscopy: Analytical Approach to Solid Dispersions and Mapping of Drugs. Pharm Res. 16 (1999): 1109-1113.

Brittain, H. G. Effects of mechanical processing on phase composition. J Pharm Sci. 91 (2002): 1573-1580.

Bugay, E. D. Characterization of the solid-state: spectroscopic techniques. Adv Drug Deliver Rev. 48 (2001): 43-65.

Bugay, E. D. and Brittain, G. H. P Soc Photo-opt Ins. (2006). 271-312.

Byrn, R. S., Pfeiffer, R. R., Stephenson, G., Grant, W. J. D. and Gleason, B. W. Solid-State Pharmaceutical Chemistry. Chem Mater. 6 (1994): 1148-1158.

Byrn, R. S., Pfeiffer, R. R. and Stowell, G. J. Sol St Phen. (1999).

Byrn, S., Pfeiffer, R., Ganey M., Hoiberg, C. and Poochikian, G. Pharmaceutical solids: a strategic approach to regulatory considerations. Pharm Res. 12 (1995): 945-954.

Cao, W., Bates, S., Peck, E. G., Wildfong, L.D. P., Zhihui, Q. and Morris, R. K. Quantitative determination of polymorphic composition in intact compacts by parallel-beam X-ray powder diffractometry. J Pharm Biomed Anal. 30 (2002): 1111-1119.

Cao, W., Mullarney, P. M., Hancock, C. B., Bates, S. and Morris, R. K. Modeling of Transmitted X-ray Intensity Variation with Sample Thickness and Solid Fraction in Glycine Compacts. J Pharm Sci. 92 (2003): 2345-2353.

Chan, K. H. a. D. E. Polymorphic Transformation of some drugs under compression. Drug Dev Ind Pharm. 11 (1985): 315-332.

Chesalov, A. Y., Baltakhinov, P. V., Drebushchak, N. T., Boldyreva, V. E., Chukanov, B. N. and Drebushchak, A. V. FT-IR and FT-Raman spectra of five polymorphs of chlorpropamide. Experimental study and ab initio calculations. J Mol Struct. 891 (2008): 75-86.

Chieng, N., Rehder, S., Saville, D., Rades, T. and Aaltonen J. Quantitative solid-state analysis of three solid forms of ranitidine hydrochloride in ternary mixtures using Raman spectroscopy and X-ray powder diffraction. J Pharm Biomed Anal. 49 (2009): 18-25.

Connolly, R. J Introd XRPD. (2007): 1-9.

Drebushchak, A. V., Drebushchak, N. T., Chukanov, V. N. and Boldyreva, V. E. A new gamma-polymorph of chlorpropamide: 4-chloro-N-(propylaminocarbonyl) benzenesulfonamide. Acta Crystallogr B. 63 (2007): 355-357.

Drebushchak, N. T., Chesalov, A. Y. and Boldyreva. V. E. A new polymorph of chlorpropamide: 4-chloro-N-(propylaminocarbonyl)benzenesulfonamide. Acta Crystallogr B. 62 (2006): 4393-4395.

Drebushchak, A. V., Drebushchak, N. T., Chukanov, V. N. and Boldyreva, V. E. Transitions among five polymorphs of chlorpropamide near the melitng point. J Therm Anal Calorim. 93 (2008): 343-351.

Drebushchak, A. V., Drebushchak, N. T., Chukanov, V. N. and Boldyreva, V. E. Two polymorphs of chlorpropamide: the d-form and the high-temperature-form. Acta Crystallogr B. 64 (2008): 623-625.

Eiliazadeh, B., Pitt, K. and Briscoe, B. Effects of punch geometry on powder movement during pharmaceutical tabletting processes. Int J Solids Struct. 41 (2004): 5967-5977.

Furuyama, N., Hasegawa, S., Hamaura, T., Yada, S., Nakagami, H., Yonemochi, E. and et al. Evaluation of Solid-State Forms Present in Tablets by Raman Spectroscopy. Int J Pharm. 361 (2008): 12-18.

Gendrin, C., Roggo, Y. and Collet, C. Pharmaceuticalapplications of vibrational chemicalimaging and chemometrics: Areview. J Pharm Biomed Anal. 48 (2008): 533-553.

Gowen, A., O'Donnell, P. C., Cullen, J. P. and Bell, J. E. S. Recent applications of Chemical Imaging to pharmaceutical process monitoring and quality control. Eu J Pharm Sci. 69 (2008): 10-22.

Haefele, F. T. and P., K. Confocal Raman Microscopy in Pharmaceutical Development. Springer Series Opti. 158 (2011) : 165-202.

Hollricher, O. and I., W. High-Resolution Optical and Confocal Microscopy. 158 (2011): 1-20.

Izolani, O. A., Moraes, T. M. and Te´ llez S, A. C. Fourier transform Raman spectroscopy of drugs: quantitative analysis of 1-phenyl-2,3-dimethyl-5-pyrazolone-4-methylaminomethane sodium sulfonate: (dipyrone). J Raman Spectros. 34 (2003): 837-843.

Karpinski, H., P. Polymorphism of Active Pharmaceutical Ingredients. Chem Eng Technol. 29 (2006).

Koivisto, M. H. Depth Profiling of Compression-Induced Disorders and Polymorphic Transition on Tablet Surfaces with Grazing Incidence X-ray Diffraction. Pharm Res. 23 (2006): 813-820.

Kojima, T. O., S. Murase, N., Katoh F. Mano, T. and Matsuda, Y. Crystalline Form Information from Multiwell Plate Salt Screening by Use of Raman Microscopy. Pharm Res. 23 (2006): 806-811.

Kontoyannis, G. C. Quantitative determination of $CaCO_3$ and glycine in antacid tablets by Laser Raman Spectroscopy. J Pharm Biomed Anal. 13 (1995): 73-76.

Lin-Vien, D., Colthup, N.B., Fateley, W.G. and Grasselli, J.G. The handbook of Infrared and Raman characteristic frequencies of organic molecules. Acad Press. (1991): 503.

Lin, W., Jiang, J., Yang, H., Ozaki, Y., Shen, G. and Yu, R. Characterization of Chloramphenicol Palmitate Drug Polymorphs by Raman Mapping with Multivariate Image Segmentation Using a Spatial Directed Agglomeration Clustering Method. 78 (2006): 6003-6011.

Lin, Y. S. Grinding and compression processes affecting the solid-state transition of famotidine polymorphs. J Pharm Sci. 2 (2007): 211-219.

Matsumoto, T., Kaneniwa, N., Higuchi S. and Otsuka, M. Effects of Temperature and Pressure During Compression on Polymorphic Transformation and Crushing Strength of Chlorpropamide Tablets. J Pharm Pharmacol. 43 (1991): 74-78.

Mazel, V., Delplace, C., Busignies, V., Faivre, V., Tchoreloff, P. and Yagoubi, N. Polymorphic transformation of anhydrous caffeine under compression and grinding: a re-evaluation. Drug Dev Ind Pharm. 37 (2011): 832-840.

Morris, R. K., Nail, L. S., Peck, E. G. and et al. Advances in pharmaceutical materials and processing. PSTT. 1 (1998): 235-246.

Newman, W. A. and Byrn, R. S. Solid-state analysis of the active pharmaceutical ingredient in drug products. Drug Discov Today 8 (2003): 8.

Newton, M. J., Haririan, I. and Podczeck, F. The influence of punch curvature on the mechanical properties of compacted powders. Powder Technol. 107 (2000): 79-83.

Otsuka, M., Matsumoto, T. and Kaneniwa, N. Effects of the Mechanical Energy of Multi-tableting Compression on the Polymorphic Transformations of Chlorpropamide. J Pharm Pharmacol. 41 (1989): 665-669.

Otsuka, M., Matsuda, Y. Effects of Environmental Temperature and Compression Energy on Polymorphic Transformation During Tabletting. Drug Dev Ind Pharm. 19(1993): 2241-2269.

Picker-Freyer, M. K., Liao, X., Zhang, G. and Wiedmann, S. T. Evaluation of the Compaction of Sulfathiazole Polymorphs. J Pharm Sci. 96 (2007): 2111-2124.

Pirttimaki, J., Laine, E, Ketolainen, J. and Paronen, P. Effect of grinding and compression on crystal structure of anhydrous caffeine. Int J Pharm. 95 (1993): 93-99.

Sanchez-Castillo, X. F., Anwar, J. Molecular Dynamics Simulations of Granular Compaction. Chem Mater. 15 (2003).

Sasic, S. Raman Mapping of Low-Content API Pharmaceutical Formulations. I. Mapping of Alprazolam in Alprazolam/Xanax Tablets. Pharm Res. 24 (2007): 58-65.

Sinka, C. I., Burch, F.S., Tweed, H.J. and Cunningham, C. J. Measurement of density variations in tablets using X-ray computed tomography. Int J Pharm. 271 (2004): 215-224.

Sixsmith, D. and M., D. The effect of punch tip geometry on powder movement during the tableting process. J Pharm Pharmacol. 33 (1980): 79-81.

Skoog A. D., H., J. F. and Crouch, R. S. Principles of Instrumental Analysis Sixth Edition. (2007): 303-328.

Stephenson, A. G., Forbes, A. R. and Reutzel-Edens, M. S. Characterization of the solid state: quantitative issues. Adv Drug Deliver Rev. 48 (2001): 67-90.

Stewart, S., Priore, J. R., Nelson, P. M. and Treado, J. P. Raman Imaging. Annu Rev Anal Chem. (2012): 337-362.

Strachan, J. C., Rades, T., Gordon, C. K. and Rantanen, J. Raman spectroscopy for quantitative analysis of pharmaceutical solids. J Raman Spectros. 59 (2007): 179-192.

Suryanarayanan, R. and H., S. C. Quantitative analysis of the active ingredient in a multi-component tablet formulation by powder X-ray diffractometry. Int J Pharm. 77 (1991): 287-295.

Szep, A., Marosi, G., Marosfoi, B., Anna, P., Mohammed-Ziegler, I. and Viragh, M. Quantitative Analysis of Mixtures of Drug Delivery System Components by Raman Microscopy. Polm Adv Technol. 14 (2003): 784-789.

Taylor, S. L. and L., W. F. Evaluation of Solid-State Forms Present in Tablets by Raman Spectroscopy. J Pharm Sci. 89 (2000): 1342-1353.

Tudor, M. A., Church, J. S., Hendra, J. P., Davies, C. M. and Melia, D. C. The qualitative and quantitative analysis of chlorpropamide polymorphic mixtures by near-infrared fourier transform Raman spectroscopy. Pharm Res. 10 (1993): 1772-1776.

Ueda, H., Nambu, N. and Nagai, T. Dissolution Behavior of Chlorpropamide polymorphs. J Pharm Bull. 32 (1984): 244-250.

Vankeirsbilck, T., Bercauteren, A. Baeyens, W. and Ban der Weken, G. Applications of Raman spectroscopy in pharmaceutical analysis trends. Anat Chem. 21 (2002): 869-877.

Vyorykka, J. Confocal Raman Microscopy in Chemical and Physical characterization of coatted and printed papers. Laboratory of Forest Products Chemistry, Reports: 10 (2004).

Widjaja, E., Kanaufia, P., Lau, G., Kiong Ng, W., Garland, M., Saal, C. and et al. Detection of trace crystallinity in an amorphous system using Raman microscopy and chemometric analysis. Eu J Pharm Sci. 42 (2011): 45-54.

Wildfong, L. D. P., Morley, A. N., Moore, D. M. and Morris, R. K. Quantitative determination of polymorphic composition in intact compacts by parallel-beam X-ray powder diffractometry II Data correction for analysis of phase transformations as a function of pressure. J Pharm Biomed Anal. 39 (2005): 1-7.

Wildfong, L. D. P., Morris, R. K. Anderson, A. C. and Short, M. S. Demonstration of a shear-based solid-state phase transformation in a small molecular organic system: chlorpropamide. J Pharm Sci. 96 (2007): 1100-1113.

Yu, X. L., Furness, S. M., Raw, A., Woodland Outlaw, P. K., Nashed, E. N., Ramos, E. and et al. Scientific Considerations of Pharmaceutical Solid Polymorphism in Abbreviated New Drug Applications. Pharm Res. 20 (2003): 531-536.

APPENDICES

APPENDIX A

Table 11 The standard data of chlorpropamide Form A and Form C

Content of Form A (%)	Intensity of peak 6.6	Average intensity of peak 6.6	SD of peak 6.6	Content of Form C (%)	Intensity of peak 15.0	Average intensity of peak 15.0	SD of peak 15.0
100	3187 3245 3199	3210	31	0	0 0 0	0	0
90	2883 2815 2840	2846	34	10	60 49 0	36	32
70	2339 2297 2558	2398	140	30	204 176 147	176	29
50	1956 1807 1245	1669	375	50	310 259 287	285	26
30	1178 1232 1060	1157	88	70	314 383 416	371	52
10	470 423 413	435	30	90	474 487 503	488	15
0	0 0 0	0	0	100	508 585 562	551	40

APPENDIX B

Tests of Between-Subjects Effects

Dependent Variable: form A

Source	Type III Sum of Squares	df	Mean Square	F	Sig.	Noncent. Parameter	Observed Power[a]
Corrected Model	1759.789[b]	15	117.319	2.819	.007	42.284	.964
Intercept	36031.280	1	36031.280	865.756	.000	865.756	1.000
punch	1010.084	3	336.695	8.090	.000	24.270	.983
time	343.331	3	114.444	2.750	.059	8.250	.610
punch * time	406.374	9	45.153	1.085	.400	9.764	.435
Error	1331.785	32	41.618				
Total	39122.853	48					
Corrected Total	3091.574	47					

a. Computed using alpha = .05

b. R Squared = .569 (Adjusted R Squared = .367)

Table 12 Statistical data (two-way ANOVA) of polymorphic Form A between the various designs of punch-face and the compaction dwell times (constant compaction force) by Q-Raman.

Multiple Comparisons

Dependent Variable: form A

Tukey HSD

(I) punch	(J) punch	Mean Difference (I-J)	Std. Error	Sig.	95% Confidence Interval	
					Lower Bound	Upper Bound
CI	CC	2.9967	2.63370	.669	-4.1390	10.1323
	FI	-7.2562*	2.63370	.045	-14.3919	-.1206
	FF	-7.5939*	2.63370	.034	-14.7295	-.4582
CC	CI	-2.9967	2.63370	.669	-10.1323	4.1390
	FI	-10.2529*	2.63370	.003	-17.3885	-3.1172
	FF	-10.5905*	2.63370	.002	-17.7262	-3.4549
FI	CI	7.2562*	2.63370	.045	.1206	14.3919
	CC	10.2529*	2.63370	.003	3.1172	17.3885
	FF	-.3376	2.63370	.999	-7.4733	6.7980
FF	CI	7.5939*	2.63370	.034	.4582	14.7295
	CC	10.5905*	2.63370	.002	3.4549	17.7262
	FI	.3376	2.63370	.999	-6.7980	7.4733

Based on observed means.

*. The mean difference is significant at the .05 level.

Table 13 Statistical data (multiple comparisons) of polymorphic Form A and the various designs of punch-face (constant compaction force) by Q-Raman.

Tests of Between-Subjects Effects

Dependent Variable: form C

Source	Type III Sum of Squares	df	Mean Square	F	Sig.	Noncent. Parameter	Observed Power[a]
Corrected Model	2331.257[b]	15	155.417	4.274	.000	64.116	.998
Intercept	13299.831	1	13299.831	365.784	.000	365.784	1.000
punch	1156.077	3	385.359	10.598	.000	31.795	.997
time	965.798	3	321.933	8.854	.000	26.562	.990
punch * time	209.383	9	23.265	.640	.755	5.759	.255
Error	1163.513	32	36.360				
Total	16794.602	48					
Corrected Total	3494.771	47					

a. Computed using alpha = .05

b. R Squared = .667 (Adjusted R Squared = .511)

Table 14 Statistical data (two-way ANOVA) of polymorphic Form C between the various designs of punch-face and the compaction dwell times (constant compaction force) by Q-Raman.

Multiple Comparisons

Dependent Variable: form C

Tukey HSD

(I) punch	(J) punch	Mean Difference (I-J)	Std. Error	Sig.	95% Confidence Interval	
					Lower Bound	Upper Bound
CI	CC	1.3311	2.46170	.948	-5.3385	8.0008
	FI	-4.0171	2.46170	.376	-10.6867	2.6525
	FF	-11.2771*	2.46170	.000	-17.9467	-4.6074
CC	CI	-1.3311	2.46170	.948	-8.0008	5.3385
	FI	-5.3482	2.46170	.153	-12.0178	1.3214
	FF	-12.6082*	2.46170	.000	-19.2778	-5.9386
FI	CI	4.0171	2.46170	.376	-2.6525	10.6867
	CC	5.3482	2.46170	.153	-1.3214	12.0178
	FF	-7.2600*	2.46170	.029	-13.9296	-.5904
FF	CI	11.2771*	2.46170	.000	4.6074	17.9467
	CC	12.6082*	2.46170	.000	5.9386	19.2778
	FI	7.2600*	2.46170	.029	.5904	13.9296

Based on observed means.

*. The mean difference is significant at the .05 level.

Table 15 Statistic data (multiple comparisons) of polymorphic Form C and the various designs of punch-face times (constant compaction force) by Q-Raman.

Multiple Comparisons

Dependent Variable: form C

TukeyHSD

(I) dwell time	(J) dwell time	Mean Difference (I-J)	Std. Error	Sig.	95% Confidence Interval	
					Lower Bound	Upper Bound
0	15	-1.9171	2.46170	.863	-8.5867	4.7526
	30	-11.5597*	2.46170	.000	-18.2293	-4.8900
	60	-6.7202*	2.46170	.048	-13.3899	-.0506
15	0	1.9171	2.46170	.863	-4.7526	8.5867
	30	-9.6426*	2.46170	.002	-16.3122	-2.9729
	60	-4.8032	2.46170	.228	-11.4728	1.8665
30	0	11.5597*	2.46170	.000	4.8900	18.2293
	15	9.6426*	2.46170	.002	2.9729	16.3122
	60	4.8394	2.46170	.222	-1.8302	11.5091
60	0	6.7202*	2.46170	.048	.0506	13.3899
	15	4.8032	2.46170	.228	-1.8665	11.4728
	30	-4.8394	2.46170	.222	-11.5091	1.8302

Based on observed means.

*. The mean difference is significant at the .05 level.

Table 16 Statistic data (multiple comparisons) of polymorphic Form C and the various compaction dwell time (constant compaction force) by Q-Raman.

Tests of Between-Subjects Effects

Dependent Variable: %Form A

Source	Type III Sum of Squares	df	Mean Square	F	Sig.	Partial Eta Squared
Corrected Model	415.481[a]	15	27.699	5.382	.000	.716
Intercept	1241.355	1	1241.355	241.198	.000	.883
punch	126.159	3	42.053	8.171	.000	.434
time	141.184	3	47.061	9.144	.000	.462
punch * time	148.138	9	16.460	3.198	.007	.474
Error	164.692	32	5.147			
Total	1821.528	48				
Corrected Total	580.172	47				

a. R Squared = .716 (Adjusted R Squared = .583)

Table 17 Statistical data (two-way ANOVA) of polymorphic Form A between the various designs of punch-face and the compaction dwell times after heating (6 hours) by Q-Raman.

Tests of Between-Subjects Effects

Dependent Variable: %Form C

Source	Type III Sum of Squares	df	Mean Square	F	Sig.	Partial Eta Squared
Corrected Model	2015.560[a]	15	134.371	4.342	.000	.671
Intercept	26670.497	1	26670.497	861.746	.000	.964
punch	1468.548	3	489.516	15.817	.000	.597
time	216.696	3	72.232	2.334	.093	.180
punch * time	330.316	9	36.702	1.186	.337	.250
Error	990.380	32	30.949			
Total	29676.437	48				
Corrected Total	3005.940	47				

a. R Squared = .671 (Adjusted R Squared = .516)

Table 18 Statistical data (two-way ANOVA) of polymorphic Form C between the various designs of punch-face and the compaction dwell times after heating (6 hours) by Q-Raman.

Multiple Comparisons

Dependent Variable: %Form C

Tukey HSD

(I) punch-face	(J) punch-face	Mean Difference (I-J)	Std. Error	Sig.	95% Confidence Interval	
					Lower Bound	Upper Bound
HCI	HCC	4.7429	2.27117	.179	-1.4105	10.8964
	HFI	-10.2490*	2.27117	.000	-16.4024	-4.0956
	HFF	-4.4036	2.27117	.232	-10.5570	1.7499
HCC	HCI	-4.7429	2.27117	.179	-10.8964	1.4105
	HFI	-14.9920*	2.27117	.000	-21.1454	-8.8385
	HFF	-9.1465*	2.27117	.002	-15.2999	-2.9931
HFI	HCI	10.2490*	2.27117	.000	4.0956	16.4024
	HCC	14.9920*	2.27117	.000	8.8385	21.1454
	HFF	5.8455	2.27117	.067	-.3080	11.9989
HFF	HCI	4.4036	2.27117	.232	-1.7499	10.5570
	HCC	9.1465*	2.27117	.002	2.9931	15.2999
	HFI	-5.8455	2.27117	.067	-11.9989	.3080

Based on observed means.

*. The mean difference is significant at the .05 level.

Table 19 Statistical data (multiple comparisons) of polymorphic Form C and the various designs of punch-face after heating (6 hours) by Q-Raman.

Tests of Between-Subjects Effects

Dependent Variable: form A

Source	Type III Sum of Squares	df	Mean Square	F	Sig.	Noncent. Parameter	Observed Power[a]
Corrected Model	1183.323[b]	11	107.575	3.642	.004	40.067	.968
Intercept	25567.861	1	25567.861	865.720	.000	865.720	1.000
punch	963.731	3	321.244	10.877	.000	32.632	.997
pressure	155.392	2	77.696	2.631	.093	5.262	.473
punch * pressure	64.200	6	10.700	.362	.895	2.174	.130
Error	708.807	24	29.534				
Total	27459.992	36					
Corrected Total	1892.131	35					

a. Computed using alpha = .05

b. R Squared = .625 (Adjusted R Squared = .454)

Table 20 Statistical data (two-way ANOVA) of polymorphic Form A between the various designs of punch-face and the compaction forces (constant compaction dwell time) by Q-Raman.

Multiple Comparisons

Dependent Variable: form A

Tukey HSD

(I) punch	(J) punch	Mean Difference (I-J)	Std. Error	Sig.	95% Confidence Interval	
					Lower Bound	Upper Bound
PCI	PCC	2.2736	2.56184	.811	-4.7935	9.3407
	PFI	-9.6464*	2.56184	.005	-16.7135	-2.5793
	PFF	-8.4552*	2.56184	.015	-15.5223	-1.3881
PCC	PCI	-2.2736	2.56184	.811	-9.3407	4.7935
	PFI	-11.9200*	2.56184	.001	-18.9871	-4.8529
	PFF	-10.7288*	2.56184	.002	-17.7959	-3.6617
PFI	PCI	9.6464*	2.56184	.005	2.5793	16.7135
	PCC	11.9200*	2.56184	.001	4.8529	18.9871
	PFF	1.1912	2.56184	.966	-5.8759	8.2583
PFF	PCI	8.4552*	2.56184	.015	1.3881	15.5223
	PCC	10.7288*	2.56184	.002	3.6617	17.7959
	PFI	-1.1912	2.56184	.966	-8.2583	5.8759

Based on observed means.

*. The mean difference is significant at the .05 level.

Table 21 Statistical data (multiple comparisons) of polymorphic Form A and the various designs of punch-face (constant compaction dwell time) by Q-Raman.

Tests of Between-Subjects Effects

Dependent Variable: form C

Source	Type III Sum of Squares	df	Mean Square	F	Sig.	Noncent. Parameter	Observed Power[a]
Corrected Model	606.660[b]	11	55.151	1.170	.357	12.867	.471
Intercept	9369.959	1	9369.959	198.732	.000	198.732	1.000
punch	415.480	3	138.493	2.937	.054	8.812	.622
pressure	126.636	2	63.318	1.343	.280	2.686	.261
punch * pressure	64.544	6	10.757	.228	.963	1.369	.097
Error	1131.568	24	47.149				
Total	11108.187	36					
Corrected Total	1738.228	35					

a. Computed using alpha = .05

b. R Squared = .349 (Adjusted R Squared = .051)

Table 22 Statistical data (two-way ANOVA) of polymorphic Form C between the various designs of punch-face and the compaction forces (constant compaction dwell time) by Q-Raman.

Tests of Between-Subjects Effects

Dependent Variable: form A

Source	Type III Sum of Squares	df	Mean Square	F	Sig.	Partial Eta Squared
Corrected Model	872.128[a]	11	79.284	6.817	.000	.758
Intercept	3247.497	1	3247.497	279.237	.000	.921
pressure * punch	253.396	6	42.233	3.631	.010	.476
pressure	118.204	2	59.102	5.082	.014	.298
punch	500.528	3	166.843	14.346	.000	.642
Error	279.118	24	11.630			
Total	4398.744	36				
Corrected Total	1151.246	35				

a. R Squared = .758 (Adjusted R Squared = .646)

Table 23 Statistical data (two-way ANOVA) of polymorphic Form A between the various designs of punch-face and the compaction forces after heating (6 hours) (constant compaction dwell time) by Q-Raman.

Tests of Between-Subjects Effects

Dependent Variable: form C

Source	Type III Sum of Squares	df	Mean Square	F	Sig.	Partial Eta Squared
Corrected Model	1161.603[a]	11	105.600	2.173	.054	.499
Intercept	28294.598	1	28294.598	582.238	.000	.960
pressure * punch	320.375	6	53.396	1.099	.392	.215
pressure	39.548	2	19.774	.407	.670	.033
punch	801.681	3	267.227	5.499	.005	.407
Error	1166.311	24	48.596			
Total	30622.513	36				
Corrected Total	2327.914	35				

a. R Squared = .499 (Adjusted R Squared = .269)

Table 24 Statistical data (two-way ANOVA) of polymorphic Form C between the various designs of punch-face and the compaction forces after heating (6 hours) (constant compaction dwell time) by Q-Raman.

Multiple Comparisons

Dependent Variable: form C

Tukey HSD

(I) punch-faces	(J) punch-faces	Mean Difference (I-J)	Std. Error	Sig.	95% Confidence Interval	
					Lower Bound	Upper Bound
HPCI	HPCC	1.3541	3.28621	.976	-7.7113	10.4194
	HPFI	-8.1938	3.28621	.087	-17.2591	.8716
	HPFF	-9.1790*	3.28621	.046	-18.2444	-.1136
HPCC	HPCI	-1.3541	3.28621	.976	-10.4194	7.7113
	HPFI	-9.5478*	3.28621	.036	-18.6132	-.4825
	HPFF	-10.5331*	3.28621	.019	-19.5984	-1.4677
HPFI	HPCI	8.1938	3.28621	.087	-.8716	17.2591
	HPCC	9.5478*	3.28621	.036	.4825	18.6132
	HPFF	-.9852	3.28621	.990	-10.0506	8.0802
HPFF	HPCI	9.1790*	3.28621	.046	.1136	18.2444
	HPCC	10.5331*	3.28621	.019	1.4677	19.5984
	HPFI	.9852	3.28621	.990	-8.0802	10.0506

Based on observed means.

*. The mean difference is significant at the .05 level.

Table 25 Statistical data (multiple comparisons) of polymorphic Form C and the various designs of punch-face after heating (6 hours) (constant compaction dwell time) by Q-Raman.

APPENDIX C

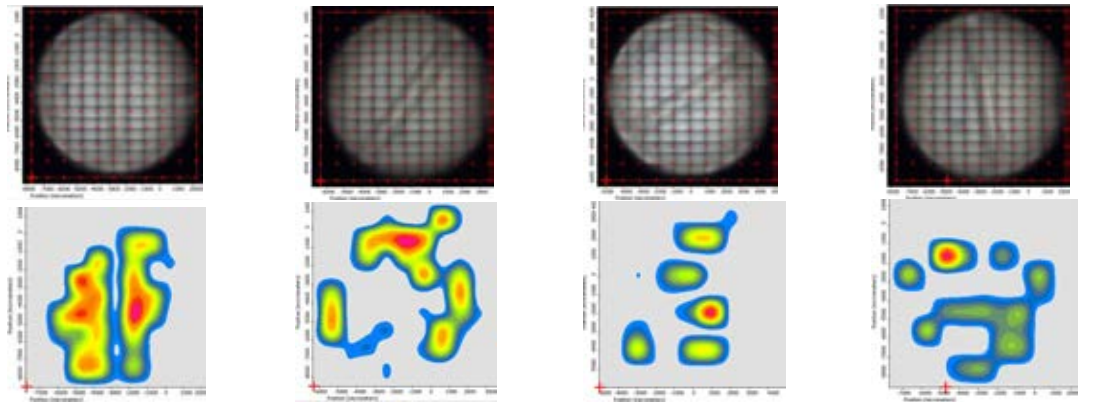
HCI 0 min Form A HCI 15 min Form A HCI 30 min Form A HCI 60 min Form A

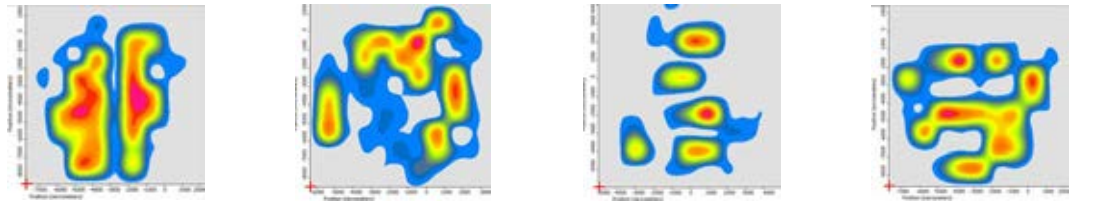
HCI 0 min Form C HCI 15 min Form C HCI 30 min Form C HCI 60 min Form C

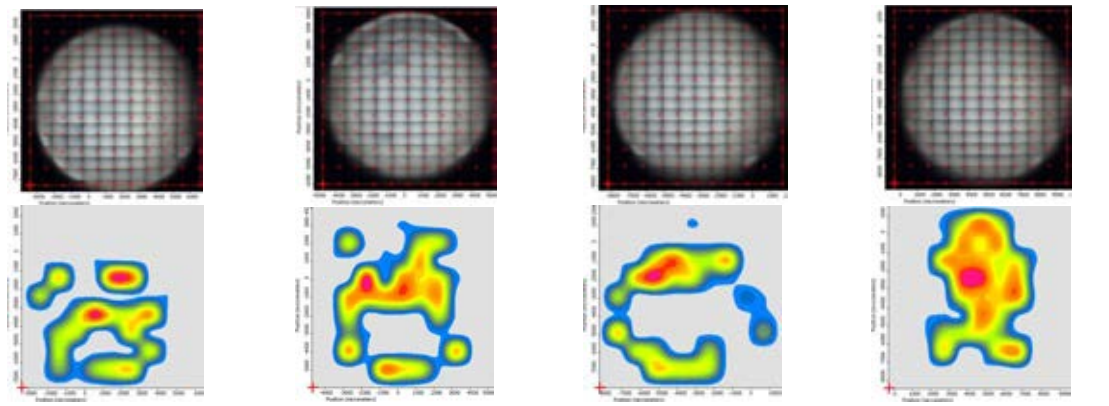
HCC 0 min Form A HCC 15 min Form A HCC 30 min Form A HCC 60 min Form A

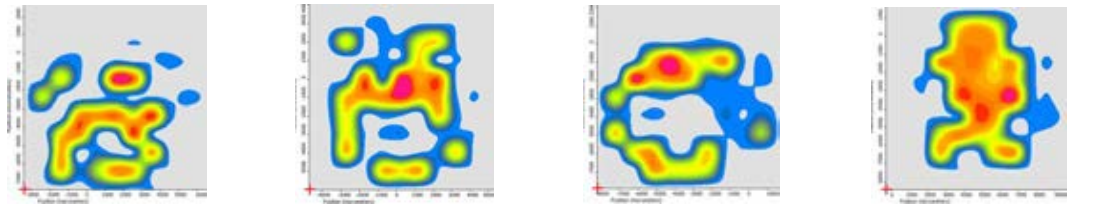
HCC 0 min Form C HCC 15 min Form C HCC 30 min Form C HCC 60 min Form C

Figure 68 Sampling grid and chemical mapping obtain by Raman spectroscopy of heated chlorpropamide polymorphic Form A and Form C on tablet surfaces. (CI = concave, indent CC = concave FI = flat faced, indent FF = flat faced)

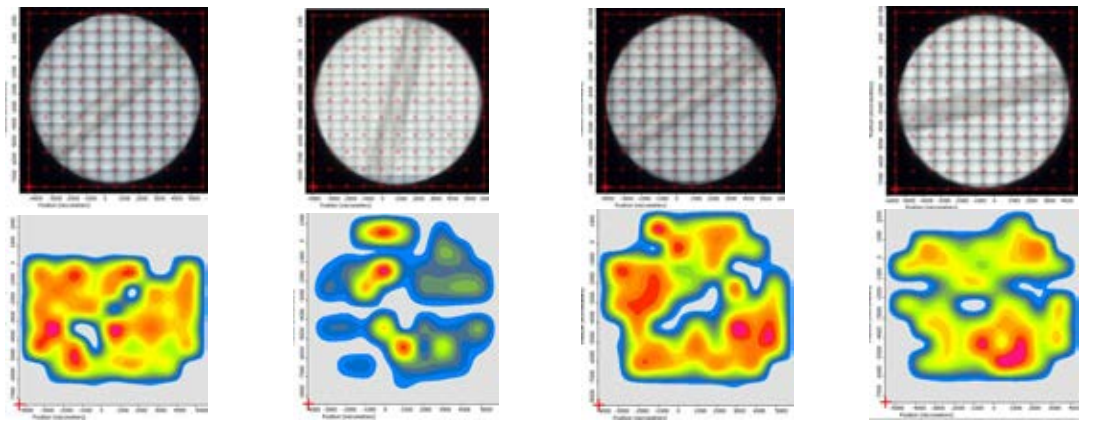

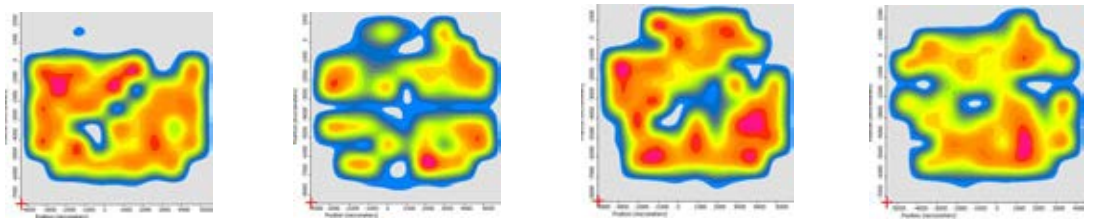

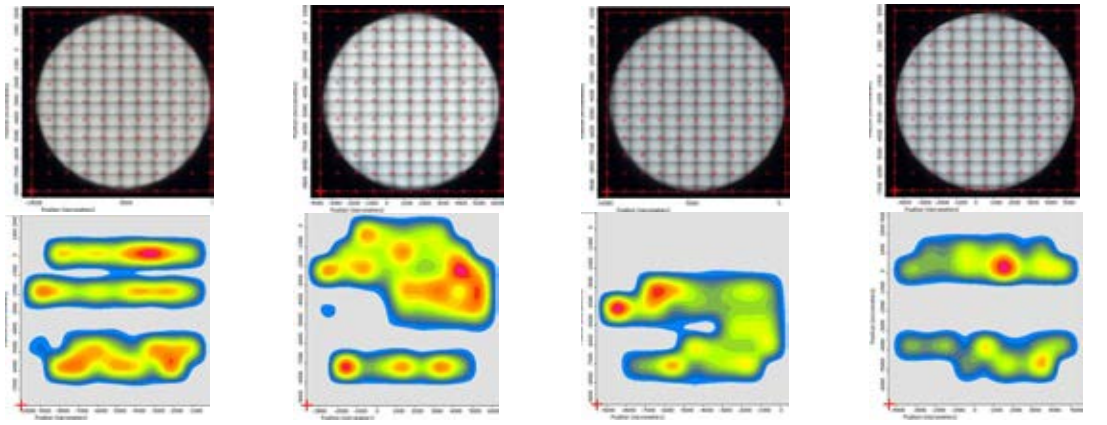

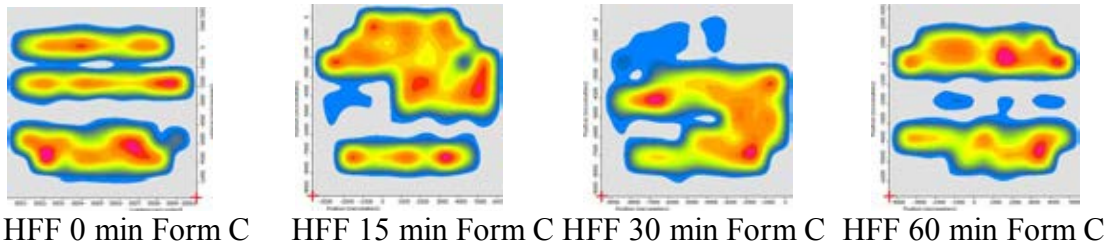

Figure 68 (cont.) Sampling grid and chemical mapping obtain by Raman spectroscopy of heated chlorpropamide polymorphic Form A and Form C on tablet surfaces. (CI = concave, indent CC = concave FI = flat faced, indent FF = flat faced)

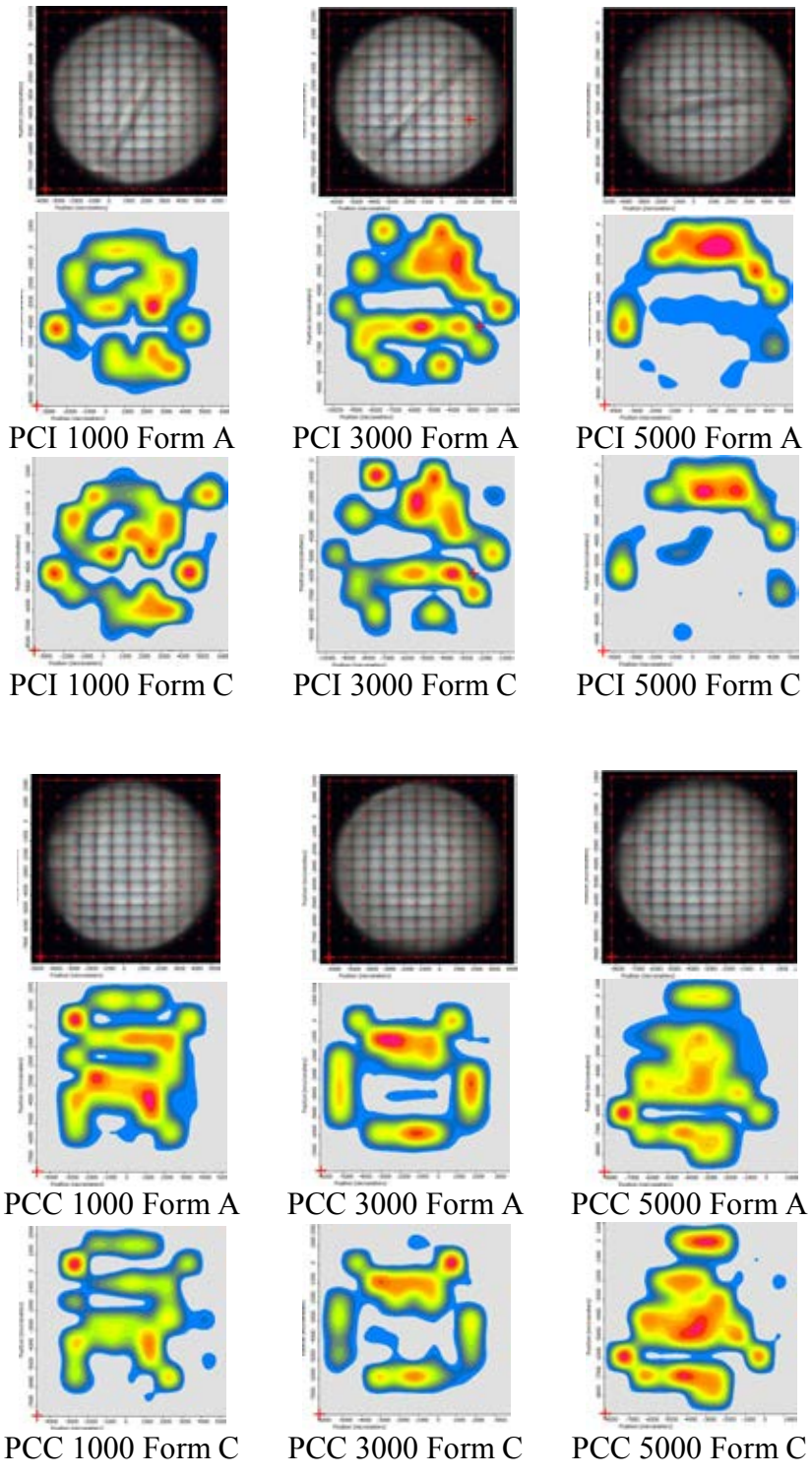

Figure 69 Sampling grid and chemical mapping obtain by Raman spectroscopy of non-heated chlorpropamide polymorphic Form A and Form C on tablet surfaces. (CI = concave, indent CC = concave FI = flat faced, indent FF = flat faced)

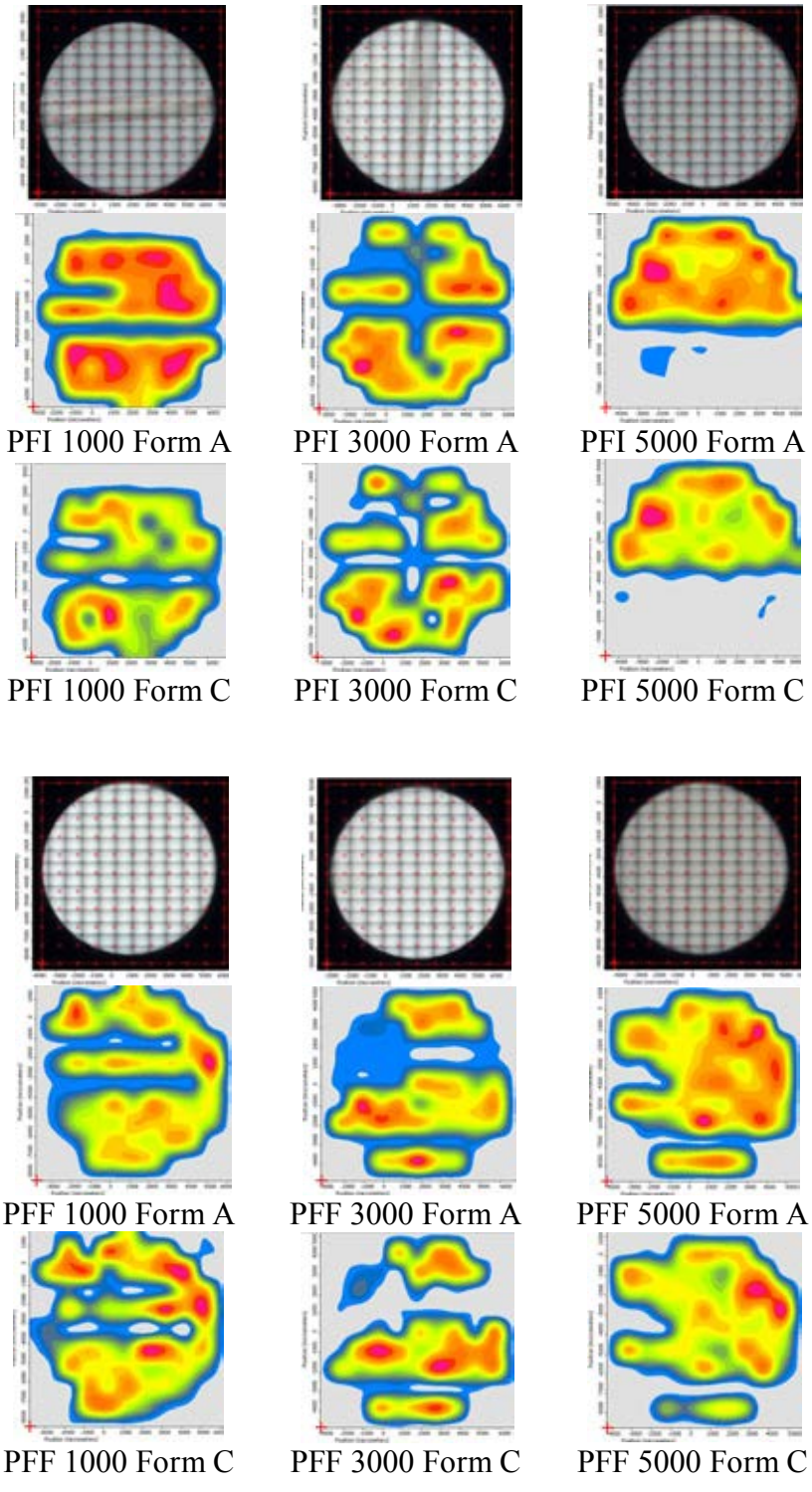

Figure 69 (cont.) Sampling grid and chemical mapping obtain by Raman spectroscopy of non-heated chlorpropamide polymorphic Form A and Form C on tablet surfaces. (CI = concave, indent CC = concave FI = flat faced, indent FF = flat faced)

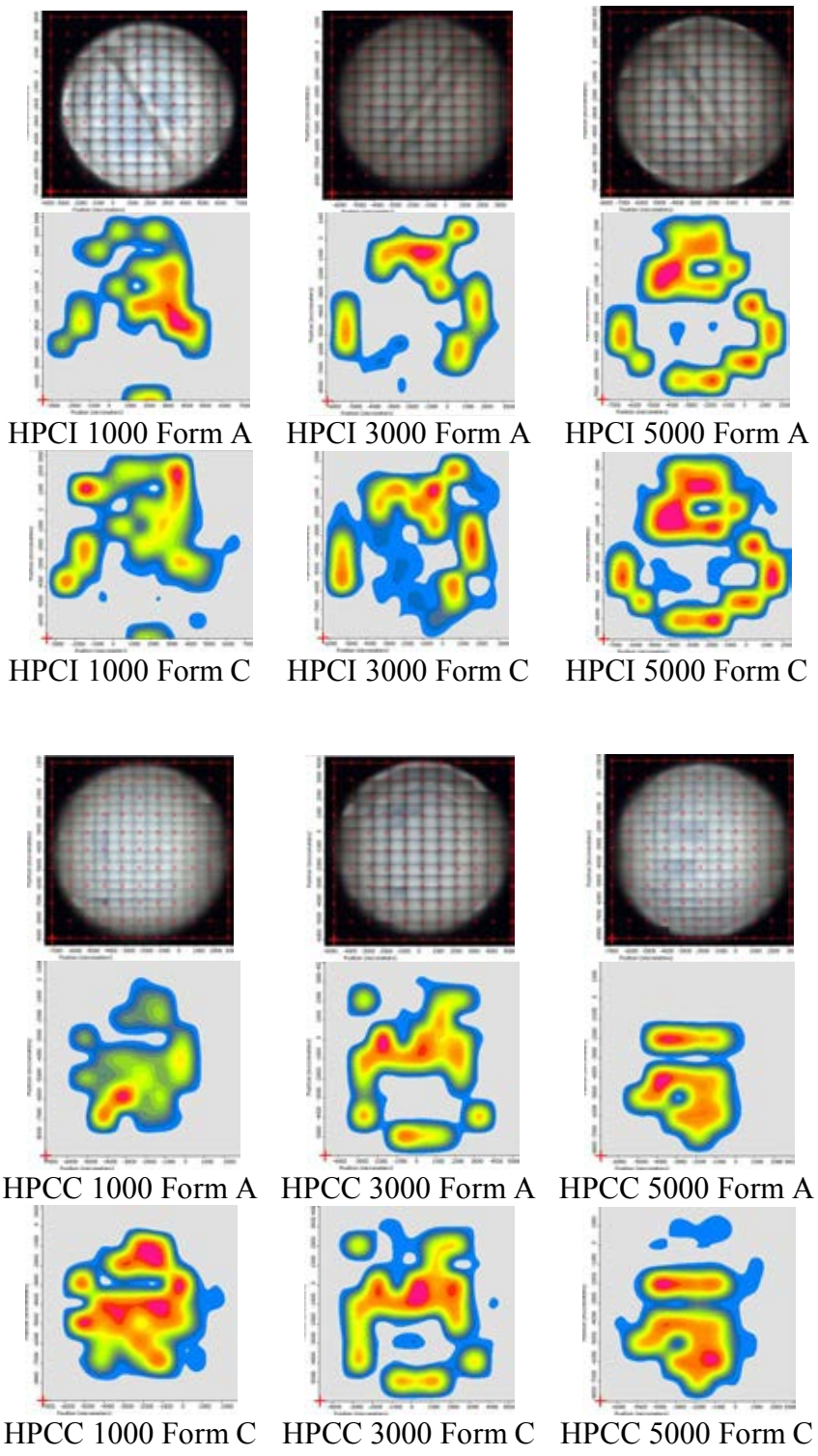

Figure 70 Sampling grid and chemical mapping obtain by Raman spectroscopy of heated chlorpropamide polymorphic Form A and Form C on tablet surfaces. (CI = concave, indent CC = concave FI = flat faced, indent FF = flat faced)

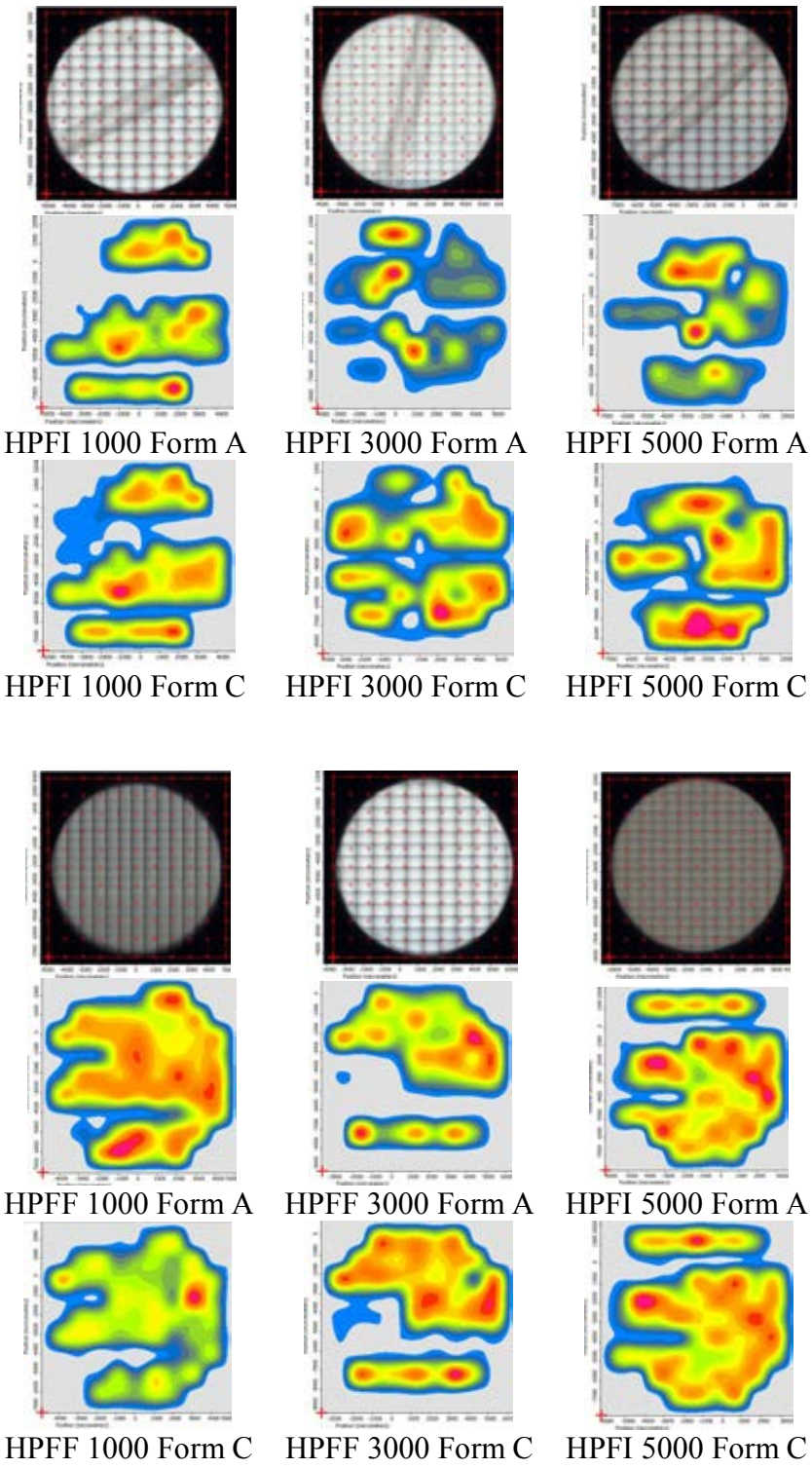

Figure 70 (cont.) Sampling grid and chemical mapping obtain by Raman spectroscopy of heated chlorpropamide polymorphic Form A and Form C on tablet surfaces. (CI = concave, indent CC = concave FI = flat faced, indent FF = flat faced)

VITA

Thanita Chotpiboolsup was born in Bangkok, Thailand, on June 20th 1986. She received Bachelor of Science in Pharmacy degree in 2009 from the Faculty of Pharmacy, Silpakorn University, Thailand. She presented a poster titled "Quantitative evaluation of chlorpropamide polymorphic transition during tabletting" at Chulalongkorn University on Jan 20, 2012.